OSU 1-D PBL Model

User's Guide

version 1.0.4

a One-Dimensional Planetary Boundary Layer Model

with Interactive
Soil Layers and Plant Canopy

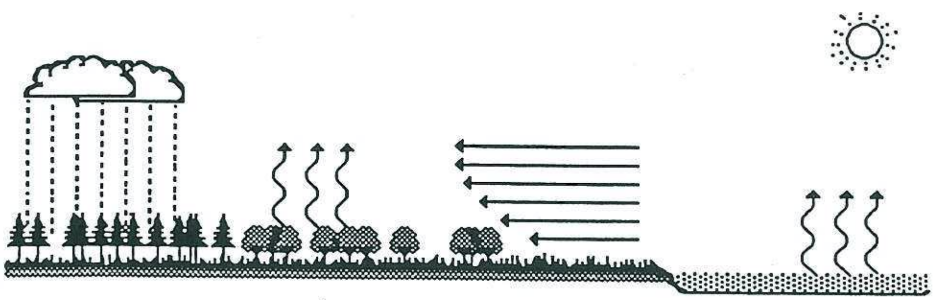

by

M. Ek and L. Mahrt

with contributions by
A. A. M. Holtslag, H.-L. Pan, P. Ruscher,
J. Kim, N. N. K. Gamage, and W. Gibson

Department of Atmospheric Sciences
Strand Agriculture Hall, Room 326
Oregon State University
Corvallis, Oregon 97331-2209 USA

March 1991

Notice for Users of OSU1DPBL 1.0.4

This model version represents work for a Phillips Laboratory contract, however the OSU1DPBL model continues to undergo change. The model and user's guide may be distributed with the permission of the OSU Atmospheric Sciences Department/Boundary Layer Research Group and Dr. S. Chang (contract monitor) of PL/GPAP.

M. Ek
Boundary Layer Research Group
Department of Atmospheric Sciences
Oregon State University
Corvallis, OR 97331-2209
tel ~~503~~ 541 [redacted] -737-5701, -737-4557
fax ~~503~~ 541 [redacted] -737-2540
Internet: ek@ats.orst.edu

michael.ek@noaa.gov

Dr. S. Chang
(PL/GPAP)
Phillips Laboratory (OLAA)
Atmospheric Sciences Division
Atmospheric Prediction Branch
Hanscom AFB, MA 01731-5000
tel 617-377-3913
Internet: chang@~~charney.gl~~.hanscom.af.mil

March 1991

Acknowledgements

Many people need to be acknowledged for their help in developing this model. Ib Troen, presently in Denmark at RisØ, conceived and implemented the basic mixing processes used in the model about 1980. A short while later Hua-Lu Pan, now at NWS/NMC, incorporated the soil and vegetation package into it, and was the principal workhorse on the model until 1988. Further model developments were made by C.-T. Chu with a cloud package (1986), Paul Ruscher at Florida State University with his thesis work on the stable boundary layer (1988), as well as modifications to the radiation package, Jinwon Kim at OSU with his thesis work on free atmospheric diffusion and gravity wave drag (1990), and Wayne Gibson at OSU for his help in general programming since 1985. Bert Holtslag at the Royal Netherlands Meteorological Institute (KNMI) worked with Hua-Lu Pan to incorporate the boundary-layer model in KNMI weather forecast models, and provided improved formulations for surface fluxes and profile functions, many of which were incorporated into the model when he visited OSU in the summer of 1989. Thanks also go to our previous and present contract monitors, Ken Mitchell now at NWS/NMC, and Ken Yang and Sam Chang at PL for their help in model testing and numerous suggestions and comments. A more detailed list of scientists involved in the development of this model is given on the next page.

Paul Ruscher, Hua-Lu Pan, Nimal Gamage, Jinwon Kim, Wayne Gibson, and Bert Holtslag also helped write parts of this user's guide. Special thanks also go to Astrid Peterson, Susanna M. Bremer, and Jacob H. Jensen for their help with the word processing and graphics involved in creating this comprehensive user's guide.

As this has been an effort by many people over a number of years, we apologize if we have forgotten anything anyone has done, or left anyone out of these acknowledgements.

OSU1DPBL Model Researchers

Scientist	Present Location	Contribution	Years
Ib Troen	Risø National Lab. Roskilde, Denmark	Implemented mixing processes in PBL	1980-82
Larry Mahrt	Oregon State Univ.	Involved with all model packages	1980-91
James Paumier	Computer Sciences. Corporation Research Triangle Park, NC	Canopy/ transpiration packages	1981-83
Michael Ek	Oregon State Univ.	Evaporation formulation Cover package/ other model improvements	1981-82 1988-91
Hua-Lu Pan	NWS/NMC Washington, D.C.	Implemented soil/ vegetation package	1982-88
Paul Ruscher	Florida State Univ. Tallahassee, FL	Stable boundary layer/ modifications to radiation package	1982-88
C.-T. Chu	Chicago, IL	Cloud package	1984-86
Wayne Gibson	Oregon State Univ.	General programming	1985-91
Bert Holtslag	KNMI The Netherlands	Improved surface flux formulations/ profile functions	1986-89
Jinwon Kim	LL National Lab. Livermore, CA	Gravity wave drag/ Free atmospheric mixing	1987-91

Present and former contract monitors:

Sam Chang/ Ken Yang	Phillips Lab. Hanscom AFB, MA	suggestions/comments	1989-91 1987-89
Ken Mitchell	NWS/NMC Washington, D.C.	suggestions/comments/ model testing	1980-87

OSU 1-D PBL Model
User's Guide
version 1.0.4

Table of Contents

Oregon State University One-Dimensional Planetary Boundary Layer Model

User's Guide

version 1.0.4

Chapter 1. Introduction

The Oregon State University one-dimensional planetary boundary-layer (OSU1DPBL) model simulates the atmosphere, soil, and vegetated surface. The planetary boundary-layer model (Troen and Mahrt, 1986) is coupled with an active two-layer soil model (Mahrt and Pan, 1984) and a primitive plant canopy model (Pan and Mahrt, 1987). While many modifications have been made, the individual components from the original model have been examined previously in the references listed above as well as by Mahrt et al. (1984), Mahrt et al. (1987), and Mahrt et al. (1991). The equations used in this composite model are comprehensive enough to approximate the physical processes thought to be most important, yet simple enough to allow both crude and high-resolution diurnal model simulations to be run in a few minutes on a personal computer under a variety of diverse atmospheric conditions. The model is also robust with respect to atmospheric stability and has been run for long integrations under a variety of diverse conditions for many different locations around the globe. The model is being used by a number of governmental agencies, industrial organizations, and academic institutions for many different sensitivity experiments in local weather forecasting, air pollution, soil chemistry, and soil hydrology, either as a stand-alone model or in concert with larger scale models. For example, the surface evaporation scheme from the model is currently being used in National Weather Service forecast models. It has also been incorporated into 3-D global models such as the PL/GPAP global spectral model (Brenner et al., 1984) and the KNMI regional operational air mass transformation model (Holtslag et al., 1990). (See the Appendix for additional users.)

This user's guide serves as a basic informational tool for anyone who wishes to study the physical basis of the model, run the present version, or examine the computer code. Development of the model equations and a brief description of the computational procedures are presented in Chapter 2. Also included in this chapter are some simple diagrams showing the physical processes simulated by the model, and a flowchart for the model including the primary subroutines.

In Chapter 3, the steps needed to run the model are outlined, and the structure of the input data file and the model output sequence is explained. The program source code for the model is outlined in Chapter 4, including descriptions of the COMMON blocks and the SUBROUTINE calling arguments.

In the Appendix is a list of current OSU1DPBL users. Also, changes from previous model versions (1.0.1, 1.0.2, 1.0.3) are discussed, along with proposed changes, plus model limitations. A comprehensive list of references for the model and this user's guide are then given. Lastly, a full listing of the model (OSU1DPBL1.0.4.for) and the program to read binary model output and convert it to a readable form (PRINT1DPBL.for) are given.

This model has been financed by the Phillips Laboratory, Hanscom AFB, Massachusetts, under contracts F19628-81-K-0046, F19628-84-K-0044, and F19628-88-K-0001.

Chapter 2.
Model Equations and Numerical Methods

In this chapter we describe the physics and numerical methods employed in the model. Model equations are described in section 2.1. A brief description of the computational procedure follows in section 2.2. In section 2.3 schematics are presented which describe the general boundary-layer, soil, and plant processes in the model (Figures 1-3), plus some more specific figures. Section 2.4 contains a generalized flowchart of the model. Sections 2.5 to 2.11 describe numerical methods and other physics used in the model -- the finite differencing methods used for model computations, the snow cover model, the radiation Richardson number, the development of potential evaporation and surface temperature, and the relation between canopy resistance and the plant coefficient. Note that equation numbers are sequential within each section of this chapter.

2.1 Model Equations

In order to close the system of equations and determine the turbulent mixing, boundary conditions near the earth's surface must be provided. To obtain these conditions, an atmospheric surface-layer parameterization is used. The exchange of sensible and latent heat flux between the surface layer and the underlying surface requires knowledge of the soil and ocean surface conditions.

This section is divided into six subsections, each describing individual aspects of the planetary boundary-layer (PBL) and soil models. Turbulent mixing within the PBL is described in 2.1.1; free atmospheric mixing is given in 2.1.2; local generation of turbulence in the stable boundary layer is presented in 2.1.3; the surface-layer model of the atmosphere is given in 2.1.4; the soil model with soil hydrology and thermodynamics, and canopy transpiration and water balance is found in 2.1.5; the surface energy balance calculation, used to incorporate the impact of radiative heating effects on both the boundary and soil layers, is discussed in 2.1.6; the boundary-layer cloud parameterization follows in 2.1.7; and the total downward radiation is given in 2.1.8.

Unless otherwise indicated, the units of temperature are in degrees Kelvin (K), velocity in meters per second (m s^{-1}), humidity in kilograms per kilogram (kg kg^{-1}, nondimensional) and height and length in meters (m). Units for each of the remaining terms are indicated in the text.

2.1.1 Boundary-layer model

The model forecasts the tendencies due to turbulent mixing of the potential temperature (θ), specific humidity (q), and horizontal components of the wind ($\mathbf{V}_h$, or u and v) in subroutine PBLL. The set of prognostic equations is

$$\frac{\partial \mathbf{V}_h}{\partial t} = \frac{\partial}{\partial z}\left(K_m \frac{\partial \mathbf{V}_h}{\partial z}\right) - w\left(\frac{\partial \mathbf{V}_h}{\partial z}\right) \tag{1a}$$

$$\frac{\partial \theta}{\partial t} = \frac{\partial}{\partial z}\left(K_h \left(\frac{\partial \theta}{\partial z} - \gamma_\theta\right)\right) - w\left(\frac{\partial \theta}{\partial z}\right) \tag{1b}$$

$$\frac{\partial q}{\partial t} = \frac{\partial}{\partial z}\left(K_h \frac{\partial q}{\partial z}\right) - w\left(\frac{\partial q}{\partial z}\right) \tag{1c}$$

To simplify the presentation, only the vertical diffusion terms due to boundary-layer turbulent mixing, and the advection terms due a prescribed vertical motion field are kept in the equations. Details of the complete equations may be found in Troen and Mahrt (1986). Units are m s^{-2} in (1a), K s^{-1} in (1b), and s^{-1} in (1c).

The counter-gradient correction for potential temperature (γ_θ, K m^{-1}) which is included in (1b) following Troen and Mahrt (1986), is parameterized for the boundary layer as

$$\gamma_\theta = \begin{cases} 0 & ,\text{stable} \\ C\dfrac{(w'\theta')_s}{w_s h} & ,\text{unstable} \end{cases} \tag{2}$$

The counter-gradient correction (γ_θ) is evaluated in terms of the surface flux of potential temperature (see section 2.1.4 for a discussion of fluxes), the boundary-layer depth (h), a nondimensional constant C, set to 8.5 following Holtslag (1987), modified from the value of 6.5 employed by Troen and Mahrt (1986), and the velocity scale (w_s, m s^{-1}) of the boundary layer defined as

$$w_s = u_* \, \phi_m^{-1}\left(\frac{z_s}{L}\right) \tag{3}$$

In (3), u_* (m s^{-1}) is the surface friction velocity, z_s is the top of the surface layer (currently 0.1h in the model), and L is the Monin-Obukhov length; u_* and L will also be described in section 2.1.4. ϕ_m is the nondimensional profile function which is specified in (10a) below. In the neutral limit as $L \rightarrow \pm\infty$, the velocity scale $w_s \rightarrow u_*$. In the free convection case as $\mathbf{V} \rightarrow 0$, $u_* \rightarrow 0$ and

$$w_s \rightarrow \left[\frac{7 z_s g k (w'\theta_v')_s}{\theta_{sv}}\right]^{1/3} \tag{4}$$

The coefficient of diffusivity for momentum (K_m, m^2 s^{-1}) in the unstable case is

$$K_m = w_s \, h \, k \, \frac{z}{h}\left(1 - \frac{z}{h}\right)^p \quad . \tag{5}$$

with p set equal to 2.0 and $u_* \, \phi^{-1}(z/L)$ replacing w_s in the stable case. The eddy diffusivity for heat (K_h, m^2 s^{-1}) is related to the eddy diffusivity for momentum in terms of the turbulent Prandtl number (Pr, nondimensional)

$$K_h = K_m \, Pr \tag{6}$$

where for the unstable case

$$Pr = \left[\frac{\phi_h\left(\frac{z}{L}\right)}{\phi_m\left(\frac{z}{L}\right)} + C \, k \, \frac{z}{h}\right]_{z=z_s} \tag{7}$$

Pr is determined as the value at the top of the surface layer (z_s =

0.1h) using surface-layer similarity theory. For the stable and neutral cases the Prandtl number is assumed to be a constant (currently 1.0 in the model).

As shown in Eq. 7, the counter-gradient term occurring in the heat equation is also absorbed in the Prandtl number. The nondimensional profile functions (ϕ_m and ϕ_h) have their standard definition and will be defined formally below. The resulting prediction equation for potential temperature will therefore not explicitly contain the counter-gradient term and is actually identical in form to Eq. 1a (Troen and Mahrt, 1986).

The boundary-layer height (z_i, Figure 4) is diagnosed as

$$z_i = \frac{Ri_{cr}\theta_{ov}\left|\mathbf{V}(h)\right|^2}{g\ (\theta_v(h) - \theta^*_{ov})} \tag{8}$$

where Ri_{cr} (nondimensional) is the critical Richardson number, θ_{ov} is the reference virtual potential temperature at the first model above the surface, g (m s^{-2}) is the gravitational acceleration, $\theta_v(h)$ is the virtual potential temperature at model level h, and $\mathbf{V}(h)$ is the horizontal wind velocity at level h (the first model level above the surface). This approach to diagnosing the PBL height also requires the specification of a low-level potential temperature (θ^*_{ov}). We define $\theta_{ov}{}^*$ in the following way

$$\theta^*_{ov} = \left\{ \begin{array}{ll} \theta_{ov} & ,\text{stable} \\ \theta_{ov} + C\dfrac{\overline{(w'\theta_v')_s}}{w_s} & ,\text{unstable} \end{array} \right\} \tag{9}$$

When the boundary layer is unstable, the virtual potential temperature at the top of the surface layer in (9) is enhanced by thermal effects in an amount that is proportional to the surface sensible heat flux. In the neutral limit as $w_s \rightarrow u_*$, the correction to the surface temperature vanishes so that $\theta^*_{ov} \rightarrow \theta_{ov}$ with the result that the modified bulk Ri number (in Eq. 8) reduces to the usual one.

The nondimensional profile functions for the shear and temperature gradients are defined as follows

$$\phi_m = \begin{cases} 6.0 & \text{,very stable} \\ 1.0 + 5.0\frac{z}{L} & \text{,stable} \\ \left(1.0 - 15\frac{z}{L}\right)^{-1/3} & \text{,unstable} \end{cases} \tag{10a}$$

and

$$\phi_h = \begin{cases} 6.0 & \text{,very stable} \\ 1.0 + 5.0\frac{z}{L} & \text{,stable} \\ \left(1.0 - 15\frac{z}{L}\right)^{-1/2} & \text{,unstable} \end{cases} \tag{10b}$$

These formulations are taken from Businger et al. (1971) with modifications by Holtslag (1987), and are functions of the height coordinate (z) and the Monin-Obukhov length scale (L). For the very stable case ($z/L > 1.0$), we set $z/L = 1.0$ so that the profile functions remain constant. In the model code, ϕ_h appears implicitly as a form of ϕ_m and the Prandtl number.

2.1.2 Free atmospheric mixing

Eddy diffusivities above the boundary layer are computed as

$$K_h = \ell_h^2 \left| \frac{dV_h}{dz} \right| \qquad (11a)$$

$$K_m = \ell_m^2 \left| \frac{dV_h}{dz} \right| \qquad (11b)$$

or using the eddy Prandtl number

$$K_m = K_h Pr \qquad (11c)$$

where ℓ_h and ℓ_m are the mixing lengths for heat and momentum, respectively, and are assumed to be dependent upon the gradient Richardson number (Ri) computed across a model layer.

For stably-stratified cases ($Ri > 0$), the formulations for the mixing length and eddy Prandtl number are adopted from the atmospheric observations by Kim and Mahrt (1991a) as

$$\ell_h = \ell_{0,h} \left(e^{-8.5Ri} + 0.15/(Ri + 3.0)\right) \qquad (12a)$$

$$Pr = 1.5 + 3.08Ri \qquad (12b)$$

where $\ell_{0,h}$ is the asymptotic mixing length estimated as 50 m from observations in the free atmosphere. The relationships (11a), (11c), (12a), and (12b) complete the formulation for eddy diffusivity in a stably-stratified free atmosphere.

For the case of an unstably-stratified free atmosphere ($Ri < 0$), observations are not currently available and we adapt the eddy diffusivity formulation introduced by Louis *et al.* (1981). Eddy diffusivities from the relationship (11a-b) with mixing lengths are

$$\ell_m = \ell_{0,m} \left[1 - \frac{10Ri}{1 + 15|Ri|^{1/2}(\ell_{0,m}/\Delta z)^2(\Delta z/z)^{1/2}[(1+\Delta z/z)^{1/3} - 1]^{3/2}}\right]^{1/2} \qquad (13a)$$

$$\ell_h = \ell_{0,h} \left[1 - \frac{15Ri}{1 + 15|Ri|^{1/2}(\ell_{0,h}/\Delta z)^2(\Delta z/z)^{1/2}[(1+\Delta z/z)^{1/3} - 1]^{3/2}}\right]^{1/2} \qquad (13b)$$

where $\ell_{0,m}$ is the asymptotic mixing length for momentum transfer, Δz is the grid spacing, and z is the distance from the ground. The asymptotic mixing length for heat transfer $\ell_{0,h}$ is the same as the stable case, and the asymptotic mixing length for momentum transfer $\ell_{0,m}$ is determined from the Prandtl number at neutral stability and the asymptotic mixing length for heat transfer as

$$\ell_{0,m} = \sqrt{1.5}\, \ell_{0,h}. \qquad (14)$$

The relationships (13-14) completes the formulation for the eddy diffusivity in the unstably-stratified free atmosphere.

2.1.3 Local generation of turbulence in the stable boundary layer

To consider the local generation of turbulence in the upper part of stable boundary layer we apply the free atmospheric eddy diffusivity formulation (11-14) in the upper 70 % of the stable boundary layer. It is assumed that the boundary layer parameterization (2-10) is valid in the lower 30 % of the stable boundary layer. In applying the free atmospheric eddy diffusivity formulation (11-14) in the stable boundary layer, the asymptotic mixing length $\ell_{0,h}$ is adjusted as

$$\ell_{0,h} = \min(50, kz) \tag{15}$$

where k is the von Karman constant (0.4) and z is the distance from the ground surface. Eddy diffusivities in the upper 70 % of the stable boundary layer are computed from the boundary layer formulation (2-10) or from the free atmospheric formulation (11-14), whichever yields larger values.

2.1.4 Surface-layer model

The surface fluxes are calculated in subroutines PBLL and SFLX and are parameterized following Mahrt (1987) for the stable case and following Louis et al. (1982) for the unstable case (with modifications by Holtslag and Beljaars, 1989) as

$$u_*^2 = C_m \, |\mathbf{V}_0| \tag{16a}$$

$$(\overline{w'\theta'})_s = C_h \, (\theta_s - \theta_0) \tag{16b}$$

$$(\overline{w'q'})_s = C_h \, (q_s - q_0) \tag{16c}$$

where C_m and C_h are the surface exchange coefficients for momentum and heat, respectively (m s^{-1}). C_m and C_h are defined so that the wind speed factor is absorbed in them. $|\mathbf{V}_0|$ is the wind speed evaluated at the first model level above the surface.

The potential temperature (θ_0) and specific humidity (q_0) are taken at the first model level above the surface while the surface potential temperature (θ_s) and specific humidity (q_s) are obtained from the surface energy balance.

The surface exchange coefficients are

$$C_m = k^2 \, |\mathbf{V}_0| \, \frac{F1(z, z_{0M}, Ri_B)}{\left(\ln\left(\frac{z}{z_0}\right)\right)^2} \tag{17a}$$

$$C_h = \frac{k^2}{R} \, |\mathbf{V}_0| \, \frac{F2(z, z_{0M}, z_{0H}, Ri_B)}{\ln\left(\frac{z}{z_0}\right) \ln\left(\frac{z}{z_{0H}}\right)} \tag{17b}$$

where k is the nondimensional von Kármán constant (0.40) and R, estimated at 1.0, is the ratio of the drag coefficients for momentum and heat in the neutral limit and is taken from Businger et al. (1971) with modification by Holtslag and Beljaars (1989).

C_m and C_h are functions of the wind speed evaluated at the first model level above the surface ($|\mathbf{V}_0|$), the height of the first model layer above the surface (z), the roughness length for momentum (z_{0M}) which depends on surface characteristics, and the bulk Richardson number for the surface layer (Ri_B) which will be described later. In addition, C_h is also a function of the roughness length for heat (z_{0H}).

For C_m, the function F1 is defined as

$$F1 = \begin{cases} e^{-aRi_B} & ,\text{stable} \\ 1 - \dfrac{10Ri_B}{1+7.5\left[\dfrac{k^2}{\left(\ln\left(\dfrac{z}{z_{0M}}\right)\right)^2}10\right]\left(-Ri_B\dfrac{z}{z_{0M}}\right)^{1/2}} & ,\text{unstable} \end{cases} \quad (18)$$

and for C_h, the function F2 is defined as

$$F2 = \begin{cases} e^{-aRi_B} & ,\text{stable} \\ 1 - \dfrac{15Ri_B}{1+7.5\left[\dfrac{k^2}{\ln\left(\dfrac{z}{z_{0M}}\right)\ln\left(\dfrac{z}{z_{0H}}\right)}10\right]\left(-Ri_B\dfrac{z}{z_{0M}}\right)^{1/2}} & ,\text{unstable} \end{cases} \quad (19)$$

where a is a constant currently equal to 1.0 in the model.

The bulk Richardson number for the surface layer is defined as

$$Ri_B = \frac{g\ z\ (\theta_{ov} - \theta_{sv})}{\theta_{0v}|\mathbf{V}_0|^2} \quad (20)$$

The bulk-Richardson number is a function of the height (z), the difference between the virtual potential temperature of air at the first model level (θ_{0v}) and the surface virtual potential temperature (θ_{sv}) which corresponds to the surface temperature from the surface energy balance, and the air speed at the first model level ($|\mathbf{V}_o|$).

The length scale for the surface layer is the Monin-Obuhkov length

$$L = -\frac{\theta_{sv} u_*^3}{gk\overline{(w'\theta_v')}_s} \quad (21)$$

The Monin-Obukhov length scale (L) is defined using the surface virtual potential temperature (θ_{sv}), friction velocity (u_*), and the virtual heat flux at the surface. It is used in the nondimensional profile functions described in Eqs. 10a-b.

The tendency equations for the surface layer are the same as those for the boundary layer (Eqs. 1a-c) except that the eddy diffusivities for the surface layer are

$$K_m = u_* \; k \; z \; \phi_m^{-1}\left(\frac{z}{L}\right)\left(1 - \frac{z}{h}\right)^p \quad (22)$$

$$K_h = K_m \; Pr^{-1} \quad (23)$$

where ϕ_m now has a dependence on z/L instead of on z_s/L. The dimensionless function ϕ_m is defined in Eq. 10a. As a modification to surface-layer similarity theory, the term $(1 - z/h)^p$ remains in K_m for proper matching with the mixed layer.

The only variables needed to close the surface-layer model are q_s and θ_s; they are available from the the soil model (2.1.5) and the surface energy balance calculation (2.1.6), respectively.

2.1.5 Soil model

The soil model has been described previously by Mahrt and Pan (1984) and Pan and Mahrt (1987). The soil hydrology is modelled in subroutine SFLX with the prognostic equation for the nondimensional volumetric water content (Θ)

$$\frac{\partial \Theta}{\partial t} = \frac{\partial}{\partial z}\left(D(\Theta)\frac{\partial \Theta}{\partial z}\right) + \frac{\partial K(\Theta)}{\partial z} \quad (24)$$

The coefficients of diffusivity (D, m^2 s^{-1}) and hydraulic conductivity (K, m s^{-1}) are functions of the volumetric water content (Mahrt and Pan, 1984). Through the extremes of wet and dry soil conditions, the coefficients D and K can vary by several orders of magnitude and, therefore cannot be treated as constants. The layer integrated form of Eq. 24 for the ith layer is

$$\Delta z_i \frac{\partial \Theta}{\partial t} = \left(D(\Theta)\frac{\partial \Theta}{\partial z} + K(\Theta) \right)_{z_{i+1}} - \left(D(\Theta)\frac{\partial \Theta}{\partial z} + K(\Theta) \right)_{z_i} \qquad (25)$$

Eq. 25 is valid for a layer $[z_i, z_{i+1}] = \Delta z_i$. At the surface of the soil, the evaporation is called the direct evaporation. For direct evaporation (E_{dir}, m s^{-1}) at the air-soil interface (z=0), we have

$$E_{dir} = \left[-D(\Theta)\left(\frac{\partial \Theta}{\partial z}\right)_0 - K(\Theta_0) \right](1-\sigma_f) + I(1-\sigma_f) \qquad (26)$$

where I (m s^{-1}) is the infiltration rate (which is equal to rainfall less runoff) and σ_f (nondimensional, between 0 and 1) is the plant shading factor. The evaporation (E, m s^{-1}) can proceed at a potential rate (E_p) when the apparent soil moisture at the surface (Θ_{sfc}) is greater than the air dry value (Θ_d), i.e., that is when the soil is sufficiently wet (demand control stage). When the soil dries out, the evaporation can only proceed at the rate by which the soil can diffuse water upward from below (flux control stage) in which case $\Theta_{sfc} = \Theta_d$ and $E < E_p$. (E_p will be discussed below.)

The canopy evaporation of free water (E_c) is formulated as

$$E_c = E_p \, \sigma_f \left(\frac{C^*}{S'} \right)^n \qquad (27)$$

where S' (m), the saturation water content for a canopy surface, is a constant usually chosen to be 0.002 meters (2 mm), and n (nondimensional) is taken to be 0.5 (Pan and Mahrt, 1987). The canopy water content (C^*, m) changes as

$$\frac{dC^*}{dt} = \sigma_f \text{ Precip} - E_c \qquad (28)$$

Precipitation increases the canopy water content first while evaporation decreases C^*. Eq. 28 is in units of m s^{-1}.

The model also incorporates transpiration (E_t) in the following manner

$$E_t = E_p \, \sigma_f \, k_v \frac{\sum_{i=1}^{2}[\Delta z_i g(\Theta_i)]\left[1-\left(\frac{C^*}{S'}\right)^n\right]}{\sum_{i=1}^{2}[\Delta z_i]} \qquad (29)$$

where k_v is the nondimensional plant resistance factor or plant coefficient (PC) with a value between 0 and 1. The canopy resistance (RC) may be used instead of the plant coefficient. See section 2.10 for a discussion of PC and RC. The nondimensional transpiration rate function $g(\Theta_i)$ is defined as

$$g(\Theta) = \begin{cases} 1 & , \Theta > \Theta_{ref} \\ \dfrac{\Theta - \Theta_{wilt}}{\Theta_{ref} - \Theta_{wilt}} & , \Theta_{ref} \geq \Theta > \Theta_{wilt} \\ 0 & , \Theta_{wilt} \geq \Theta \end{cases} \qquad (30)$$

The transpiration limit Θ_{ref} and Θ_{wilt} refer, respectively, to an upper reference value, which is the Θ value where transpiration begins to decrease due to a deficit of water, and the plant wilting factor, which is the Θ value where transpiration stops (Mahrt and Pan, 1984).

Total evaporation is obtained by adding the direct soil evaporation, the transpiration and the canopy evaporation

$$E = E_{dir} + E_c + E_t \qquad (31)$$

The total evaporation cannot exceed the potential evaporation (E_p, defined in Eq. 39). After obtaining the evaporation, the surface specific humidity (q_s) is calculated from

$$q_s = q_0 + \frac{E}{\rho_0 C_h} \qquad (32)$$

This quantity is the specific humidity at the surface which allows E to be calculated from the bulk aerodynamic relationship; q_s is also used in the calculation of vertical profiles of moisture. ρ_0 (kg m^{-3}) is the air density at the surface, and C_h is the exchange coefficient for moisture, described section 2.1.4.

Soil thermodynamics are treated with a prognostic equation for soil temperature (T) such that

$$C(\Theta) \frac{\partial T}{\partial t} = \frac{\partial}{\partial z}\left(K_T(\Theta)\frac{\partial T}{\partial z}\right) \qquad (33)$$

The volumetric heat capacity (C, J m^{-3} K^{-1}) and the thermal conductivity (K_T, W m^{-1} K^{-1}) of the soil are both functions of the soil water content (Θ). The heat capacity (C) is linearly related to Θ, whereas the coefficient of thermal diffusivity (K_T) is a highly nonlinear function of Θ and increases by several orders of magnitude from dry to wet soil conditions. The layer-integrated form of Eq. 33 for the ith layer is

$$\Delta z_i C(\Theta_i)\frac{\partial T_i}{\partial t} = \left(K_T(\Theta)\frac{\partial T}{\partial z}\right)_{z_{i+1}} - \left(K_T(\Theta)\frac{\partial T}{\partial z}\right)_{z_i} \qquad (34)$$

The upper boundary condition for the soil thermodynamic model is the soil heat flux, G (W m^{-2}), an important component in the surface energy balance. It is found from

$$K_T(\Theta)\left(\frac{\partial T}{\partial z}\right)_{z=0} = G \qquad (35a)$$

The soil system is closed except for the potential evaporation which is defined in the next section. For the two-level soil model, at 2.5 cm

$$\left(\frac{\partial T}{\partial z}\right)_{z=0} = \frac{\theta_s - T_{1soil}}{\Delta z} \tag{35b}$$

2.1.6 Surface energy balance

Surface temperature is calculated from the surface energy balance method

$$(1-\alpha)S\downarrow + L\downarrow - \sigma\theta_s^4 = G + H + L\cdot E \tag{36}$$

where each term is expressed in W m^{-2}. The first term on the left-hand side of Eq. 36 is the downward solar radiation (defined as positive downward). The nondimensional coefficient α is the surface albedo and is a function of surface characteristics. The second term on the left-hand side is the downward atmospheric radiation (positive downward). The third term on the left-hand side is the upward terrestrial radiation (positive upward); the coefficient σ is the Stefan-Boltzmann constant (5.6696×10^{-8} W m^{-2} K^{-4}). The first term on the right-hand side of Eq. 36 is the soil heat flux (positive downward) defined in Eq. 35a. The second term on the right-hand side is the sensible heat flux (positive upward). It is defined as

$$H = \rho_0 \, c_p \, C_h \, (\theta_s - \theta_0) \tag{37}$$

and is a function of the air density (ρ_o), the specific heat for air (c_p = 1004.5 J kg^{-1} K^{-1}), the exchange coefficient (C_h, Eq. 17), and the difference between the surface temperature (θ_s) and the air potential temperature at the first model level (θ_o). The last term on the right-hand side of Eq. 36 is the latent heat flux (positive upward) where L (J kg^{-1}) is the latent heat of phase change; E is calculated from Eq. 31.

The potential evaporation is needed to compute the actual evaporation from Eq. 31. The usual Penman relationship cannot be employed since the surface temperature is needed to compute the net radiation. Instead, as a first step, we evaluate the surface energy balance for the reference state of the surface (with the same albedo) but in a saturated condition

$$(1-\alpha)S\downarrow + L\downarrow - \sigma\theta_s'^4 = G + H' + L \cdot E_p \tag{38}$$

where

$$E_p = \rho_0 \, C_h \, (q_s^*(\theta_s') - q_0) \tag{39}$$

and

$$H' = \rho_0 \, c_p \, C_h \, (\theta_s' - \theta_0) \tag{40}$$

The temperature variable (θ_s') which appears in Eqs. 38-40 is a fictitious temperature the surface would have if the soil is sufficiently wet to evaporate at the potential rate. The variable $q^*_s(\theta_s')$ in Eq. 39 is the saturation specific humidity for this fictitious temperature. Thus θ_s' should be used for temporary evaluation of C_m in Eq. A3 of Troen & Mahrt (1986).

Over water, the prescribed sea surface temperature (SST) is prescribed so that q_s is the saturated surface specific humidity (q^*_s), which is calculated directly from SST. This over-water q_s is then used in the bulk aerodynamic formula for evaporation (Eq. 16 times $\rho_0 L_v$). Since θ_s' (SST in this case) and thus q^*_s are already known, there is no need to evaluate the surface energy balance over water.

A more formal derivation of the potential evaporation (E_p) and actual surface temperature (θ_s) can be found in section 2.9.

2.1.7 Boundary-layer clouds

Fractional cloud cover in the boundary layer is calculated in subroutine CLOUD and follows Ek and Mahrt (1991). The model predicts cloud cover using the generalized equation

$$CLC = f(\overline{RH}, \sigma_{RH}) \tag{41}$$

where CLC is the fractional cloud cover, RH (bar) is the maximum relative humidity in the boundary layer, and σ_{RH} is the standard deviation of relative humidity which accounts for the turbulent and subgrid mesoscale variations in relative humidity (Figure 5). The turbulent variability of relative humidity is formulated in terms of boundary-layer similarity theory whereas the mesoscale subgrid variability is specified as a function of grid size based on HAPEX analyses. With unstable conditions, boundary-layer clouds first form at lower relative humidities compared to the stable case. The fractional cloud cover is then the area under a Gaussian curve greater than RH = 1.0, and is approximated by a ninth-order polynomial fit to a Gaussian distribution (see the figure describing the cloud cover formulation in section 2.3).

2.1.8 Downward radiation

The model includes a simple radiation package which in subroutine SUN gives the total downward radiation, a combination of incoming solar (shortwave) plus downward atmospheric (longwave) radiation.

The incoming solar radiation is calculated following the method of ~~Kasten and Czeplak~~ Collier and Lockwood (~~1980~~ 1974). The clear sky value is reduced due to the solar elevation and presence of boundary-layer clouds (Figure 6). The equation for incoming solar radiation as it reaches the ground is

$$S\downarrow = [1 - (1-t)CLC^{n}]\ S_{CS}\downarrow \qquad (42)$$

where $S\downarrow$ is the net incoming solar radiation (below clouds but above the ground), t is a fraction dependent on the solar radiation transmitted through the clouds which depends on sun angle following Liou (1976), CLC is the fractional cloud cover, n is an empirically derived coefficient (1.0 in the model), and $S_{CS}\downarrow$ is the clear sky solar radiation adjusted for solar elevation. When n = 1, t is the actual fraction of solar radiation transmitted through the clouds.

Atmospheric (downward longwave) radiation is parameterized using a method from Satterlund (1979) with a modification for clouds following Paltridge and Platt (1976). The expression for atmospheric radiation is then

$$L\downarrow = \varepsilon\ \sigma\ T_{ref}^{4} + c_2\ CLC \qquad (43)$$

where L$\downarrow$ is the downward atmospheric radiation (W m^{-2}); ε is the emissivity of the atmosphere, a function of the temperature and moisture at the reference level in the model (currently 200 m); T_{ref} is the temperature at the reference height (200 meters in the model); CLC is the fractional cloud cover; and c_2 is an empirically derived constant equal to 60 W m^{-2}.

The user also has the option of specifying an effective atmospheric temperature (T_{eff}) in order to determine the atmospheric radiation from the simple relation $L\downarrow = \sigma T_{eff}^4$.

2.2 Computational Procedures

The computational procedures described in this section are also illustrated in general following the flowchart in figure x.

Computationally, we begin by determining the external forcing of the incoming solar radiation (Eq. 42), reduced by a fractional cloud cover (Eq. 41) and calculated for the previous time step. Fractional cloud cover plus profiles of temperature and moisture from the previous time step are then used for the calculation of downward atmospheric radiation (Eq. 43). This gives the total downward radiation.

Next, the fictitious surface energy balance for an open water surface (or a saturated land surface evaporating without resistance) is used to obtain potential evaporation (Eqs. 38-40). The key quantity to be determined in these equations is the skin temperature (θ_s') which the surface would achieve if it was saturated. Eqs. 38 and 40 are used to form a prediction for θ_s' which is then used to predict potential evaporation from Eq. 39. Both the soil heat flux G and the exchange coefficients take on their values from the previous time step.

As a test, the potential evaporation is imposed upon the upper part of the soil by requiring the upward flux of water in the soil to equal the potential rate. Eq. 39 is then solved for the surface value of soil moisture which would be required to produce a sufficiently strong gradient for the soil water flux to equal the potential demand. If this test gradient requires the surface soil moisture value to be less than the air-dry value, the potential demand cannot be met. In this case, the evaporative flux is set equal to the maximum value which can be supplied by the soil, that is, Eq. 26 with the surface soil moisture equal to the air-dry value (Eq. 26 serves to determine the top boundary condition for Eq. 25). On the other hand, if the test value of the surface soil moisture is greater than the air-dry value, the test value is retained and the soil moisture flux (bare soil contribution) proceeds at the potential rate. Given the bare soil evaporation and the potential evaporation, the contributions from plant transpiration and reevaporation of canopy water are determined giving the total surface soil moisture flux. The soil hydrology package is then updated.

When precipitation occurs, it wets the plant canopy first until the plant holding capacity is reached, then wets the ground surface by dripping through the plant canopy. Reevaporation from the plant canopy occurs at the potential rate given by Eq. 27 until the canopy water is depleted as determined by Eq. 28. Transpiration from plants is evaluated using Eqs. 29-30 and the potential evaporation determined from (38).

With Eq. 35a, the soil heat flux is obtained using the soil thermodynamic model from Eq. 34. In the finite difference form for Eq. 35a, the skin temperature θ_s appears as an unknown. Also an unknown in Eq. 36, θ_s can be solved for, thus allowing the other components of the surface energy balance to be determined. When snow cover is present, changes are needed for the interface; these changes are described in section 2.6.

Having obtained θ_s with Eq. 36 and q_s with Eq. 32, we use the surface-layer parameterization (Eqs. 16a-c) to obtain the surface stress, sensible heat flux, and latent heat flux. Variables used in Eqs. 16a-c are further defined in Eqs. 17-20. In addition, we calculate the Monin-Obukhov scale height (Eq. 21) and the similarity diffusivity profiles K_m and K_h (Eqs. 22 and 23) for the surface layer. The nondimensional profile functions for shear- and thermal-gradients are then computed from Eqs. 10a-b.

In the boundary-layer model, we then determine the height of the boundary layer (Eq. 8). The diffusivity coefficients above the surface layer are obtained with Eqs. 5-7. Finally, the

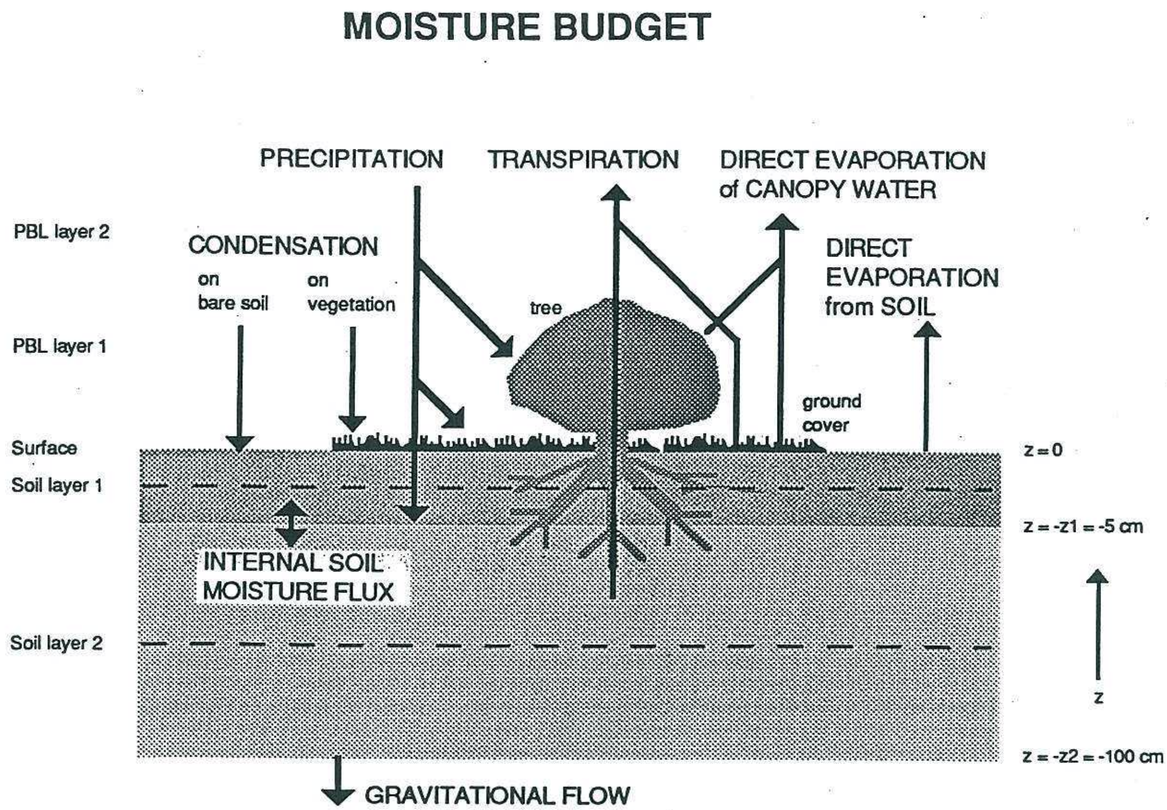

Figure 2. Geometry of the moisture budget in the model. Arrows indicate fluxes computed by the model; dashed lines indicate the mid-level of each soil layer which is the location of the computed soil water content ($\Theta 1$ at -2.5 cm and $\Theta 2$ at -52.5 cm).

tendencies of wind velocity, potential temperature, and specific humidity are calculated with Eqs. 1a-c.

2.3 Diagrams of Boundary-Layer Processes in OSU1DPBL

The diagrams in this section represent some of the physical processes simulated in the OSU1DPBL model.

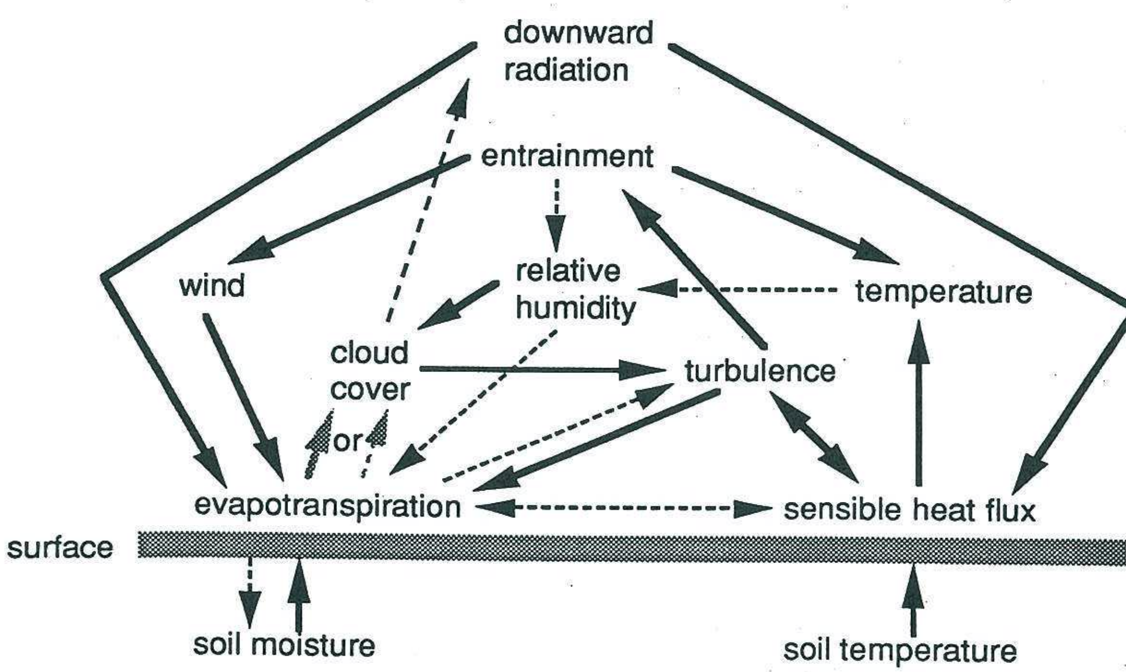

Figure 1. Suspected important interactions between surface evapotranspiration and boundary-layer development for conditions of daytime surface heating. Solid arrows indicate the direction of those feedbacks which are normally positive (leading to increases of the recipient variable). Dashed arrows indicate negative feedbacks. Two consecutive negative feedbacks make a positive one. Depending on conditions, cloud cover can lead to positive or negative feedbacks.

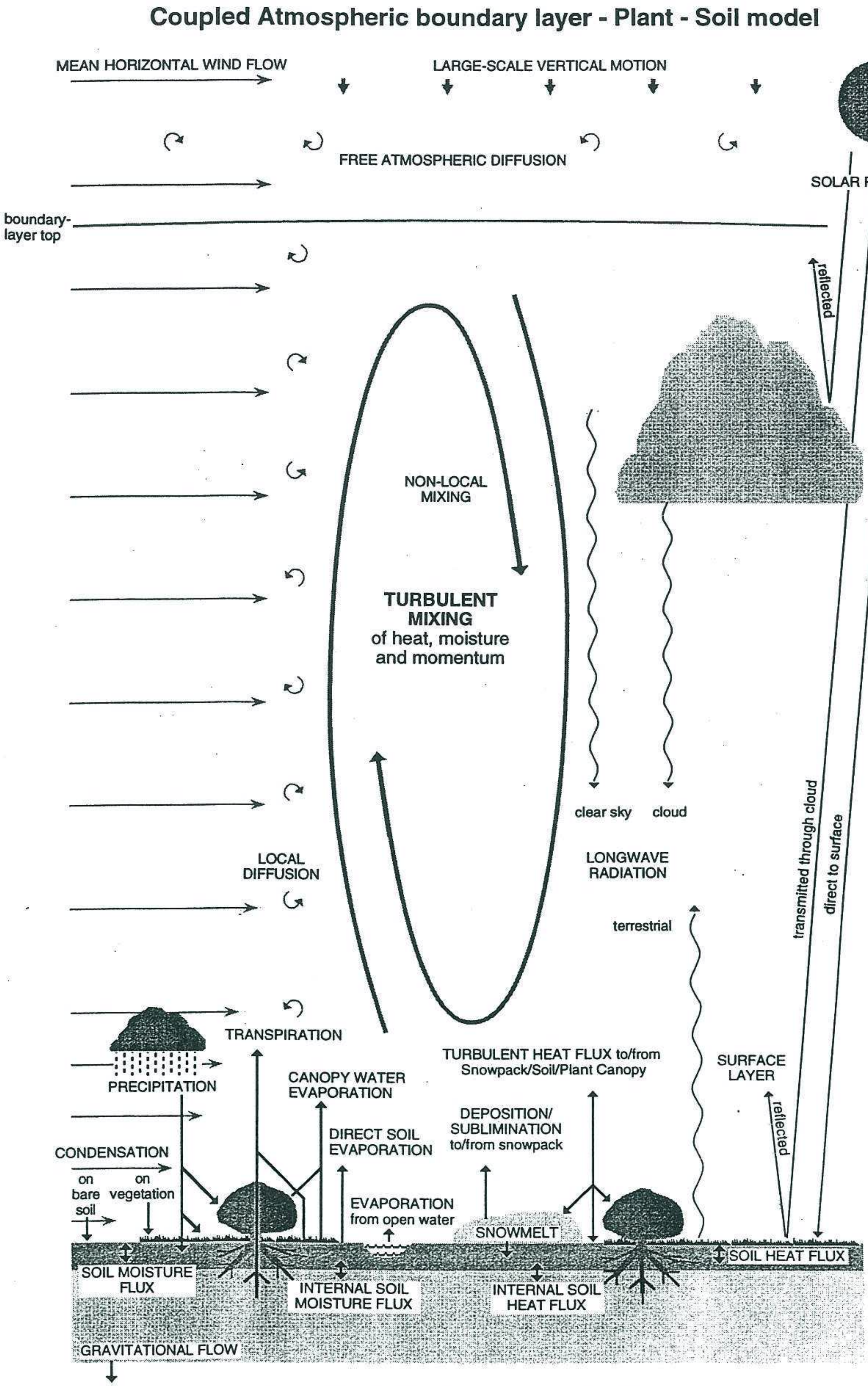

SURFACE MOISTURE and HEAT BUDGETS

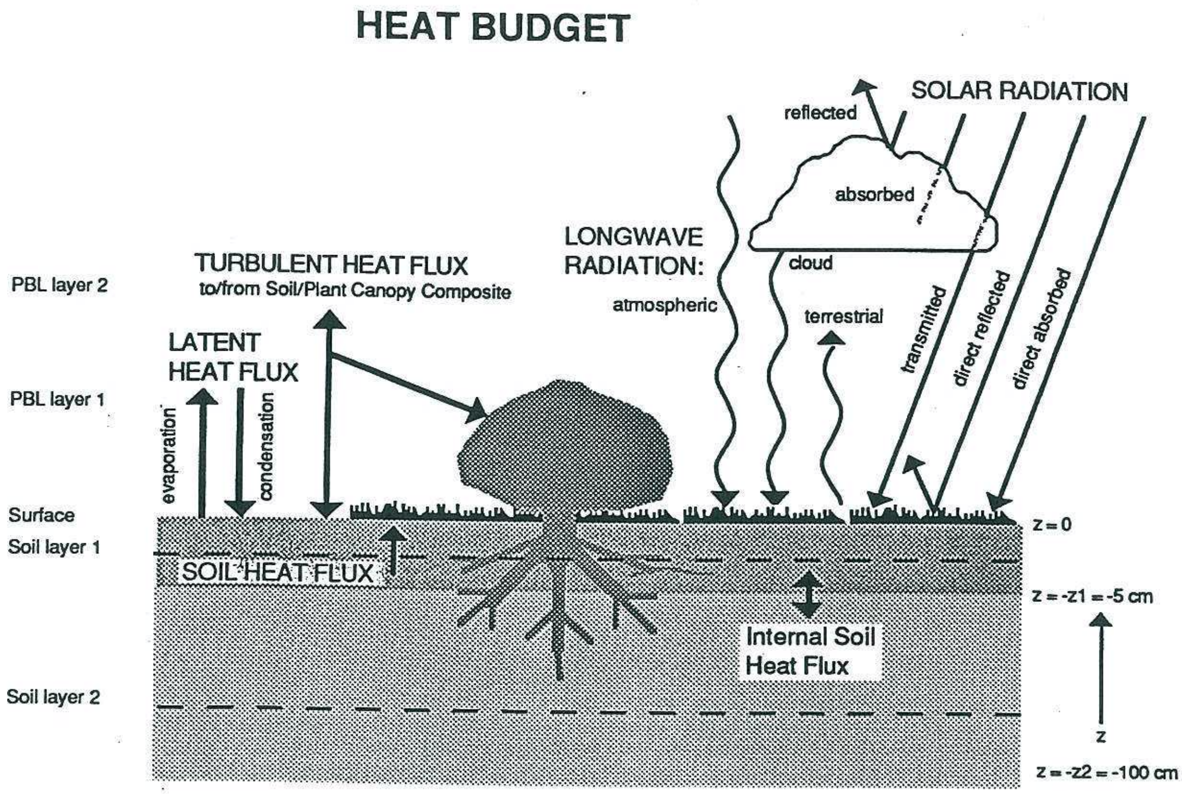

Figure 3. Geometry of the model heat budget. Terms in UPPERCASE letters represent terms of the surface energy balance. Arrows indicate fluxes computed by the model; dashed lines indicate the mid-level of each soil layer which is the location of the computed soil temperatures (T1 at -2.5 cm and T2 at -52.5 cm).

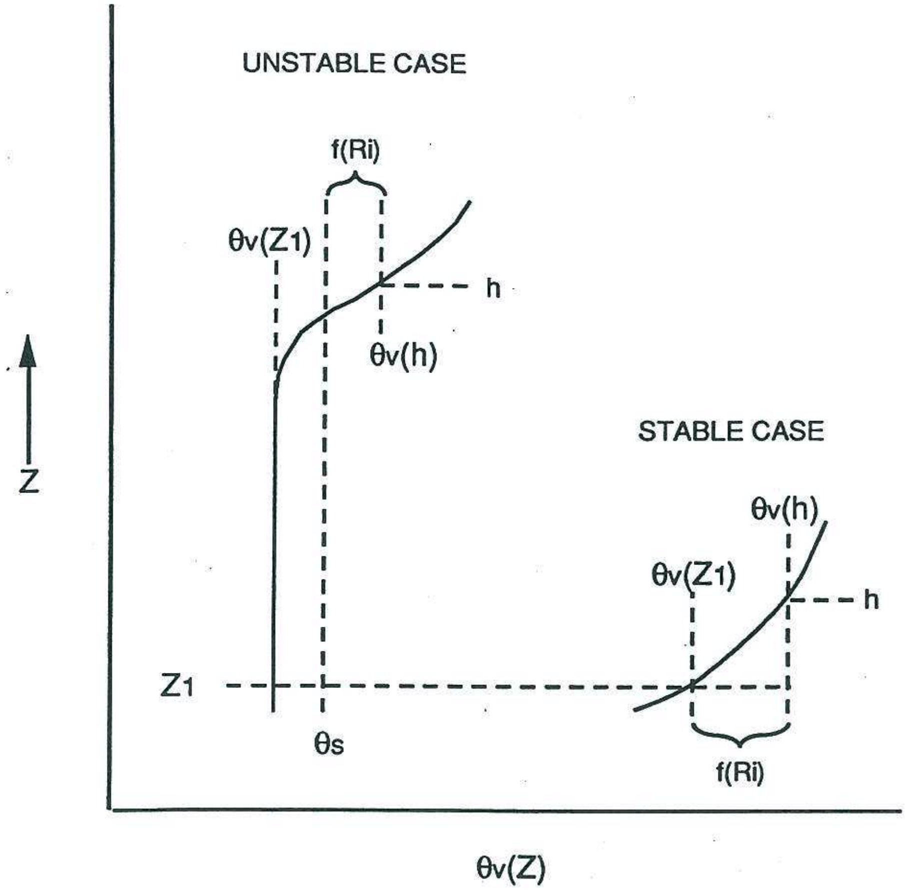

Figure 4. Determining the boundary-layer height in OSU1DPBL for unstable and stable cases. Z is height; $\theta_v(Z)$ is the virtual potential temperature at a given height, $\theta_v(Z_1)$ is the virtual potential temperature at the first model level, θ_s is the surface temperature as determined from the surface energy balance, h is boundary-layer top, $\theta_v(h)$ is the virtual potential temperature at the boundary-layer top, and f(Ri) refers to a function of the layer Richardson number.

Fractional Cloud Cover =
f(maximum RH in PBL, σ_{RH} at that level)

- determine level of maximum RH in PBL
- determine moisture flux at that level
- determine σ_w at that level

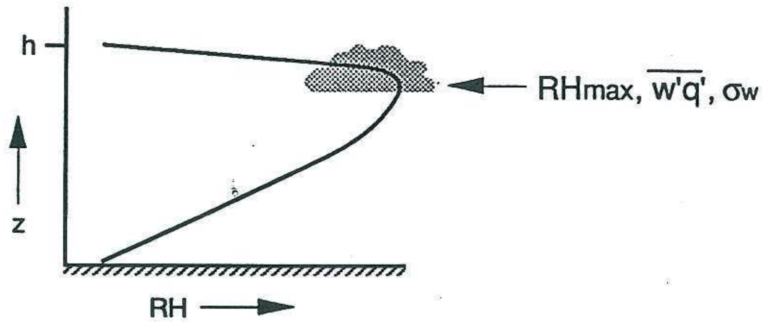

→ unstable conditions: $\sigma_w = fct(z/h, w^*, u^*)$

→ stable conditions: $\sigma_w = fct(z/h, u^*)$

- $\sigma_{RHturb} = a + b * f(\overline{w'q'}, \sigma_w, q_{sat})$

- $\sigma_{RHmeso} = c + d * f(\Delta x)$, where Δx is the horizontal grid size

- $\sigma_{RH} = [(\sigma_{RH\text{-}turb})^{**}2 + (\sigma_{RH\text{-}meso})^{**}2]^{**}0.5$

- Fractional Cloud Cover determined from normal distribution of RH: (use polynomial fit of normal distribution for analytical calculation of cloud cover)

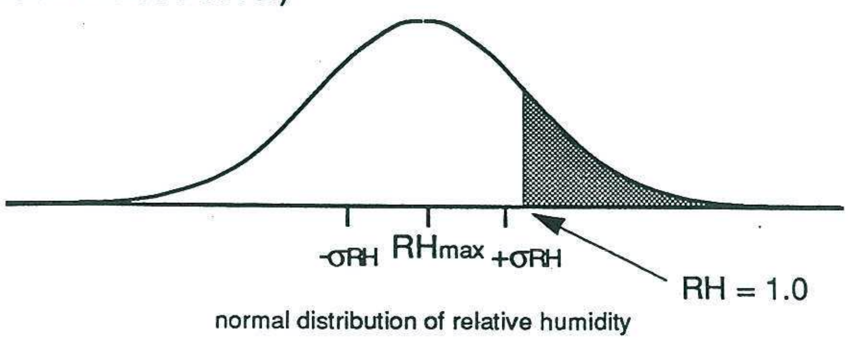

Figure 5. Steps in determining fractional boundary-layer cloud cover.

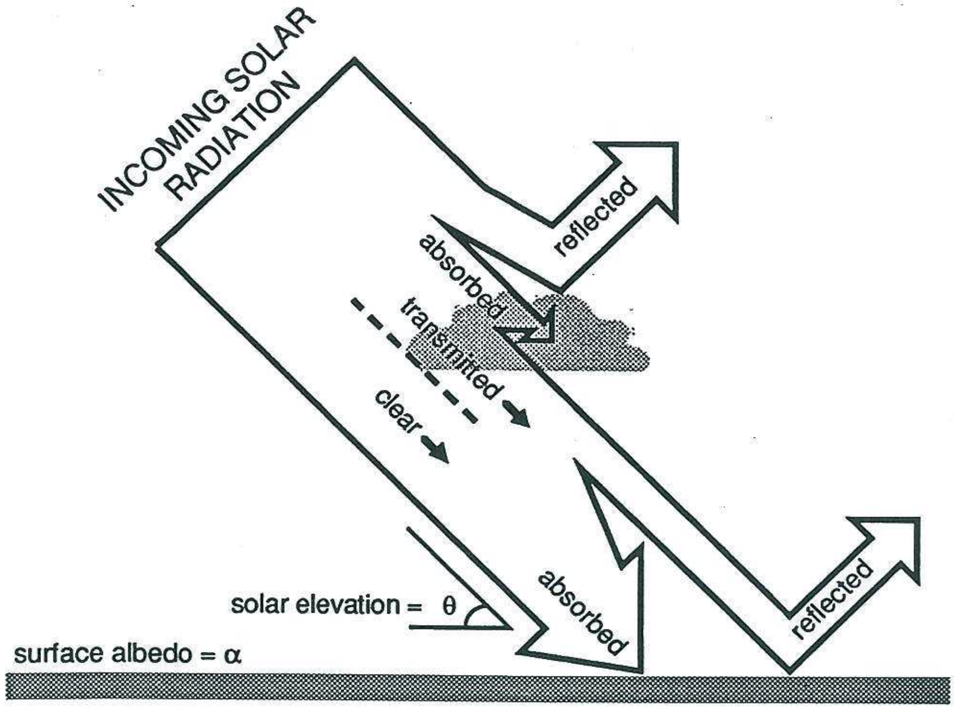

INCOMING SOLAR RADIATION = CLEAR

Fractional coud cover = CLC

Fraction of solar radiation transmitted through clouds =
$TRANSM = 0.06 + 0.17 \sin \theta$

Fraction of solar radiation reflected/absorbed by clouds =
$OPAQUE = 1 - TRANSM$

Solar radiation below cloud level =
$SOLAR = CLEAR\ (1 - CLC * OPAQUE)$

Solar radiation absorbed at surface = $(1 - \alpha)$ SOLAR

Figure 6. Incoming solar radiation interaction with cloud cover and the terms used in the calculation of the net solar radiation.

2.4 OSU1DPBL Model Flowchart

For a quick understanding of the model code the table below lists important variables from the equations described in section 2.1 and their location in the model code, followed by a generalized flowchart of the model.

Equation in section 2.1	Variables	Subroutine	Symbol in Code	Key lines in code
2.1.1				
1a-c	$\partial(\mathbf{v},\theta,q)/dt$	PBLDRV	UN,VN,RN,QN	1233-1236 1478-1481
2	γ_θ	PBLL	CGH	6661-6669
3-4	w_s	PBLL	WSC	6659
5-6	K_m, K_h	PBLL	PBLK	6828-6893
7	Pr^{-1}	PBLL	PRINV	6647-7165
8	z_i	PBLL	HPBL	6598-6698
9	θ^*_{ov}	PBLL	TLV	6657-6701
10a-b	ϕ_m, ϕ_h	PBLL	PHIM	6827-6857
2.1.2				
11a-11c	as in 5-6			
12a	l_h	PBLL	XLH	6803-6823
12b	Pr	PBLL	PRDT	6810-6813
13a-b,14	$l_m, l_h, l_{0,m}$	PBLL	XLH	6803-6823
2.1.3				
15	$l_{0,h}$	PBLL	XLHL	6803-6823
2.1.4				
16a-c	$u^*, (w'\theta')_s, (w'q')_s$	PBLL	USTAR,HEAT,EVAP	6554-6564
17a-b	C_m, C_h	SFCXCH	CM,CH	3908-3998
18-19	F1,F2	SFCXCH	implicit	3908-3998
20	Ri_B	SFCXCH	RIB	3936
21	L	PBLL	XL	6570-6574
22-23	as in 5-6			

Equation in section 2.1	Variables	Subroutine	Symbol in Code	Key lines in code
2.1.3				
24-25	$\partial\Theta/dt$	SRT	RHSTT	3374-3394
26	E_{dir}	SEDIR	EDIR	3223
27	E_c	SEC	EC	3306
28	dC^*/dt	SRC	RHSCT	3433
29	E_t	SET	ET	3096,3270
30	$g(\Theta)$	SET	GX	3261-3267
31	E	SMFLX	EVAP	3106
32	q_s	SFLX	Q1	1890,2189
33-34	$C(\Theta)\partial T/\partial t$	HRT	RHSTS	2891,2912
35a-b	G	HFLX	S	2819
2.1.4				
36	θ_s	SHFLX	TS	2788
37	H	PBLL	HEAT	6558
38-40	E_p	SFLX	EP	2041
2.1.5				
41	CLC	CLOUD	CLC	7505-7654
2.1.6				
42	$S\downarrow, S_{cs}\downarrow$	SUN	SOLAR, CLEAR	7407,7405
43	$L\downarrow$	SUN	TDOWN	7418-7466

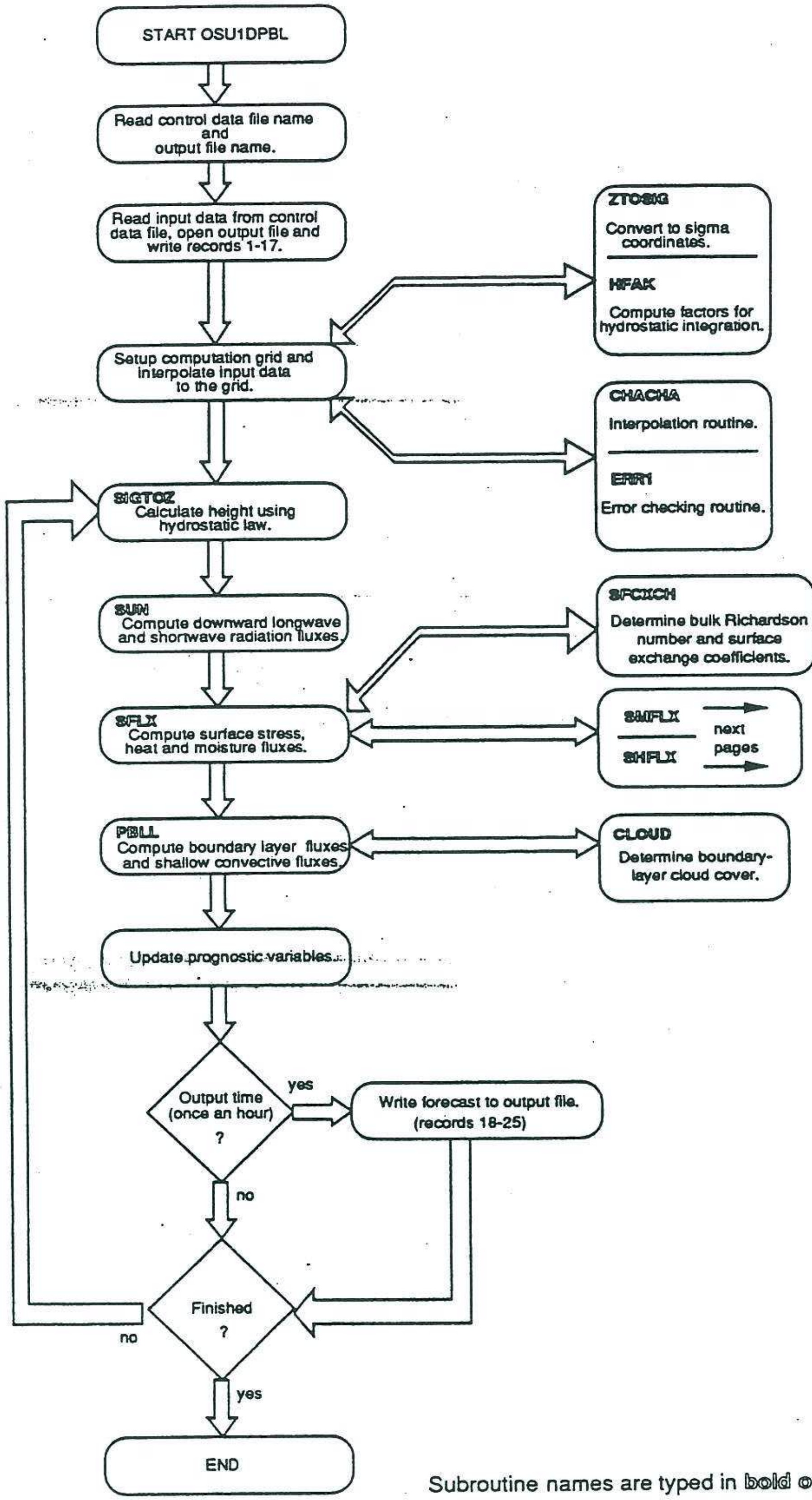

Subroutine names are typed in **bold outline** style

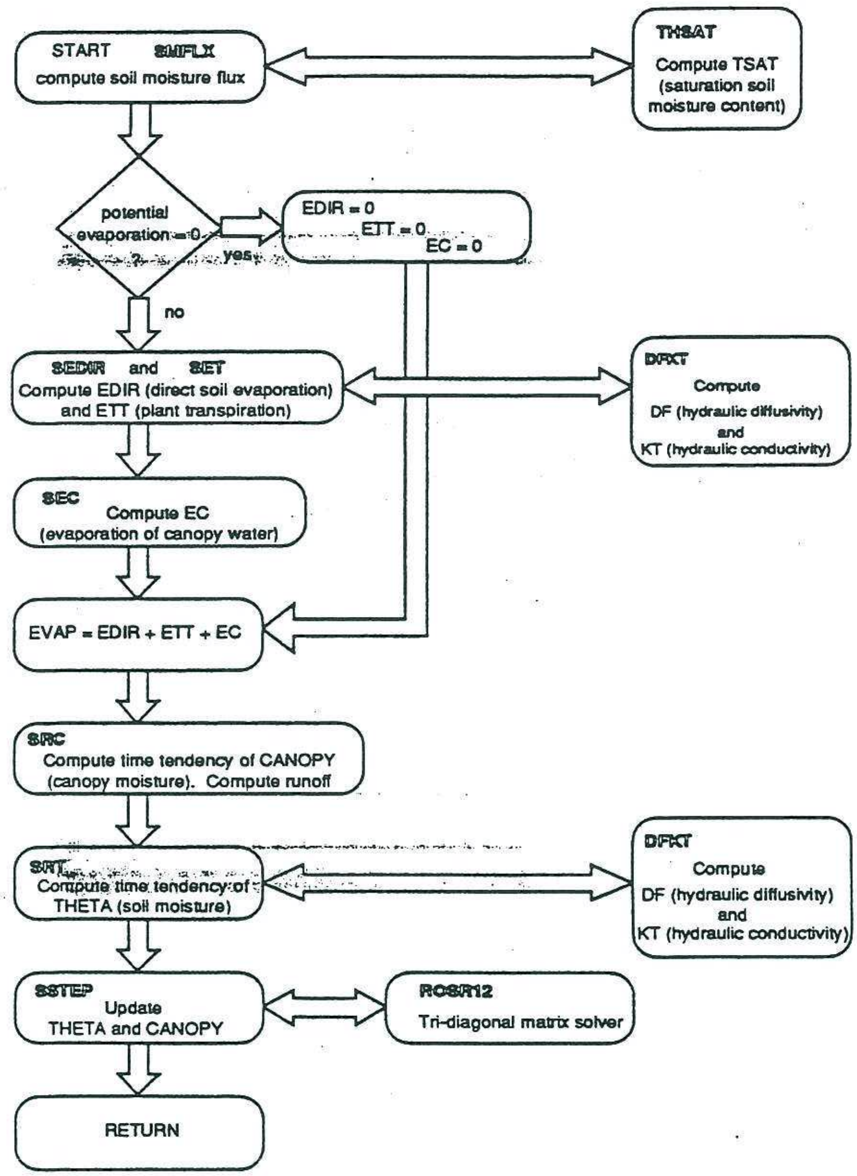
START SMFLX
compute soil moisture flux
THSAT
Compute TSAT
(saturation soil moisture content)
potential evaporation = 0 ?
yes
EDIR = 0
ETT = 0
EC = 0
no
SEDIR and SET
Compute EDIR (direct soil evaporation) and ETT (plant transpiration)
DFKT
Compute
DF (hydraulic diffusivity)
and
KT (hydraulic conductivity)
SEC
Compute EC
(evaporation of canopy water)
EVAP = EDIR + ETT + EC
SRC
Compute time tendency of CANOPY (canopy moisture). Compute runoff
SRT
Compute time tendency of THETA (soil moisture)
DFKT
Compute
DF (hydraulic diffusivity)
and
KT (hydraulic conductivity)
SSTEP
Update
THETA and CANOPY
ROSR12
Tri-diagonal matrix solver
RETURN

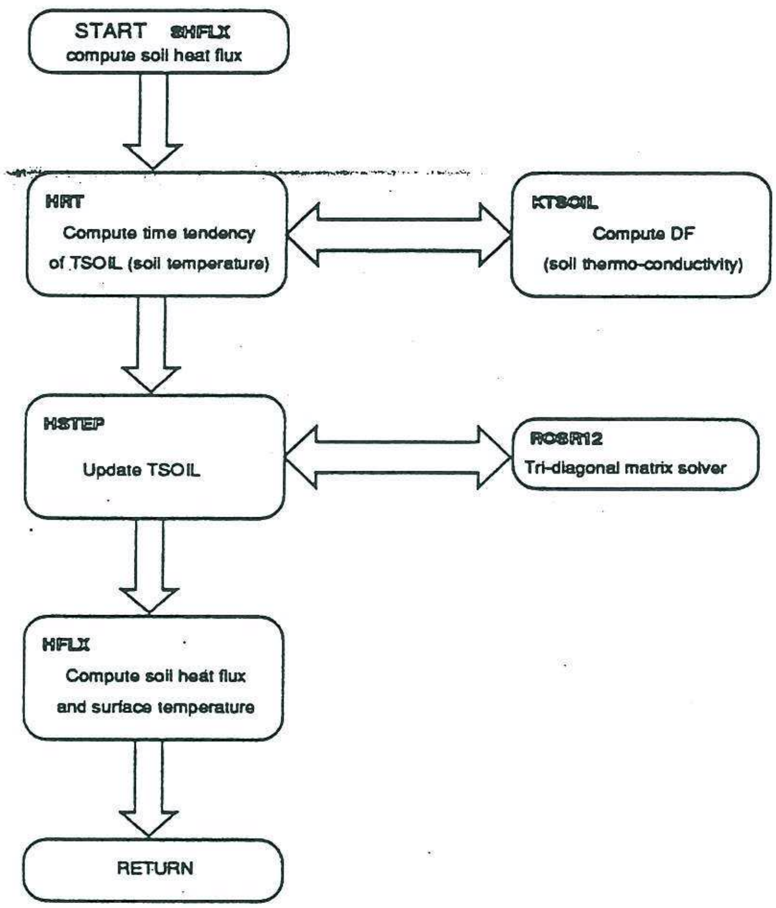
START SHFLX
compute soil heat flux
HRT
Compute time tendency
of TSOIL (soil temperature)
KTSOIL
Compute DF
(soil thermo-conductivity)
HSTEP
Update TSOIL
RCSR12
Tri-diagonal matrix solver
HFLX
Compute soil heat flux
and surface temperature
RETURN

2.5 Finite Differencing Techniques

The OSU1DPBL model employs different schemes for the numerical simulation of each of the different physical processes depending on the stability and other characteristics of the terms being approximated. This section contains a description of (1) the Leap-frog method used for time-stepping in the boundary layer, (2) the fully implicit Crank-Nicholson time integration scheme with the Galerkin technique for atmospheric diffusion, (3) the Crank-Nicholson scheme used for time integration in the soil and plant canopy, and (4) the Euler forward differencing scheme used for diffusion in the soil.

2.5.1 Time-stepping in the boundary layer

To illustrate the method of time-stepping in the boundary layer, we first consider the model equation

$$\frac{\partial \psi}{\partial t} = f(\psi, t) \qquad (1)$$

The implicit Leap-Frog scheme (with centered time differencing) for Eq. 1 would then be

$$\frac{1}{2\Delta t}\left(\psi^{n+1} - \psi^{n-1}\right) = f(\psi^{n+1}, t^{n+1}) + \text{error} \qquad (2)$$

where the error is $O(\Delta t^2)$.

This method is not self-starting. Thus a first step using the Euler forward scheme is needed to start an integration. This scheme has a computational mode and a special procedure is implemented nominally every 25 steps to reduce this instability problem. Once every few Leap-Frog time-integration steps, the Euler forward scheme is used to prevent separation of the two different branches (Fig. 7).

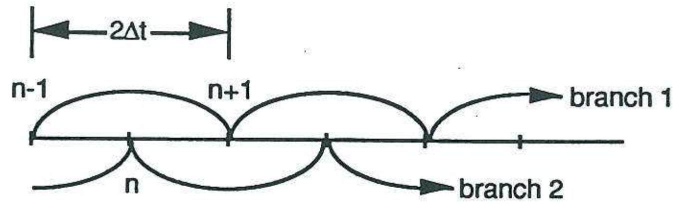

Fig. 7. Grid for the Leap-Frog scheme.

2.5.2 Finite-element formulations for atmospheric diffusion

The diffusion equation for the vertical mixing is given as

$$\frac{\partial u}{\partial t} = \frac{\partial}{\partial z}\left(K\frac{\partial u}{\partial z}\right) \tag{3}$$

where the unknown u can be momentum, potential temperature, moisture, or a (conservative) tracer; t is time; z is the vertical coordinate; and the coefficient of diffusivity K is a function of stability. The fully implicit Cranck-Nicholson scheme (Marchuk, 1974) is selected for time integration; the solution follows closely the procedure in Ahlberg et al. (1967).

The method proceeds as follows. The finite difference form of the diffusion equation (Eq. 3) is

$$\frac{u^{+} - u^{-}}{2\Delta t} = \frac{\partial}{\partial z}\left(K\frac{\partial u^{+}}{\partial z}\right) \tag{4}$$

where the superscripts + and − denote time level $t+\Delta t$ and $t-\Delta t$, respectively. We now put the equation in the form of the Sturm-Liouville equations where

$$-2\Delta t\frac{\partial}{\partial z}\left(K\frac{\partial u^{+}}{\partial z}\right) + u^{+} = u^{-} \tag{5}$$

We next expand the variables u^{+} and u^{-} into an element series of a modified Chapeau basis function $\phi_{i,j}$ for which

$$u^+ = \sum U^+_{j,i} \ \phi_{j,i} \tag{6a}$$

$$u^- = \sum U^-_{j,i} \ \phi_{j,i} \tag{6b}$$

where j=1,J indicate the basis sets defined for each layer $[z_i, z_{i+1}]$ and $\phi_{i,j}$ is nonzero only in the domain $[z_i, z_{i+1}]$. The summation index (j) runs from 1 to 2 for linear elements since there are only two nonzero elements over each interval. The linear elements are defined as

$$\phi_{i,1} = \frac{z_{i+1} - z}{z_{i+1} - z_i},$$

$$\phi_{i,2} = \frac{z - z_i}{z_{i+1} - z_i}$$

where the superscript denotes the interval over which the element function is to be applied (Figure 8).

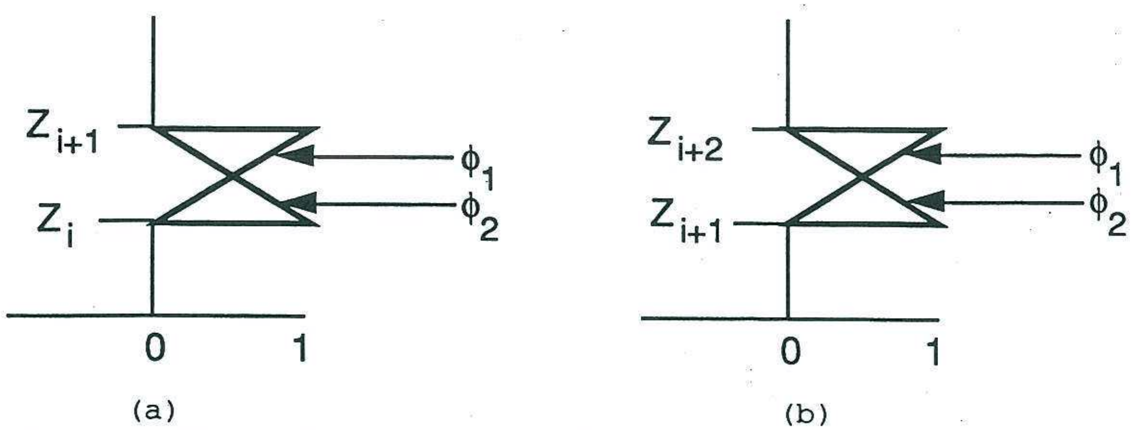

Figure 8. Basis function used in OSU1DPBL vertical diffusion scheme for the domain (a) z_i to z_{i+1} and (b) z_{i+1} to z_{i+2}.

We substitute Eqs. 6a-b into Eq. 5 to form

$$-2\Delta t \frac{\partial}{\partial z}\left(K \frac{\partial}{\partial z}\left(\sum U^+_{j,i} \ \phi_{j,i}\right)\right) + \sum U^+_{j,i} \ \phi_{j,i} = \sum U^-_{j,i} \ \phi_{j,i} \tag{7}$$

Applying the Galerkin criterion, we multiply Eq. 7 by the element of the basis function and integrate to produce

$$-\int_{z_i}^{z_{i+1}} \phi_{i,j} 2\Delta t \frac{\partial}{\partial z}\left(K\frac{\partial}{\partial z}\left(\sum U^+_{j,i}\ \phi_{j,i}\right)dz + \int_{z_i}^{z_{i+1}} \phi_{i,j} \sum U^+_{j,i}\ \phi_{j,i} dz\right.$$

$$= \int_{z_i}^{z_{i+1}} \phi_{i,j} \sum U^-_{j,i}\ \phi_{j,i} dz \qquad (8)$$

Integration by parts yields

$$\int_{z_i}^{z_{i+1}} (2\Delta t) K \frac{\partial}{\partial z}\left(\sum U^+_{j,i}\ \phi_{j,i}\right)\frac{\partial \phi_{i,j}}{\partial z} dz + \int_{z_i}^{z_{i+1}} \phi_{i,j}\left(\sum U^+_{j,i}\ \phi_{j,i}\right)dz =$$

$$\int_{z_i}^{z_{i+1}} \phi_{i,j} \sum U^-_{j,i}\ \phi_{j,i} dz + \int_{z_i}^{z_{i+1}} (2\Delta t) \frac{\partial}{\partial z}\left(\phi_{i,j} K \frac{\partial}{\partial z}\left(\sum U^+_{j,i}\ \phi_{j,i}\right)\right)dz$$

where the second term on the right-hand side is the boundary-flux term and makes the application of the Neumann boundary conditions a natural procedure. Further,

$$(2\Delta t)\sum_{j=1}^{2} U^+_j \int_{z_i}^{z_{i+1}} K \frac{\partial \phi_{j,i}}{\partial z}\frac{\partial \phi_{i,j}}{\partial z} dz + \sum_{j=1}^{2} U^+_j \int_{z_i}^{z_{i+1}} \phi_{j,i}\phi_{i,j} dz =$$

$$\sum_{j=1}^{2} U^-_j \int_{z_i}^{z_{i+1}} \phi_{j,i}\phi_{i,j} dz - (2\Delta t)(\phi_{i,j}(z_{i+1})\tau(z_{i+1}) - \phi_{i,j}(z_i)\tau(z_i))$$

where the boundary stress at nodes z_i and z_{i+1} are explicitly included as τ. Labelling the vertical coordinate of the grid as z_1, z_2, ..., z_n, we will apply the integration over the interval $[z_i, z_{i+1}]$. Only nonzero terms appear in the equations for i and i+1. For i

$$(2\Delta t)\left(\frac{U^+_i}{\Delta z^2}\int_{z_i}^{z_{i+1}} K dz - \frac{U^+_{i+1}}{\Delta z^2}\int_{z_i}^{z_{i+1}} K dz\right) + \frac{\Delta z}{3}U^+_i + \frac{\Delta z}{6}U^+_{i+1} =$$

$$\frac{\Delta z}{3}U^-_i + \frac{\Delta z}{6}U^-_{i+1} + (2\Delta t)\tau(z_i) \qquad (9)$$

where

$$\Delta z = z_{i+1} - z_i$$

while the equation i+1 is:

$$(2\Delta t)\left(-\frac{U_i^+}{\Delta z^2}\int_{z_i}^{z_{i+1}} K dz + \frac{U_{i+1}^+}{\Delta z^2}\int_{z_i}^{z_{i+1}} K dz\right) + \frac{\Delta z}{6}U_i^+ + \frac{\Delta z}{3}U_{i+1}^+ =$$

$$\frac{\Delta z}{6}U_i^- + \frac{\Delta z}{3}U_{i+1}^- - (2\Delta t)\tau(z_{i+1}) \quad (10)$$

Our philosophy has been to transform u in terms of the basis set (modified Chapeau) with the U coefficients substituted into the equation of motion. We will now solve for U using matrix representation and construct the total variable from summing the basis set. In anticipation of a matrix representation of these equations, we will define the following:

$$B_{i,i} = \frac{2\Delta t}{\Delta z^2}\int_{z_i}^{z_{i+1}} K dz,$$

$$B_{i,i+1} = \frac{-2\Delta t}{\Delta z^2}\int_{z_i}^{z_{i+1}} K dz,$$

$$A_{i,i} = \frac{\Delta z_i}{3},$$

$$A_{i,i+1} = \frac{\Delta z_i}{6}, \text{ and}$$

$$\tau_i = \tau(z_i).$$

Eq. 9 now becomes

$$(B_{i,i}+A_{i,i})U_i^+ + (B_{i,i+1}+A_{i,i+1})U_{i+1}^+ = A_{i,i}U_i^- + A_{i,i+1}U_{i+1}^- + (2\Delta t)\tau_i$$

Similarly, Eq. 10 becomes

$$(B_{i,i+1}+A_{i,i+1})U_i^+ + (B_{i,i}+A_{i,i})U_{i+1}^+ = A_{i,i+1}U_i^- + A_{i,i}U_{i+1}^- - (2\Delta t)\tau_{i+1}$$

Adding the second equation for interval $[z_i, z_{i+1}]$ and the first equation for $[z_{i+1}, z_{i+2}]$, we can cancel the internal stress term to close the equation set and obtain

$$(B_{i,i+1} + A_{i,i+1})U_i^+ + (B_{i,i} + B_{i+1,i+1} + A_{i,i} + A_{i+1,i+1})U_{i+1}^+ + (B_{i+1,i+2} + A_{i+1,i+2})U_{i+2}^+ = A_{i,i+1}U_i^- + (A_{i,i} + A_{i+1,i+1})U_{i+1}^- + A_{i+1,i+2}U_{i+2}^-$$

We will define another set of new variables to further simplify the notation

$$A'_{i,i} = (A_{i,i-1} + A_{i,i+1})$$

$$A'_{i,i+1} = A_{i,i+1} = \frac{\Delta z_i}{6}$$

$$A'_{i+1,i} = A'_{i,i+1}$$

$$B'_{i,i} = B_{i-1,i-1} + B_{i,i} = -B'_{i,i-1} - B'_{i,i+1}$$

$$B'_{i,i+1} = B_{i,i+1} = -\frac{(2\Delta t)}{\Delta z_i^2}\int_{z_i}^{z_{i+1}} K dz$$

$$B'_{i+1,i} = B'_{i,i+1}$$

We now obtain the matrix equation representation

$$(B' + A')\, U^+ = A'\, U^- + \begin{bmatrix} 2\Delta t \tau_1 \\ 0 \\ 0 \\ . \\ . \\ 0 \\ -2\Delta t \tau_N \end{bmatrix}$$

provided we define the coefficients in the first and the last row as

$$A'_{1,1} = \frac{\Delta z_1}{3}$$

$$A'_{1,2} = \frac{\Delta z_1}{6},$$

$$A'_{N-1,N} = \frac{\Delta z_{N-1}}{6}$$

$$A'_{N,N} = \frac{\Delta z_{N-1}}{3}$$

$$B'_{1,1} = \frac{2\Delta t}{\Delta z_1^2}\int_{z_1}^{z_2} K dz$$

$$B'_{1,2} = -B'_{1,1}$$

$$B'_{N,N} = \frac{2\Delta t}{\Delta z_{N-1}^2}\int_{z_{N-1}}^{z_N} K dz$$

$$B'_{N-1,N} = B'_{N,N}$$

Standard methods can now be applied to solve the tridiagonal matrix equation to obtain the updated values of u.

Application of the Technique for Minimally Diagnosed Boundary Layer

No special modification of the above methodology is required when the boundary layer is at its minimum allowable depth in the OSU1DPBL model (h = the first model level above the surface). The diffusivity profile theoretically vanishes at z = h. In practice, however, K is calculated at intermediate levels and the vertical flux divergence is calculated at the prognostic levels. This is ensured provided that the diffusivity calculation recognizes that the boundary layer is a constant flux layer, with zero diffusion above. Hence the flux divergence is nonzero at the boundary-layer top when the boundary layer is at its minimum allowable depth.

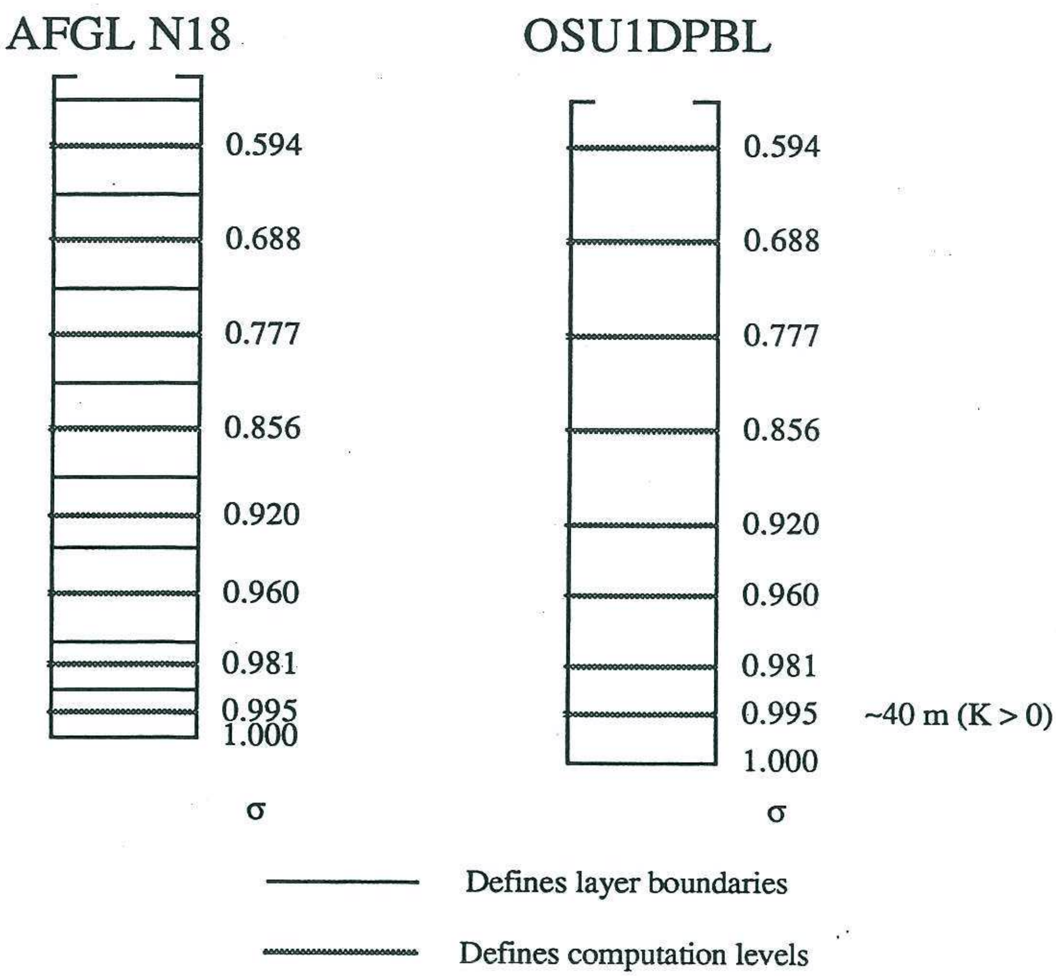

The figure above shows the vertical staggering of the grid for A18 resolution in the AFGL GSM and OSU1DPBL. Note that the computational levels match in sigma coordinates although the GSM uses explicit vertical staggering. OSU1DPBL calculates u, v, θ, and q at the computation levels and K and $\partial/\partial z[u,v,\theta,q]$ at the layer boundaries (between computational levels).

2.5.3 Time-stepping in the soil and plant canopy

The Crank-Nicholson time integrator is also called the Trapezoidal approximation (Figure 9). It is devised as a "better than Euler" scheme because it is a combination of the Euler forward and Euler backward schemes. Using Eq. 1 to illustrate the method, the Euler forward scheme would be

$$\frac{1}{\Delta t}(\psi^{n+1} - \psi^{n}) = f(\psi^{n}, t^{n}) + \frac{1}{2}(\Delta t)\ \psi'' + \text{Error} \qquad (11)$$

The Euler Backward scheme for Eq. 1 would be

$$\frac{1}{\Delta t}(\psi^{n+1} - \psi^{n}) = f(\psi^{n+1}, t^{n+1}) - \frac{1}{2}(\Delta t)\ \psi'' + \text{Error} \qquad (12)$$

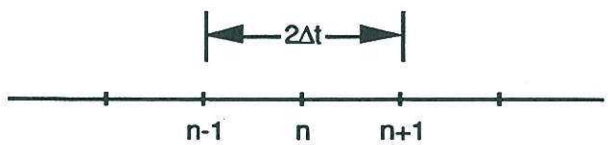

Fig. 9. The grid for the trapezoidal scheme.

The Euler forward scheme overdamps the solution while the Euler backward scheme underdamps it. This observation gives rise to the Crank-Nicholson scheme which can be viewed as an average of the two schemes shown above. The Crank-Nicholson scheme for Eq. 1 would be

$$\frac{1}{\Delta t}(\psi^{n+1} - \psi^{n}) = \frac{1}{2}[f(\psi^{n+1}, t^{n+1}) + f(\psi^{n}, t^{n})] + \text{Error} \qquad (13)$$

A few comments about the scheme are in order here. The Euler forward scheme and the Euler backward scheme are globally accurate to $O(\Delta t^1)$; the Crank-Nicholson scheme is accurate to $O(\Delta t^2)$. The Crank-Nicholson scheme is also absolutely stable with no computational mode and with slight to moderate phase retardation (see Baer and Simons (1970) for a good graphical representation).

2.5.4 Finite differencing in the soil layer

The vertical flux of water at the interface between the two soil layers is computed from the gradient between the midlevels of the two soil layers, and from the hydraulic diffusivity and conductivity evaluated from the soil moisture content of the wetter of the two soil layers. The latter "upstream" diffusivity is invoked because wetting fronts seem to propagate vertically and are based on the hydraulic properties in the wetter soil behind the front. When compared to high resolution models, this procedure reduces truncation errors as effectively as does employing the more complicated finite element approximation. It is also used to determine the soil heat flux.

At the bottom of the model, the hydraulic diffusivity is assumed to be zero so that the soil water flux is due only to the gravitational term $K(\theta)$. The soil heat flux is computed in terms of a vertical temperature gradient determined using a specified temperature at an imaginary level 1 meter below the bottom of the model.

2.6 Modelling the Snow Cover

The OSU1DPBL combined boundary-layer and soil model was originally developed in an effort to parameterize boundary-layer heat and moisture transport for a global forecast model (Brenner et al., 1984). In order to implement the boundary-layer package in a global model, or as a stand-alone model, it is necessary to include the effects of snow cover (Tuccillo, 1987).

Snow cover serves as the upper boundary of the earth's surface, thereby affecting the boundary layer as well as the soil. Although snow cover reduces the available energy at the surface because of its high albedo for solar radiation and high emissivity in the spectral range of most terrestrial radiation, its insulative properties greatly reduce heat loss from the soil (Gray and Male, 1981). The thermal conductivity of new snow is roughly an order of magnitude less than that of most soils. As snow "ages", its albedo decreases while its thermal conductivity increases which generally remains less than that of moist soil.

The nocturnal cooling which is usually balanced by the soil heat flux (Oke, 1978) may lead to much cooler surface temperatures in the presence of snow. Siberia, northwestern North America, and Antarctica are among the regions where intense radiative cooling occurs which causes the formation of air masses characterized by very low surface temperature and strong surface inversions.

In its present stage, the model does not predict precipitation; rather precipitation is specified as an input to the model. We categorize fallen precipitation as snow when both the temperature at 850 mb is below 0°C and the dew point temperature at the first model level above the surface is below 0°C. The first step in the model is to make an estimate of the heat flux between the soil and the snow by using the relationship

$$G = \kappa_s \frac{T_s - T_{soil}}{h_s} \qquad (1)$$

where k_s is the thermal diffusivity for snow, T_s is the "skin" temperature, T_{soil} is the top-layer soil temperature (in the present model, the top layer is 5 cm thick), and h_s is the depth of the snow layer (assumed to be ten times the water-equivalent snow depth).

The thermal diffusivity for snow depends on the porosity of snow. It can vary from 0.063 W K^{-1} m^{-1} for new snow with a porosity of 0.95, to 0.71 W K^{-1} m^{-1} for packed snow with porosity of 0.5 (comparable to clay). Unless we try to resolve the snow surface into many layers and monitor the "age" of each layer, we cannot model the porosity of the snow pack. Here, we choose the value of 0.13 W K^{-1} m^{-1} for k_s which corresponds to a porosity of 0.8. The soil-surface temperature is assumed to be the same as the top-layer averaged soil temperature. This assumption is supported by observations that the largest thermal gradient below the snow surface is near the top of the snow layer due to weak thermal diffusion within the snow layer (Oke, 1978). When snow falls over warm soil, the snow heat flux may lead to snow melt.

The calculation of the snow heat flux enables one to calculate the potential evaporation E_p using the surface energy balance

$$(1-\alpha)S\downarrow + L\downarrow - \sigma T'^4 = G + \rho_0 c_p C_h |\mathbf{v}|(T'-T_0) + LE_p \quad (2)$$

where

$$E_p = \rho_0 C_h |\mathbf{v}|(q_s(T')-q_0) \quad (3)$$

The albedo (α) is assigned a constant value of 0.7; the normal change of snow albedo with age of snow pack is not included. The terms on the left-hand side of (2) are the downward short- and longwave radiative flux and the upward longwave radiative flux. The terms on the right-hand side are the snow, sensible, and latent heat fluxes. The skin temperature T' is the temperature of the surface if the snow surface is evaporating at the potential rate. While the units of E_p in the surface energy balance are kg m^{-2} s^{-1}, typical soil hydrological applications use the units m s^{-1}. The conversion is accomplished using the density of water (r_w = 10^3 kg m^{-3}). This formula is most appropriate for melted water in the snow. Otherwise, C_h describes sublimation which may depend primarily on solar radiation and snow temperature.

The snow evaporates/sublimates at the following rate

$$E = \begin{bmatrix} E_p, & h_s \geq E_p\Delta t \\ \frac{h_s}{\Delta t}, & h_s < E_p\Delta t \end{bmatrix} \quad (4)$$

where E is in m s^{-1}. When the depth of the snow layer is thick, it will evaporate at the potential rate for an entire time step. When the snow layer is thin so that it cannot maintain the potential rate, we assume the snow to evaporate evenly and completely over the time interval Δt.

When the evaporation rate E is determined, the skin temperature T_s is calculated by solving the surface energy balance (Eq. 2) again

$$(1-\alpha)S\downarrow + L\downarrow - \sigma T_s^4 = D_s\frac{T_s-T_{soil}}{h_s} + \rho_0 c_p C_h |\mathbf{v}|(T_s-T_0) + LE \quad (5)$$

where T_s recognizes evaporation/sublimation of the snow from Eq. 4. If the resulting skin temperature is above the melting point of snow (T_c = 273.16 K), the amount of snow melt h_m is calculated as follows

$$(1-\alpha)S\downarrow + L\downarrow - \sigma T_c^4 = D_s \frac{T_c - T_{soil}}{h_s} + \rho_0 c_p C_h |\mathbf{v}| (T_c - T_0) + LE + L_i h_m \quad (6)$$

where L_i is the latent heat of fusion and T_c is the snow temperature which recognizes both evaporation/sublimation, and melting of snow.

In the model, it is arbitrarily assumed that when precipitation falls, it has the same temperature as that of the lowest atmospheric model layer. Conversion of warm rain to ice or snow may be an important process during warm front passages and is included in the model. Excess snow melt from Eq. 6 is allowed to drip into the top soil layer. Soil temperature is updated by accounting for heat flux (G) across the snow-soil interface.

2.7 Radiation Richardson Number

The radiation Richardson number was developed by Mahrt and Ek (1984) in a study which examined the relationship between atmospheric stability and potential evaporation. Although not widely used heretofore, the radiation Richardson number is appealing in that it does not rely on estimates of fluxes to estimate low-level stability; rather, the sensible heat flux is treated as a residual from the surface energy balance. The radiation Richardson number (Ri_{rad}) is defined as

$$Ri_{rad} \equiv -\frac{g}{\theta} \frac{(R_n + Q_G)\, z}{u^3} \quad (1)$$

where θ is the mean potential temperature, u is a velocity scale, z is the height of the wind speed observation, g is the gravitational acceleration, R_n is the net radiation (defined as positive upwards), and Q_G is the heat flux (to the soil). The radiation Richardson number has been used by Ken Mitchell to compare model predictions with observations where the surface flux information is not available.

The flux Richardson number is

$$Ri_f \equiv \frac{\frac{g}{\theta}\,\overline{w'\theta'}}{\frac{\partial \overline{V}}{\partial z}\,\overline{w'V'}} \tag{2}$$

with the surface heat flux

$$Q_H = R_n - Q_G \approx \overline{w'\theta'} \tag{3}$$

Typically the radiation Richardson number will have the same sign as other formulations of the Richardson number (such as the flux form above or the low-level bulk form, both of which are available in the model as RIF and RIB, respectively). The range for Ri_{rad} has been seen to have slightly larger magnitudes, in part due to the role of the soil heat flux. There is no special significance in terms of a known critical radiation Richardson number (of 0.25, for example), and no direct comparisons of the magnitude of Ri_{rad} to the other forms should be attempted.

A regression relationship between Ri_{rad} and z/L (Mahrt and Ek, 1984) can be used to estimate Ri_f for comparison with the model prediction of Ri_f. The cube root of z/L is correlated to $(Ri_{rad})^{1/3}$ with a correlation coefficient of 0.90 in the unstable case and 0.77 in the stable case. The regression relationship for the unstable case is

$$\left(\frac{z}{L}\right)^{1/3} = -8.64\,(Ri_{rad})^{1/3} - 0.09 \tag{4}$$

and for the stable case

$$\left(\frac{z}{L}\right)^{1/3} = -15.29\,(Ri_{rad})^{1/3} - 0.13 \tag{5}$$

Both relationships predict that z/L approaches $\sim -10^{-3}$ as the net radiation vanishes. This small constant has no special significance for the near neutral case but rather improves the fit over the range of the values of the radiation Richardson number. A higher order model is not justified because of the very approximate nature of this development.

2.8 Stable Boundary Layer

By itself, the usual similarity theory for the stable boundary layer leads to a significant overestimation of surface cooling. This is due to (a) failure to consider subgrid-scale spatial variability where vertical fluxes can occur in part of the grid even with large Richardson number based on grid averaged variables (Mahrt, 1987), (b) poor vertical resolution where turbulence may occur in thinner layers, perhaps intermittently, even when the Richardson number over the model layer is large, (c) neglect of clear air radiative cooling, (d) neglect of gravity wave momentum transport, and (e) use of a temperature from the surface energy balance (instead of temperature at z_0) to compute the surface-layer Richardson number.

To compensate for such inadequacies, various mechanisms have been employed (often unreported) which include capping the allowable value of the Richardson number or specifying a minimum wind speed. We use the area-averaged exchange coefficient relationship of Mahrt (1987) where the exchange coefficient for momentum is proportional to $\exp(-Ri_{bulk})$ with the Kondo et al. (1978) modification to the nondimensional gradients.

The above modifications lead to significant improvements of model performance in the nocturnal boundary layer (Ruscher, 1987). However, a future rederivation may include explicit dependence on (a) vertical resolution, (b) wind speed, and (c) subgrid characteristics such as standard deviation of subgrid terrain height (surface inhomogeneity).

2.9 Potential Evaporation and Surface Temperature

2.9.1 Potential Evaporation

The potential evaporation is used to compute the actual evaporation in the model. The derivation of potential evaporation closely follows Mahrt and Ek (1984). Many terms not defined in this section are found in section 2.1. The usual Penman relationship is modified since the surface temperature is needed to compute the net radiation. As a first step, we evaluate the surface energy balance for the reference state of a saturated surface.

$$(1-\alpha)S\downarrow + L\downarrow - \sigma\theta_s^4 = G + H' + L_vE_p \tag{1}$$

where $(1-\alpha)S\downarrow + L\downarrow$ is the total downward radiation, the upward longwave radiation, $\sigma\theta_s{}^4$, is linearized as

$$\sigma\theta_s^4 \approx \sigma T_0^4 \left(1 + 4\left(\frac{\theta_s - T_0}{T_0}\right)\right)$$

G is the soil heat flux, the sensible heat flux which uses a saturated surface temperature appropriate for the potential evaporation and is defined as

$$\begin{aligned} H' &= \rho c_p C_h(\theta_s - \theta_0) \\ &= \rho c_p C_h[(\theta_s - T_0) - (\theta_0 - T_0)] \end{aligned}$$

and L_vE_p is the potential evaporation (L_v is latent heat). θ_s is the surface temperature, and θ_0 and T_0 are the potential and actual temperatures at the first model level, respectively. The surface energy balance may then be rewritten as

$$\begin{aligned} (1-\alpha)S\downarrow + L\downarrow - \sigma T_0^4 - 4\sigma T_0^4\left(\frac{\theta_s - T_0}{T_0}\right) &= \\ G + \rho c_p C_h[(\theta_s - T_0) - (\theta_0 - T_0)] + L_vE_p \end{aligned} \tag{2}$$

Combining terms and solving for L_vE_p

$$\begin{aligned} L_vE_p = (1-\alpha)S\downarrow + L\downarrow - \sigma T_0^4 - G + \rho c_p C_h(\theta_0 - T_0) \\ - (\theta_s - T_0)\left(\frac{4\sigma T_0^4}{T_0} + \rho c_p C_h\right) \end{aligned} \tag{3}$$

The latent heat flux is approximated as

$$
\begin{aligned}
L_vE_p &= \rho L_v C_h\ (q_s^* - q_0) \\
&= \rho L_v C_h\ [(q_s^* - q_0^*) + (q_0^* - q_0)] \\
&= \rho L_v C_h \left[\left(\frac{q_s^* - q_0^*}{\theta_s - T_0}\right)(\theta_s - T_0) + (q_0^* - q_0)\right] \\
&\approx \rho L_v C_h \left[\left(\frac{dq_s}{dT}\right)(\theta_s - T_0) + (q_0^* - q_0)\right]
\end{aligned}
$$

where q_s^* is the surface saturation specific humidity. q_0 and q_0^* are the actual and saturation specific humidities at the first model level, respectively. Solving for $\theta_s - T_0$ from the above expression

$$
\theta_s - T_0 = \frac{\left[\dfrac{L_vE_p}{\rho L_v C_h} - (q_0^* - q_0)\right]}{\left(\dfrac{dq^*}{dT}\right)}
$$

Substituting the above expression for $\theta_s - T_0$ into Eq. 3, noting that $\rho T_0 \approx p_{sfc}/R_d$, and solving for E_p

$$
E_p = \left(\frac{\left[\dfrac{R_n}{\rho c_p C_h} + (\theta_0 - T_0)\right]\Delta + (r + 1)A}{\Delta + r + 1}\right)\frac{\rho c_p C_h}{L_v}
$$

$$
R_n = (1 - \alpha)S\downarrow + L\downarrow - \sigma T_0^4 - G
$$

$$
\Delta = \frac{dq^*}{dT}\frac{L_v}{c_p}
$$

$$
r = \frac{4\sigma T_0^4 R_d}{p_{sfc} c_p C_h}
$$

$$
A = (q_0^* - q_0)\frac{L_v}{c_p}
$$

From the notation in the OSU1DPBL model code,

$$\rho c_p C_h = RCH$$

$$L_v = ELV$$

$$\Delta = DELTA$$

$$r + 1 = RR$$

$$A = A$$

$$\frac{R_n}{\rho c_p C_h} + (\theta_0 - T_0) = RAD$$

We define an expression for potential evaporation used in the model as

$$E_p = \left(\frac{RAD \cdot DELTA + RR \cdot A}{DELTA + RR}\right)\frac{RCH}{ELV}$$

2.9.2 Surface Temperature

To define the surface temperature, θ_s, we start with the surface energy balance similar to Eq. 1 except we use the actual evaporation E instead of the potential E_p. Note that $E = \beta E_p$ where β is a factor multiplied by the potential evaporation to get the actual evaporation. The surface energy balance then becomes

$$(1-\alpha)S\downarrow + L\downarrow - \sigma\theta_s^4 = G + H + \beta L_v E_p$$

Using similar approximations from the previous section, we can rewrite this surface energy balance as

$$(1-\alpha)S\downarrow + L\downarrow - \sigma T_0^4 - 4\sigma T_0^4\left(\frac{\theta_s - T_0}{T_0}\right) =$$

$$G + \rho c_p C_h[(\theta_s - T_0) - (\theta_0 - T_0)] + \beta L_v E_p$$

Noting that

$$F = (1 - \alpha)S\downarrow + L\downarrow$$

$$G = K_T(\Theta)\frac{(\theta_s - T_{1soil})}{\Delta z}$$

where the terms in G are defined in the model physics chapter. Using the definition of r from above, we can now write the surface energy balance as

$$\frac{F - \sigma T_0^4}{\rho c_p C_h} - \frac{K_T(\Theta)(\theta_s - T_{soil})}{\Delta z \rho c_p C_h} = (r + 1)(\theta_s - T_0) - (\theta_0 - T_0) + \frac{\beta L_v E_p}{\rho c_p C_h}$$

Combining terms and solving for θ_s

$$\theta_s = \frac{T_0 + \dfrac{\dfrac{F - \sigma T_0^4}{\rho c_p C_h} + (\theta_0 - T_0) - \dfrac{\beta L_v E_p}{\rho c_p C_h}}{r + 1} + \dfrac{K_T(\Theta) T_{1soil}}{\Delta z \rho c_p C_h (r+1)}}{1 + \dfrac{K_T(\Theta)}{\Delta z \rho c_p C_h (r+1)}}$$

Using the terms in the OSU1DPBL model code noted in the previous section,

$$EPSCA = \frac{L_V E_P}{\rho c_p C_h}$$

$$\Delta z = -0.5 \cdot ZSOIL(1)$$

$$YY = T_0 + \frac{\dfrac{(F - \sigma T_0^4)}{RCH} + (\theta_0 - T_0) - \beta EPSCA}{RR}$$

$$ZZ = \frac{K_T(\Theta)}{\Delta z \cdot RCH \cdot RR}$$

$$ZZ1 = ZZ + 1$$

The surface temperature θ_s is now given by

$$\theta_s = \frac{YY + ZZ \cdot T_{1soil}}{ZZ1}$$

2.10 Canopy Resistance

To account for the reduction in transpiration due to internal plant physiology, OSU1DPBL uses a plant coefficient (PC). The PC is multiplied by the potential evaporation and a value for the soil moisture deficit to obtain plant transpiration. The usual convention in meteorology is to express this reduction in terms of a canopy resistance (RC). The two expressions, PC and RC, can be related to each other by equating the expression for transpiration used in OSU1DPBL and in Monteith (1965). The following relation is obtained for use in the model (Holtslag and Ek, 1990)

$$RC = \frac{\frac{(RR + DELTA)}{PC} - (DELTA + RR)}{RR \cdot CH}$$

For $0 < PC \leq 1$,

$$RR = \frac{4\sigma\ T_0^4\ R_d}{p_{sfc} C_h\ c_p} + 1$$

$$DELTA = \frac{L_v}{c_p}\ \frac{dq_s}{dT}$$

RR and DELTA are dimensionless quantities; σ is the Stefan-Boltzmann constant (5.67×10^{-8} W m^{-2} K^{-4}); T_0 is the air temperature at the first model level; R_d is the gas constant for dry air (287 J kg^{-1} K^{-1}); p_{sfc} is the surface pressure (Pa); CH is the surface exchange coefficient for heat and moisture (m s^{-1}); c_p is the specific heat for dry air (1004.5 J kg^{-1} K^{-1}); L_v is the latent heat of vaporization (2.5×10^6 J kg^{-1}); and dq_s/dT is the slope of the saturation specific humidity curve (K^{-1}).

The user has the choice of specifying either a plant coefficient or a canopy resistance in the OSU1DPBL model.

2.11 Gravity wave drag

The deceleration of the mean flow due to gravity wave stress divergence is written as

$$\left(\frac{\partial U}{\partial t}\right)_w = \frac{1}{\rho}\frac{\partial \tau}{\partial z} \tag{1}$$

where U is the component of the mean wind vector $\mathbf{V}$ parallel to the surface wind vector $\mathbf{V}_0$ determined as

$$U = \frac{\mathbf{V}\cdot\mathbf{V}_0}{|\mathbf{V}_0|} \tag{2}$$

and τ is the wave stress obtained from the velocity perturbation $\tilde{u}$ and $\tilde{w}$ due to wave motion as

$$\tau = -\rho\overline{\tilde{u}\tilde{w}} \tag{3}$$

The wave stress is computed from layer to layer beginning at the model level immediately above the maximum height of the topographic variation (Fig.10). The surface gravity wave stress τ_0 is obtained for a linear sinusoidal gravity wave as

$$\tau_0 = \frac{1}{2}\rho_0 U_0 N_0 k h_0^2 \tag{4}$$

where the subscript $_0$ represents the values at the ground surface assumed as the level of the top of the subgrid-scale topography and k is the horizontal wavenumber of the topography. The amplitude of the gravity wave at the surface, h_0, is determined by the relationship

$$h_0 = \mathbf{min}\left(\eta_0,\ 0.32\frac{U_0}{N_0}\right) \tag{5}$$

where η_0 is the height of the surface topography (Kim and Mahrt, 1991b).

When the incident wave stress (Fig. 1, τ_i) for a model layer exceeds the saturated wave stress τ^* for the layer, wave breaking occurs and the outgoing wave stress from the layer (Fig. 1, τ_{i+1}) is replaced with the (super)saturated wave stress. Otherwise, wave stress is conserved across the layer and the outgoing wave stress τ_{i+1} is the same as the incident wave stress τ_i for the layer.

The (super)saturated wave stress for a layer is given as

$$\tau^* = \frac{1}{2}\rho U N k (h_m\gamma)^2\left(1 + \frac{(h_m\ell_0)^2}{4}\right) \tag{6}$$

where h_m is the surface amplitude of (super)saturated gravity wave, ℓ_0 is the vertical wavenumber at the surface given as

$$\ell_0 = \frac{U_0}{N_0} \tag{7}$$

and γ is defined as

$$\gamma = \left(\frac{\rho_0 U_0 N_0}{\rho U N}\right)^{1/2}. \tag{8}$$

The surface amplitude of the (super)saturated wave for a layer at height z can be obtained as

$$h_m = \frac{1+S}{\ell_0 \gamma'} \qquad \cos\phi = 0 \tag{9a}$$

$$h_m = \frac{1}{\ell_0 \cos\phi}\left[1 - \sqrt{1 - \frac{2(1+S)}{\gamma'}\cos\phi}\right] \qquad \cos\phi < 0 \tag{9b}$$

$$h_m = \frac{1}{\ell_0 \cos\phi}\left[1 + \sqrt{1 - \frac{2(1+S)}{\gamma'}\cos\phi}\right] \qquad \cos\phi > 0 \tag{9c}$$

where S is the degree of supersaturation, ϕ is the vertical phase of the gravity wave obtained by using the WKB approximation as

$$\phi(z) = \int^{z} \ell(z')dz' \tag{10}$$

and γ' represents the vertical variation of the mean flow and is defined as

$$\gamma' \equiv \frac{\gamma(z)\ell(z)}{\ell_0} = \left(\frac{N(z)}{N_0}\right)^{1/2} \left(\frac{U(z)}{U_0}\right)^{-3/2} \left(\frac{\rho(z)}{\rho_0}\right)^{-1/2}. \tag{11}$$

When $\cos\phi > \gamma'/2(1+S)$, the contribution from the first-order lower boundary condition suppresses the wave steepening enough to prevent wave breaking and wave stress is conserved. For the saturated wave stress $S = 0$ in (9a-c). Solutions for the zero-order lower boundary condition are given by (9a).

The degree of supersaturation, $S(z) \equiv (\partial\delta/\partial z)_{max} - 1$, is given as

$$S(z) = \frac{3}{2}\frac{(\pi/\ell)(\sqrt{2}H/3L)^{1/2}}{(\pi/\ell)(H/3\sqrt{2}L)^{1/2} + H} \tag{12}$$

where L is the horizontal length scale of the gravity wave and H is the equivalent scale height defined as

$$H = \frac{D}{\ln[\gamma^2(z+D)/\gamma^2(z)]}$$

where D is the depth of the layer.

Having determined the vertical profile of the gravity wave stress, deceleration of the mean wind component parallel to the surface wind is obtained for each model layer from (1). Finally, acceleration of the zonal and meridional components of the mean flow is obtained by

$$\left(\frac{\partial u}{\partial t}\right) = \left(\frac{\partial U}{\partial t}\right)_w \frac{u_0}{|\mathbf{V}_0|} \tag{13a}$$

$$\left(\frac{\partial v}{\partial t}\right) = \left(\frac{\partial U}{\partial t}\right)_w \frac{v_0}{|\mathbf{V}_0|} \tag{13b}$$

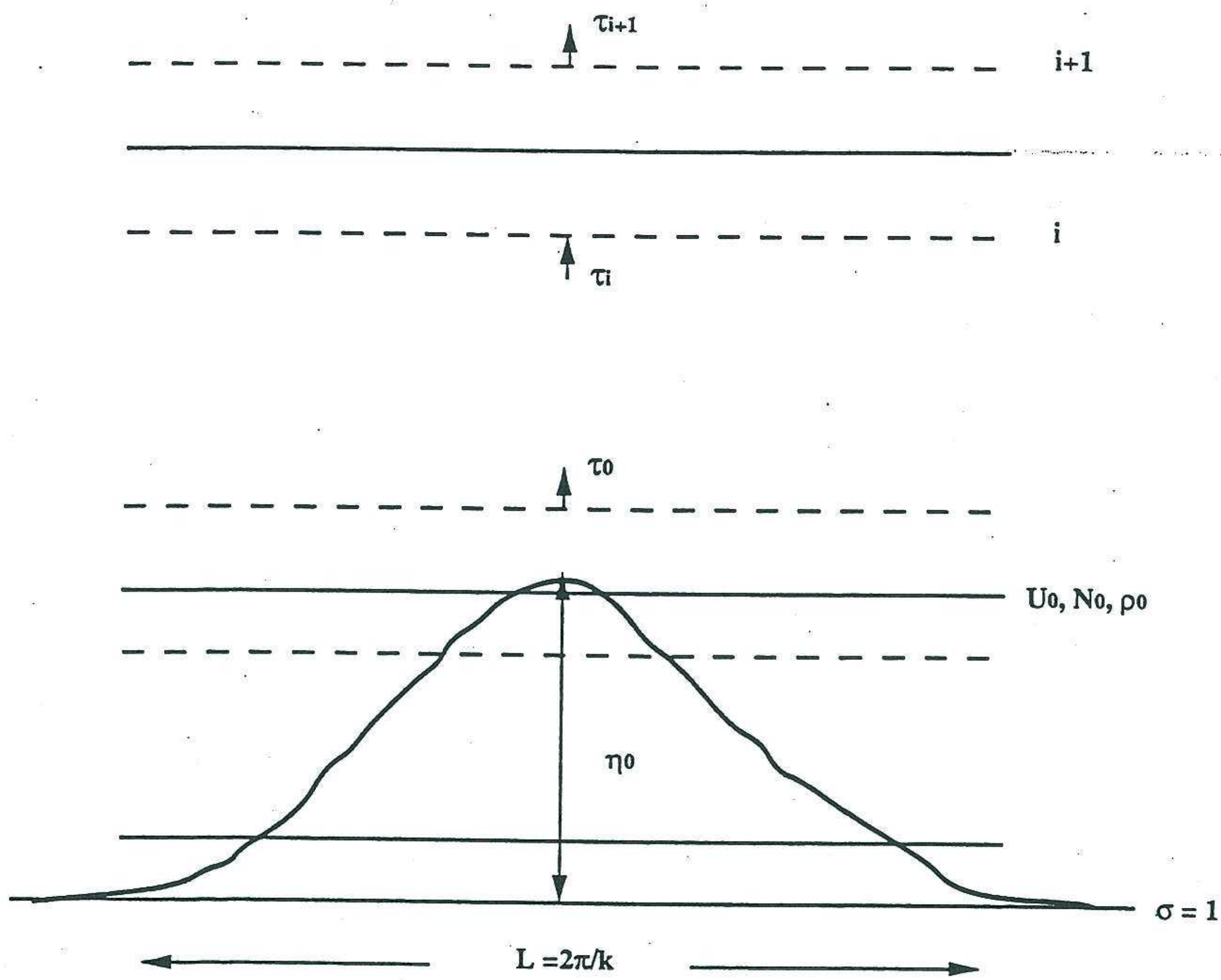

Fig. 10 Schematic diagram for the computation of gravity wave drag

Thin solid horizontal lines: full model level where the prognostic variables (u, v, θ, q) are carried.

Thin dashed horizontal lines: layer interface where the flux variables ($u'w'$, $q'w'$, τ) are carried.

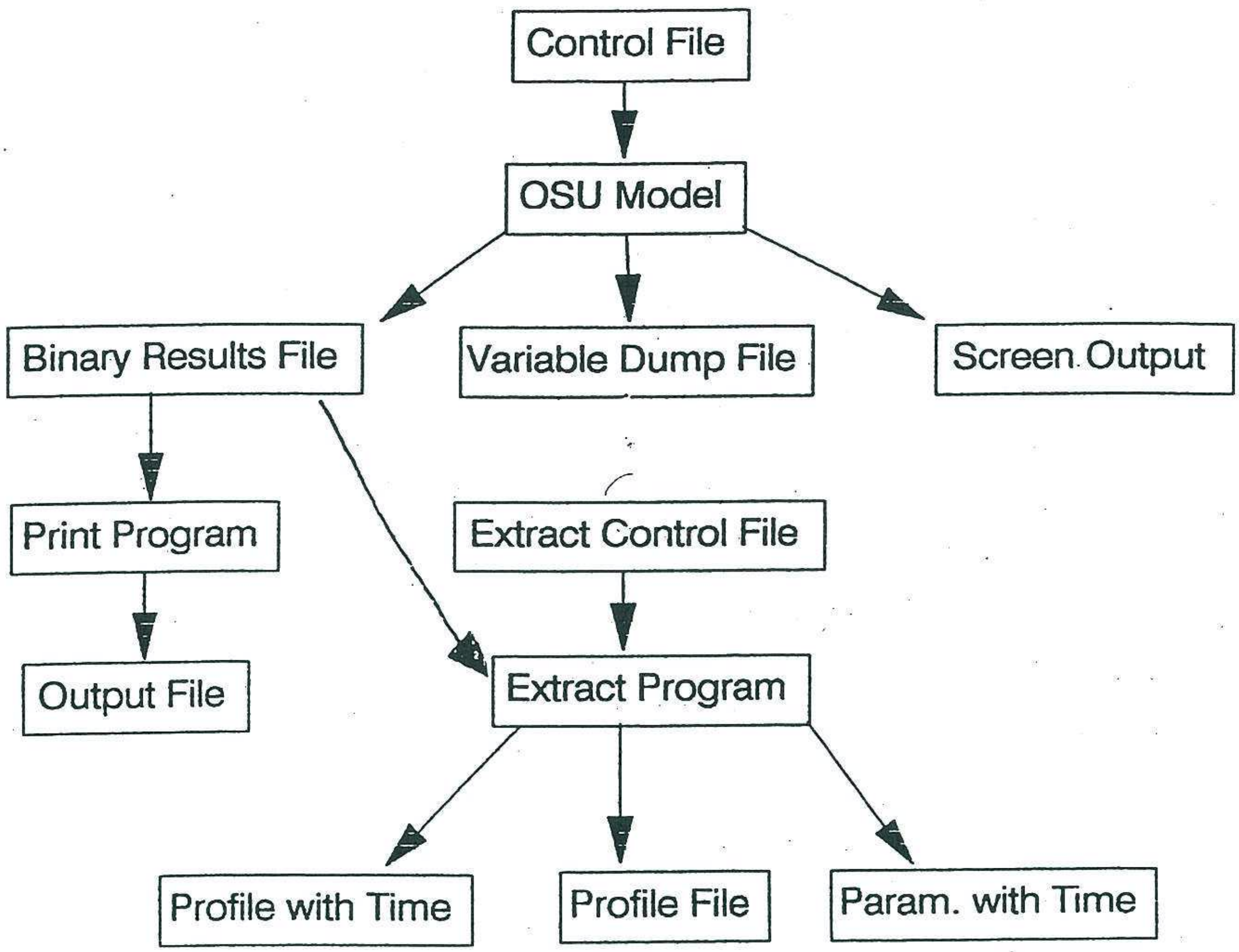

Flow chart for using the Oregon State University One Dimensional Planetary Boundary Layer model.

Chapter 3. Running OSU1DPBL

The following is a brief description of the steps required to run OSU1DPBL 1.0.4. The assumption is made that the user of this model is capable of compiling, linking, and running FORTRAN programs and is familiar with his/her local operating system.

The model is written in ANSI FORTRAN standard 5.0 (FORTRAN 77). The code has also been successfully ported to machines including the Burroughs, CRAY-X/MP™, CDC Cyber 930, Apple Macintosh™ II using MACTRAN Plus (1988), DEC VAX 11/750 operating under VMS (4.2) and Sun workstations. Most users should encounter no difficulties in adapting the model for use in their own operating system environment.

Prior to actually running the model, the user must set up an input (***control***) file. This file contains the initial parameters and data required by the model. An example ***control*** file with description is given in section 3.1.

The model is now ready to run. Once the program has started the user is asked for two files. The first file name requested is the ***control*** file. The second file is the name of the ***output*** (binary) file, discussed below. A third file is also created at this time, which is a dump of the initial model parameters and is nearly identical to the ***control*** file. An example dump file is given in section 3.2.1. The dump file can be kept as a record, or can be immediately viewed on a multitasking/ multiuser computer system and the program aborted if any errors are found.

The ***output*** file is stored as a binary file to minimize disk space usage, so it is not possible to view the output directly unless the data is once again read and output as formatted (ASCII) data. Running PRINT1DPBL.for (Appendix D.2) allows the user to read the model (binary) ***output*** results and rewrite the data as formatted output for viewing. This program contains source code for reading the data and can be modified for whatever type of post analysis desired.

While the program PRINT1DPBL has been supplied, it is necessary to describe each record and field within each record that the program reads. A list of the symbolic variable names, their meaning and units is given in sections 3.2.2 and 3.2.3 below. The list represents a single dump for a single time step forecast. In actuality, records 1-17 (described in section 3.2.2) are dumped once, at the initial time (t=0). The remainder of the output, records 18-25 (described in section 3.2.3), are by default output to the binary file every hour. A change to the OSU1DPBL1.0.4 driver program (PBLDRVR, approximately line #1563, Appendix D.1) can be made if more or less frequent output is desired.

The gravity wave package is included in the present model version but is still being modified. The separate output files from the gravity wave model that are generated in subroutine PRTFLX are used only for testing and improving the gravity wave model. A description of these output files is not included except within the model code of subroutine PRTFLX.

3.1 Control File

The sample ***control*** (input) file listed below illustrates the format for input of data to the model.

All parameters not input in the control file have default settings in the model code described in sections 3.2.2 and 4.1.2. The default settings are initialized in the model code through BLOCK DATA program segments A1 through A4 (see Appendix D.1). If a user wishes to change any of these parameters, either the control file must be modified, or the initial program defaults within the program code (BLOCK DATA program segments A1 through A4) need to be changed.

The sample control file below lists the boundary layer input data, followed by the program input variable names. Model output for this control file follows in section 3.2.

```
1 1 0 0                                           = IFHF,IFCRI,IFSNO,IFCLD
600. 12.0                                         = DELTAT,TEND
TEST CASE DRY DESERT AIR                          = TEXTI
20.0 10.0 0.0 0.1 0.01 0.0 0.23                   = SLA,SLO,TZONE,Z0,Z0H,ZD0,ALBEDO
6 21.0 6.0                                        = MO,DY,TIMEIS
100000.0                                          = PSFC
0.0                                               = CLC
0.0 0.002                                         = CMC,SCANOP
0.0 0.0 0.0 0.0                                   = PRST,PREND,PRCIP,ESD
1 0.05 0.3 1 0.07 0.25 0.4                        = ISOIL,TWILT,SIGMAF,IFTC,TSO0,TSOREF,PC
0.08 0.08                                         = WSOIL(1), WSOIL(2)
2                                                 = NUG
5.00 0.00  6.00                                   = UGI,VGI,TGI
5.00 0.00 18.00
25 1                                              = MZ1, IWUNIT
   0.0   0.00   0.00   0.00   20.7   3.0          = DZ,UNM,VNM,WNM,RNM,QNM
  50.0   5.00   0.00   0.01   20.4   3.0
 100.0   5.00   0.00   0.01   20.1   3.0
 150.0   5.00   0.00   0.01   19.8   3.0
 200.0   5.00   0.00   0.01   19.5   3.0
 250.0   5.00   0.00   0.01   19.2   3.0
 300.0   5.00   0.00   0.01   18.9   3.0
 350.0   5.00   0.00   0.01   18.6   3.0
 400.0   5.00   0.00   0.01   18.3   3.0
 500.0   5.00   0.00   0.01   17.7   3.0
 600.0   5.00   0.00   0.03   17.1   3.0
 700.0   5.00   0.00   0.03   16.5   3.0
 800.0   5.00   0.00   0.03   15.9   3.0
 900.0   5.00   0.00   0.03   15.3   3.0
1000.0   5.00   0.00   0.05   14.7   3.0
1200.0   5.00   0.00   0.05   13.5   2.0
1400.0   5.00   0.00   0.05   12.3   1.0
1600.0   5.00   0.00   0.07   11.1   1.0
1800.0   5.00   0.00   0.07    9.9   1.0
2000.0   5.00   0.00   0.07    8.7   1.0
2400.0   5.00   0.00   0.07    6.3   1.0
2800.0   5.00   0.00   0.07    3.9   1.0
3200.0   5.00   0.00   0.05    1.5   0.5
3600.0   5.00   0.00   0.05   -0.9   0.5
4000.0   5.00   0.00   0.05   -3.3   0.5
4400.0   5.00   0.00   0.03   -5.7   0.3
```

3.2.1 Dump file

The following is an example of the dump file generated after running OSU1DPBL using the sample control file listed in section 3.1. The parameters are further described in sections 3.1, 3.2.2, and 4.1.2.

```
   PROGRAM OSUPBL1D DUMP OF INITIAL DATA

    IFHF, IFCRI, IFSNO, IFCLD =   1   1   0   0
    NOOFGR,DELTAT,TEND,RICR,PINK,KOOL =  1     600.000      12.000       .250      2.000  0
    TITLE =TEST CASE DRY DESERT AIR
    SLA, SLO, TZONE, Z0, Z0H, ZD0, ALBEDO =     20.0000     10.0000       .0000       .1000       .0100
 .0000      .2300
    MO, DY, HR =  6    21.00     6.00
    PSFC =   100000.00
    TREF =      273.160
    CLC =        .0000
    CMC =        .0000
   PRST,PREND,PRCIP,ESD,TSNOW =        .0000        .0000        .0000        .0000    273.1600
   ISOIL, TWILT, SIGMAF, IFTC, TSOO, TSOREF, PC =  1      .0500      .3000 1       .0700       .2500
 .4000
    NUG =   2
    UG, VG, TG =      5.0000      .0000      .0000
    UG, VG, TG =      5.0000      .0000    18.0000
           .000        .000        .000        .000      20.700      3.000
         50.000       5.000        .000        .010      20.400      3.000
        100.000       5.000        .000        .010      20.100      3.000
        150.000       5.000        .000        .010      19.800      3.000
        200.000       5.000        .000        .010      19.500      3.000
        250.000       5.000        .000        .010      19.200      3.000
        300.000       5.000        .000        .010      18.900      3.000
        350.000       5.000        .000        .010      18.600      3.000
        400.000       5.000        .000        .010      18.300      3.000
        500.000       5.000        .000        .010      17.700      3.000
        600.000       5.000        .000        .030      17.100      3.000
        700.000       5.000        .000        .030      16.500      3.000
        800.000       5.000        .000        .030      15.900      3.000
        900.000       5.000        .000        .030      15.300      3.000
       1000.000       5.000        .000        .050      14.700      3.000
       1200.000       5.000        .000        .050      13.500      2.000
       1400.000       5.000        .000        .050      12.300      1.000
       1600.000       5.000        .000        .070      11.100      1.000
       1800.000       5.000        .000        .070       9.900      1.000
       2000.000       5.000        .000        .070       8.700      1.000
       2400.000       5.000        .000        .070       6.300      1.000
       2800.000       5.000        .000        .070       3.900      1.000
       3200.000       5.000        .000        .050       1.500       .500
       3600.000       5.000        .000        .050       -.900       .500
       4000.000       5.000        .000        .050      -3.300       .500
   MZ1 =  25
   NSOIL =   2
   DSOIL, WSOIL, TSOIL =      -.0500       .0800     293.8600
   DSOIL, WSOIL, TSOIL =     -1.0000       .0800     293.8600
```

3.2.2 Initial output

These parameters are output only once, at initialization. An asterisk (*) indicates the parameters that are hardwired in the OSU1DPBL code and therefore not specified in the control file. Units are generally given in parenthesis following the parameter description. A sample initial model output for the control file listed in section 3.1 follows the description of each initial output record.

Record 1 IFHF,IFCRI,IFSNO,IFCLD

IFHF	Flag for soil heat flux,	1 = yes 0 = no
IFCRI	Flag for cloud-radiation interaction, 1 = cloud cover diagnosed, clouds affect radiation 0 = no clouds diagnosed -1 = clouds diagnosed, no affect on radiation	
IFSNO	Flag for snow,	1 = yes 0 = no
IFCLD	Flag for cloud diffusivity,	1 = yes 0 = no

Record 2 NOOFGR,DELTAT,TEND,RICR,PINK,KOOL

*NOOFGR	Grid resolution indicator. There are 6 grid types currently implemented. 1 ⇒ 38 level (20 m high resolution grid, default) 2 ⇒ 25 level 3 ⇒ 13 level 4 ⇒ 7 level 5 ⇒ 4 level 6 ⇒ 9 level (A18 resolution, comparable to AFGL GSM) 7 ⇒ 27 level (course resolution, levels to 10 km.) 8 ⇒ 75 level (10 m fine resolution grid, levels to 10 km.)
DELTAT	Time step (s).
TEND	Duration of the model run (hours).
*RICR	Critical Richardson number. (0.25 by default).
*PINK	p power in K profile. (2 by default).
*KOOL	Newtonian cooling index. (1=yes, 0=no, 0 by default).

Record 3 TEXTI

TEXTI	= Text string for labelling information.

Record 4 SLA,SLO,TZONE,Z0,ALBEDO

SLA	Latitude of simulation location (positive north).
SLO	Longitude of simulation location (positive east).
TZONE	Time zone of the simulation location, LST - GMT (Local standard time - Greenwich Mean Time).
Z0	Roughness length for momentum (m).
Z0H	Roughness length for heat (m).
ZD0	Displacement height of vegetation (m). If a height is specified then data from the input (control) file will be ignored at levels above the surface and <= ZD0.
ALBEDO	Albedo, 0.7 default for snow, otherwise specified in control file.

Record 5 MO,DY,TIMEIS

MO	Month of observed data.
DY	Day of observed data.
TIMEIS	Time of observed data (GMT).

Record 6 PSFC

PSFC	Surface pressure in Pa (Pa = mb x 100).

Record 7 TREF

*TREF	Reference temperature for downward longwave radiation calculation (273.16 K by default - note: this is obsolete but may be useful for other calculations).

Record 8 CLC

CLC	Fractional cloud cover.

Record 9 CMC

CMC	Canopy water (m).
SCANOP	Canopy capacity (m).

Record 10 Precipitation parameters, PRST,PREND,PRCIP,ESD,TSNOW

PRST	Precipitation start time (hours from beginning of run).
PREND	Precipitation end time (hours from beginning of

run).

PRCIP	Precipitation rate (kg m^{-2} s^{-1}).
ESD	Snow depth (m)
*TSNOW	Temperature at which snow is falling (273.16 K by default).

Record 11 ISOIL,TWILT,SIGMAF,IFTC,T0

ISOIL	Soil type (1-11, see section 4.1.2 on COMMON blocks, /SOIL1/, ISOIL, for list of soil types).
TWILT	Wilting point.
SIGMAF	Shading factor.
IFTC	Transpiration flag, 1 = yes, 0 = no transpiration or canopy evaporation of intercepted water.
TSO0	Air dry value.
TSOREF	Transpiration reduction reference value.
PC	Plant coefficient. If PC<0 then this is -RC, the canopy resistance (s/m). OSU1DPBL can accomodate either a plant coefficient or canopy resistance which is used in calculating transpiration. See 2.10 for a description of the relationship between plant coefficient and canopy resistance in OSU1DPBL.

Record 12 NUG

NUG	Number of geostrophic wind observations.

Record 13 UGI,VGI,TGI, there are NUG records.

UGI	u wind component (m s^{-1}).
VGI	v wind component (m s^{-1}).
TGI	Time of the observation from the start (s).

Record 14 NSOIL

*NSOIL	Number of soil layers, 2 by default.

Record 15 DSOIL,WSOIL,TSOIL, there are NSOIL records.

*DSOIL	Soil depth in m. (5 cm and 1 m by default)
WSOIL	Soil water content. (initially constant with depth)
*TSOIL	Soil temperature, initially set equal to the skin temperature (C).

Record 16 MZ1

MZ1	Number of observed (input) levels. This number may

be reduced depending on the value of the displacement height (see ZD0 under Record 4). While the initial atmospheric profile data is not included in the initial model output, these parameters are found in the control file and in the dump file, so they will be described here for completeness.

DZ — Height above surface (m).

UNM — u wind component (m s^{-1}).

VNM — v wind component (m s^{-1}).

WNM — ω wind component (mb hr^{-1}).

RNM — Air temperature (C).

QNM — Mixing ratio (g kg^{-1}).

Record 17 MZ

*MZ — Number of output levels (depends on number observed).

The following is an example of the initial model output from the output file generated after running OSU1DPBL using the sample control file listed in section 3.1.

```
  IFHF, IFCRI, IFSNO, IFCLD =   1   1   0   0
  NOOFGR,DELTAT,TEND,RICR,PINK,KOOL =   1    600.000     12.000      .250      2.000  0
  TITLE =TEST CASE DRY DESERT AIR
  SLA, SLO, TZONE, Z0, Z0H, ZD0, ALBEDO =     20.0000     10.0000      .0000       .1000       .0100
.0000      .2300
  MO, DY, HR =  6   21.00    6.00
  PSFC =   100000.00
  TREF =      273.160
  CLC =        .0000
  CMC =        .0000
 PRST,PREND,PRCIP,ESD,TSNOW =        .0000       .0000       .0000       .0000    273.1600
 ISOIL, TWILT, SIGMAF, IFTC, TSOO, TSOREF, PC =  1        .0500        .3000 1       .0700        .2500
.4000
  NUM. OF GEO. WINDS =   2 UG, VG, TG
     5.0000     .0000     .0000
     5.0000     .0000   18.0000
  NUM. OF SOIL LAYER =  2 Z, THETA, TEMP
       -.0500       .0800    293.8600
      -1.0000       .0800    293.8600
  INPUT LEVEL AND OUTPUT LEVEL =  25  57
```

3.2.3 Hourly output

These parameters are output every hour; this can be changed by modifying the model code as noted earlier in this chapter. Sample model output using the control file listed in section 3.1 follows the description of each output record.

Record 18 MO,IDY,IDO,IHO,MIN,SEC

MO	Month at current time of dump.
IDY	Number of days elapsed from start time.
IDO	Day at current time of dump.
IHO	Hour at current time of dump.
MIN	Minutes at current time of dump.
SEC	Seconds at current time of dump.

Record 19 Profile data, Z,U,V,TH,T,Q,P,RH,UFLUX,VFLUX,THFLUX, QFLX,Q1,Q2,TD,ZSP,PBLK;
there will be MZ levels output.

Z	Height (m).
U	u wind component (m s^{-1}).
V	v wind component (m s^{-1}).
TH	Potential temperature (C).
T	Temperature (C).
Q	Mixing ratio (g kg^{-1}).
P	Pressure (Pa).
RH	Relative humidity (percent).
UFLUX	Zonal momentum flux (kg m^{-2} s^{-1}).
VFLUX	Meridonal momentum flux (kg m^{-2} s^{-1}).
THFLUX	Heat flux (W m^{-2}).
QFLUX	Moisture flux (W m^{-2}).
Q1	Apparent heat source (C day^{-1}).
Q2	Apparent moisture sink (C day^{-1}).
TD	Dew point temperature (C).
ZSP	Geopotential height of lifting condensation level (m); -1 if none found.
PBLK	Diffusivity coefficient due to turbulence (m^2 s^{-1}).

Record 20 RDOWN,H,G,LE,FUP,SNOFLX,SUM,FNET,EP1,THBAR,QBAR,ETOT

RDOWN	Total downward (solar + atmospheric) radiative flux (positive downward, W m^{-2}).
H	Sensible heat flux (positive upward, W m^{-2}).

G	Soil heat flux (positive downward, W m^{-2}).
LE	Latent heat flux (positive upward), W m^{-2}).
FUP	Upward surface radiative flux (positive upward, W m^{-2}).
SNOFLX	Sum of three snow fluxes (positive downward, W m^{-2}).
SUM	H + SSOIL + E - RDOWN + FUP + SNOFLX (W m^{-2}).
FNET	Net radiation (positive upwards, W m^{-2}).
EP1	Potential evapotranspiration flux (W m^{-2}).
THBAR	Layer averaged potential temperature (K).
QBAR	Layer averaged mixing ratio (g kg^{-1}).
ETOT	Accumulated evaporation (m).

Record 21 TAOX,TAOY,USTAR,WSTAR,UG,VG,GEOS,SINA,ANEM,WSC,CLC

TAOX	Surface stress (zonal direction, kg m^{-2} s^{-1}).
TAOY	Surface stress (meridonal direction, kg m^{-2} s^{-1}).
USTAR	Friction velocity (m s^{-1}).
WSTAR	Convective velocity scale (m s^{-1}).
UG	Zonal component of geostrophic wind (m s^{-1}).
VG	Meridonal component of geostrophic wind (m s^{-1}).
GEOS	Speed of geostrophic wind (m s^{-1}).
SINA	Rotation of surface wind w.r.t. geostrophic wind.
ANEM	2 meter wind speed (m s^{-1}).
WSC	Vertical velocity scale (m s^{-1}).
CLC	Cloud cover (fraction).

Record 22 HPBL,XL,RIB,RIF,RIR,TSFC,TAIR,CM,CH,CG,THERM

HPBL	Height of boundary layer (m).
XL	Monin-Obukhov length (m).
RIB	Bulk Richardson number.
RIF	Flux Richardson number.
RIR	Radiation Richardson number.
TSFC	Skin temperature (C).
TAIR	2 meter temperature (C).
CM	Momentum exchange coefficient (m s^{-1}).
CH	Sensible heat exchange coefficient (m s^{-1}).
CG	Layer averaged temperature excess (K).
THERM	Scaled virtual temperature excess (K).

Record 23 Precipitation and dew, PRCP,DEW,ACCP,ACCD

PRCP	Precipitation at time step (mm/hr).
DEW	Dew at this time step (mm/hr).

ACCP	Accumulated precipitation (mm).
ACCD	Accumulated dew (mm).

Record 24 CMC,ESD

CMC	Canopy water content (mm).
ESD	Snow depth (m).
PC	Plant coefficient, constant if specified in control file, calculated from RC if RC is specified. See description of PC, Record 11, section 3.2.2.
RC	Canopy resistance (s m^{-1}), constant if specified in control file, calculated from PC if PC is specified. See description of PC, Record 11, section 3.2.2.
SOLARN	Net downward solar radiation, (1-ALBEDO)*S (W m^{-2}).

Record 25 Soil data, DSOIL,WSOIL,TSS; there are NSOIL records.

DSOIL	Soil depth (m).
WSOIL	Volumetric water content (kg kg^{-1}).
TSS	Soil temperature (C).

The following are examples of the model output at the initial time (hour 6) and after a six hour integration (hour 12) generated after running OSU1DPBL using the sample control file listed in section 3.1.

MONTH 6 DAY 21(+ 0) HOUR 6 MIN 2 SEC 30.0

Z	U	V	TH	T	Q	P	SIGMA	RH	UFLX	VFLX	THFLX	QFLX	Q1	Q2	TD	ZSP	PBLK
4000	5.0	.0	36.8	-3.3	.5	616	.616	10.3	.00	.00	.00	.00	.0	.0	-30.3	-1	.00
3800	5.0	.0	36.0	-2.1	.5	632	.632	9.7	.00	.00	.00	.00	.0	.0	-30.0	-1	.00
3600	5.0	.0	35.1	-.9	.5	648	.648	9.1	.00	.00	.00	.00	.0	.0	-29.7	-1	.00
3400	5.0	.0	34.3	.3	.5	664	.664	8.6	.00	.00	.00	.00	.0	.0	-29.5	-1	.00
3200	5.0	.0	33.4	1.5	.5	681	.681	8.0	.00	.00	.00	.00	.0	.0	-29.2	-1	.00
3000	5.0	.0	32.6	2.7	.7	698	.698	11.3	.00	.00	.00	.00	.0	.0	-24.5	-1	.00
2800	5.0	.0	31.7	3.9	1.0	715	.715	14.2	.00	.00	.00	.00	.0	.0	-21.0	-1	.00
2600	5.0	.0	30.9	5.1	1.0	733	.733	13.4	.00	.00	.00	.00	.0	.0	-20.7	-1	.00
2400	5.0	.0	30.1	6.3	1.0	751	.751	12.7	.00	.00	.00	.00	.0	.0	-20.4	-1	.00
2200	5.0	.0	29.3	7.5	1.0	770	.770	11.9	.00	.00	.00	.00	.0	.0	-20.1	-1	.00
2000	5.0	.0	28.5	8.7	1.0	789	.789	11.3	.00	.00	.00	.00	.0	.0	-19.9	-1	.00
1900	5.0	.0	28.1	9.3	1.0	799	.799	11.0	.00	.00	.00	.00	.0	.0	-19.7	-1	.00
1800	5.0	.0	27.7	9.9	1.0	808	.808	10.7	.00	.00	.00	.00	.0	.0	-19.6	-1	.00
1700	5.0	.0	27.3	10.5	1.0	818	.818	10.4	.00	.00	.00	.00	.0	.0	-19.4	-1	.00
1600	5.0	.0	26.9	11.1	1.0	828	.828	10.1	.00	.00	.00	.00	.0	.0	-19.3	-1	.00
1500	5.0	.0	26.5	11.7	1.0	838	.838	9.8	.00	.00	.00	.00	.0	.0	-19.2	-1	.00
1400	5.0	.0	26.1	12.3	1.0	848	.848	9.5	.00	.00	.00	.00	.0	.0	-19.0	-1	.00
1350	5.0	.0	25.9	12.6	1.2	853	.853	11.8	.00	.00	.00	.00	.0	.0	-16.3	-1	.00
1300	5.0	.0	25.7	12.9	1.5	858	.858	13.9	.00	.00	.00	.00	.0	.0	-14.0	-1	.00
1250	5.0	.0	25.5	13.2	1.7	863	.863	16.0	.00	.00	.00	.00	.0	.0	-12.1	-1	.00
1200	5.0	.0	25.3	13.5	2.0	868	.868	18.1	.00	.00	.00	.00	.0	.0	-10.3	-1	.00
1150	5.0	.0	25.1	13.8	2.2	874	.874	20.0	.00	.00	.00	.00	.0	.0	-8.7	3956	.00
1100	5.0	.0	24.9	14.1	2.5	879	.879	22.0	.00	.00	.00	.00	.0	.0	-7.3	3767	.00
1050	5.0	.0	24.7	14.4	2.7	884	.884	23.8	.00	.00	.00	.00	.0	.0	-6.0	3592	.00
1000	5.0	.0	24.5	14.7	3.0	889	.889	25.7	.00	.00	.00	.00	.0	.0	-4.8	3429	.00
950	5.0	.0	24.3	15.0	3.0	895	.895	25.3	.00	.00	.00	.00	.0	.0	-4.7	3407	.00
900	5.0	.0	24.1	15.3	3.0	900	.900	25.0	.00	.00	.00	.00	.0	.0	-4.6	3385	.00
850	5.0	.0	23.9	15.6	3.0	905	.905	24.7	.00	.00	.00	.00	.0	.0	-4.5	3364	.00
800	5.0	.0	23.7	15.9	3.0	911	.911	24.3	.00	.00	.00	.00	.0	.0	-4.5	3342	.00
750	5.0	.0	23.6	16.2	3.0	916	.916	24.0	.00	.00	.00	.00	.0	.0	-4.4	3320	.00
700	5.0	.0	23.4	16.5	3.0	921	.921	23.7	.00	.00	.00	.00	.0	.0	-4.3	3298	.00
650	5.0	.0	23.2	16.8	3.0	927	.927	23.4	.00	.00	.00	.00	.0	.0	-4.2	3276	.00
600	5.0	.0	23.0	17.1	3.0	932	.932	23.1	.00	.00	.00	.00	.0	.0	-4.1	3254	.00
550	5.0	.0	22.8	17.4	3.0	938	.938	22.8	.00	.00	.00	.00	.0	.0	-4.1	3232	.00
500	5.0	.0	22.6	17.7	3.0	943	.943	22.5	.00	.00	.00	.00	.0	.0	-4.0	3210	.00
450	5.0	.0	22.4	18.0	3.0	949	.949	22.2	.00	.00	.00	.00	.0	.0	-3.9	3189	.00
400	5.0	.0	22.2	18.3	3.0	954	.954	21.9	.00	.00	.00	.00	.0	.0	-3.8	3167	.00
380	5.0	.0	22.1	18.4	3.0	957	.957	21.8	.00	.00	.00	.00	.0	.0	-3.8	3158	.00
360	5.0	.0	22.1	18.5	3.0	959	.959	21.7	.00	.00	.00	.00	.0	.0	-3.8	3150	.00
340	5.0	.0	22.0	18.7	3.0	961	.961	21.6	.00	.00	.00	.00	.0	.0	-3.7	3141	.00
320	5.0	.0	21.9	18.8	3.0	963	.963	21.5	.00	.00	.00	.00	.0	.0	-3.7	3132	.00
300	5.0	.0	21.8	18.9	3.0	966	.966	21.3	.00	.00	.00	.00	.0	.0	-3.7	3124	.00
280	5.0	.0	21.8	19.0	3.0	968	.968	21.2	.00	.00	.00	.00	.0	.0	-3.6	3115	.00
260	5.0	.0	21.7	19.1	3.0	970	.970	21.1	.00	.00	.00	.00	.0	.0	-3.6	3106	.00
240	5.0	.0	21.6	19.3	3.0	972	.972	21.0	.00	.00	.00	.00	.0	.0	-3.6	3098	.00
220	5.0	.0	21.5	19.4	3.0	975	.975	20.9	.00	.00	.00	.00	.0	.0	-3.6	3089	.00
200	5.0	.0	21.5	19.5	3.0	977	.977	20.8	.00	.00	.00	.00	.0	.0	-3.5	3080	.00
180	5.0	.0	21.4	19.6	3.0	979	.979	20.7	.00	.00	.00	.00	.0	.0	-3.5	3071	.00
160	5.0	.0	21.3	19.7	3.0	982	.982	20.6	.00	.00	.00	.00	.0	.0	-3.5	3063	.00
140	5.0	.0	21.2	19.9	3.0	984	.984	20.5	.00	.00	.00	.00	.0	.0	-3.4	3054	.00
120	5.0	.0	21.2	20.0	3.0	986	.986	20.4	.00	.00	.00	.00	.0	.0	-3.4	3045	.00
100	5.0	.0	21.1	20.1	3.0	988	.988	20.3	.00	.00	.00	.00	.0	.0	-3.4	3037	.00
80	5.0	.0	21.0	20.2	3.0	991	.991	20.2	.00	.00	.00	.00	.0	.0	-3.3	3028	.00
60	5.0	.0	20.9	20.3	3.0	993	.993	20.1	.00	.00	.00	.00	.0	.0	-3.3	3019	.00
40	4.0	.0	20.9	20.5	3.0	995	.995	20.0	.00	.00	.00	.00	.0	.0	-3.3	3010	.00
20	2.0	.0	20.8	20.6	3.0	998	.998	19.9	-2.00	.00	-26.65	10.59	.0	.0	-3.2	3001	.00
0	.0	.0	17.6	17.6	3.5	1000	1.000	28.1	-2.00	.00	-26.65	10.59	.0	.0	-1.1	-1	.00

RDOWN	+H	+G	+LE	FUP	SNOFLX	SUM	FNET	EP1	THBAR	QBAR	ETOT
320.82	-26.65	-67.95	10.59	405.06	.00	.233	-84.24	47.78	293.9	3.00	.000

TAOX	TAOY	USTAR	WSTAR	UG	VG	GEOS	SINA	ANEM	WSC	CLC
-.0200	.0000	.1416	-.5311	5.0000	.0000	5.0000	.0112	1.4083	1.5048	.0000

HPBL	OBUHK L	RIB	RIF	RIRAD	TSFC	TAIR	CM	CH	CG	THERM
198.20	9.67	.01	.27	8.45	17.57	17.11	.0100	.0070	.00000	.000

PRCP	DEW	ACCP	ACCD	CMC	ESD	PC	RC	SOLAR
.0000	.0000	.0000	.0000	.0000	.0000	.4000	508.5540	.0000

SOIL Z	SOIL Q	SOIL T
-.05	.0800	20.52
-1.00	.0800	20.70

MONTH 6 DAY 21 (+ 0) HOUR 12 MIN 5 SEC .0

Z	U	V	TH	T	Q	P	SIGMA	RH	UFLX	VFLX	THFLX	QFLX	Q1	Q2	TD	ZSP	PBLK
4012	5.0	.0	36.8	-3.3	.5	616	.616	10.3	.00	.00	.00	.00	.0	.0	-30.3	-1	.00
3812	5.0	.0	36.0	-2.1	.5	632	.632	9.7	.00	.00	.00	.00	.0	.0	-30.0	-1	.00
3612	5.0	.0	35.1	-.9	.5	648	.648	9.1	.00	.00	.00	.00	.0	.0	-29.7	-1	.00
3412	5.0	.0	34.3	.3	.5	664	.664	8.5	.00	.00	.00	.00	.0	.0	-29.5	-1	.00
3212	5.0	.0	33.4	1.5	.5	681	.681	8.0	.00	.00	.00	.00	.0	.0	-29.2	-1	.00
3012	5.0	.0	32.6	2.7	.7	698	.698	11.3	.00	.00	.00	.00	.0	.0	-24.6	-1	.00
2812	5.0	.0	31.8	3.9	1.0	715	.715	14.1	.00	.00	.00	.00	.0	.0	-21.1	-1	.00
2612	5.0	.0	30.9	5.1	1.0	733	.733	13.4	.00	.00	.00	.00	.0	.0	-20.7	-1	.00
2412	5.0	.0	30.1	6.3	1.0	751	.751	12.6	.00	.00	.00	.00	.0	.0	-20.4	-1	.00
2212	5.0	.0	29.3	7.5	1.0	770	.770	11.9	.00	.00	.00	.00	.0	.0	-20.1	-1	.00
2012	5.0	.0	28.5	8.7	1.0	789	.789	11.3	.00	.00	.00	.00	.0	.0	-19.9	-1	.00
1912	5.0	.0	28.1	9.3	1.0	799	.799	11.0	.00	.00	.00	.00	.0	.0	-19.7	-1	.00
1812	5.0	.0	27.7	9.9	1.0	808	.808	10.6	.00	.00	.00	.00	.0	.0	-19.6	-1	.00
1712	4.8	.1	26.9	10.1	1.6	818	.818	16.5	-.62	.00	-11.87	44.66	-30.8	-98.8	-14.2	-1	5.57
1612	4.6	.2	26.5	10.7	2.0	828	.828	20.3	-2.47	.65	-31.26	154.03	2.0	-63.2	-11.1	-1	19.30
1512	4.4	.3	26.3	11.6	2.2	838	.838	21.6	-4.24	1.25	-19.96	214.56	14.7	-26.5	-9.6	-1	39.54
1412	4.3	.3	26.3	12.5	2.3	848	.848	21.9	-5.58	1.60	3.05	238.44	19.4	-8.9	-8.7	-1	57.96
1362	4.2	.3	26.2	12.9	2.4	853	.853	21.8	-6.14	1.71	16.56	242.61	20.6	-3.4	-8.4	-1	71.40
1312	4.2	.3	26.2	13.4	2.4	858	.858	21.6	-6.63	1.78	30.75	243.60	21.4	.5	-8.1	3986	85.52
1262	4.1	.4	26.2	13.9	2.4	863	.863	21.3	-7.09	1.82	45.41	242.24	21.9	3.5	-7.9	3963	100.09
1212	4.1	.4	26.2	14.3	2.5	868	.868	21.1	-7.50	1.83	60.38	239.11	22.3	5.8	-7.7	3944	114.91
1162	4.1	.4	26.1	14.8	2.5	874	.874	20.7	-7.88	1.82	75.59	234.60	22.6	7.5	-7.5	3927	129.77
1111	4.0	.4	26.1	15.3	2.5	879	.879	20.4	-8.24	1.79	90.96	229.02	22.8	8.9	-7.3	3913	144.44
1061	4.0	.4	26.1	15.8	2.5	884	.884	20.0	-8.58	1.75	106.45	222.58	22.9	10.1	-7.1	3900	158.72
1011	4.0	.4	26.1	16.2	2.5	889	.889	19.7	-8.89	1.69	122.02	215.44	23.0	11.0	-7.0	3889	172.39
961	4.0	.4	26.1	16.7	2.6	895	.895	19.3	-9.19	1.61	137.67	207.73	23.1	11.7	-6.8	3879	185.23
911	3.9	.4	26.1	17.2	2.6	900	.900	18.9	-9.48	1.53	153.38	199.55	23.2	12.4	-6.7	3870	197.02
860	3.9	.4	26.1	17.7	2.6	905	.905	18.5	-9.75	1.43	169.13	190.97	23.2	12.9	-6.5	3862	207.55
810	3.9	.4	26.1	18.2	2.6	911	.911	18.2	-10.01	1.32	184.91	182.05	23.2	13.3	-6.4	3855	216.60
760	3.9	.4	26.0	18.6	2.6	916	.916	17.8	-10.26	1.19	200.72	172.85	23.3	13.7	-6.3	3848	223.94
709	3.8	.4	26.0	19.1	2.6	921	.921	17.4	-10.50	1.06	216.55	163.40	23.3	14.1	-6.2	3842	229.36
659	3.8	.4	26.0	19.6	2.6	927	.927	17.1	-10.73	.92	232.40	153.74	23.3	14.3	-6.1	3837	232.64
608	3.8	.4	26.0	20.1	2.6	932	.932	16.7	-10.95	.77	248.26	143.89	23.3	14.6	-5.9	3832	233.55
558	3.8	.4	26.0	20.6	2.6	938	.938	16.3	-11.16	.62	264.13	133.88	23.3	14.8	-5.8	3827	231.86
508	3.7	.4	26.0	21.1	2.6	943	.943	16.0	-11.37	.45	280.02	123.73	23.3	15.0	-5.7	3823	227.36
457	3.7	.5	26.0	21.6	2.6	949	.949	15.6	-11.57	.27	295.91	113.45	23.3	15.1	-5.6	3820	219.81
406	3.7	.5	26.0	22.1	2.6	954	.954	15.3	-11.76	.09	311.81	103.06	23.3	15.3	-5.5	3817	212.60
386	3.7	.5	26.0	22.3	2.6	957	.957	15.1	-11.84	.01	318.17	98.87	23.3	15.3	-5.5	3816	207.73
366	3.7	.5	26.0	22.5	2.6	959	.959	15.0	-11.91	-.07	324.54	94.67	23.3	15.4	-5.4	3815	202.29
346	3.7	.5	26.0	22.7	2.6	961	.961	14.9	-11.99	-.15	330.90	90.46	23.3	15.4	-5.4	3814	196.28
325	3.6	.5	26.0	22.9	2.7	963	.963	14.7	-12.06	-.23	337.27	86.23	23.3	15.5	-5.3	3814	189.68
305	3.6	.5	26.1	23.1	2.7	966	.966	14.6	-12.13	-.31	343.63	81.98	23.3	15.5	-5.3	3813	182.47
285	3.6	.5	26.1	23.3	2.7	968	.968	14.5	-12.20	-.40	350.00	77.72	23.3	15.6	-5.3	3813	174.63
265	3.6	.5	26.1	23.5	2.7	970	.970	14.3	-12.27	-.49	356.37	73.45	23.3	15.6	-5.2	3813	166.16
244	3.6	.5	26.1	23.7	2.7	972	.972	14.2	-12.34	-.57	362.74	69.17	23.3	15.7	-5.2	3813	157.04
224	3.6	.5	26.1	23.9	2.7	975	.975	14.1	-12.41	-.66	369.11	64.88	23.3	15.7	-5.1	3813	147.26
204	3.6	.5	26.1	24.1	2.7	977	.977	13.9	-12.47	-.76	375.48	60.57	23.3	15.7	-5.1	3813	136.79
184	3.5	.5	26.1	24.3	2.7	979	.979	13.8	-12.54	-.85	381.85	56.26	23.2	15.8	-5.1	3814	129.61
163	3.5	.5	26.1	24.6	2.7	982	.982	13.6	-12.60	-.95	388.21	51.93	23.2	15.8	-5.0	3815	112.60
143	3.5	.5	26.2	24.8	2.7	984	.984	13.5	-12.67	-1.05	394.57	47.59	23.2	15.8	-5.0	3817	95.51
123	3.5	.5	26.2	25.0	2.7	986	.986	13.4	-12.73	-1.15	400.95	43.24	23.3	15.9	-4.9	3819	78.47
102	3.4	.5	26.2	25.3	2.7	988	.988	13.2	-12.79	-1.26	407.35	38.88	23.3	15.9	-4.9	3822	61.66
82	3.4	.5	26.3	25.5	2.7	991	.991	13.1	-12.85	-1.37	413.77	34.51	23.4	15.9	-4.8	3827	45.32
62	3.3	.5	26.4	25.8	2.7	993	.993	12.9	-12.91	-1.49	420.22	30.14	23.5	15.9	-4.8	3835	29.80
41	3.2	.5	26.5	26.1	2.7	995	.995	12.7	-12.97	-1.61	426.72	25.75	23.7	16.0	-4.7	3848	15.62
21	3.1	.4	26.8	26.6	2.7	998	.998	12.4	-13.02	-1.75	433.30	21.36	24.1	16.0	-4.7	3876	.00
0	.0	.0	41.4	41.4	3.1	1000	1.000	6.2	-13.02	-1.75	433.30	21.36	.0	.0	-2.9	-1	.00

RDOWN	+H	+G	+LE	FUP	SNOFLX	SUM	FNET	EP1	THBAR	QBAR	ETOT
1062.25	433.30	59.84	21.36	555.11	.00	7.351	507.14	776.15	299.4	2.42	.014

TAOX	TAOY	USTAR	WSTAR	UG	VG	GEOS	SINA	ANEM	WSC	CLC
-.1302	-.0175	.3625	2.7367	5.0000	.0000	5.0000	.1420	.2.3378	1.7966	.0000

HPBL	OBUHK L	RIB	RIF	RIRAD	TSFC	TAIR	CM	CH	CG	THERM
1770.53	-10.27	-1.00	-.46	-11.31	41.40	28.25	.0422	.0249	.00065	1.026

PRCP	DEW	ACCP	ACCD	CMC	ESD	PC	RC	SOLAR
.0000	.0000	.0000	.0000	.0000	.0000	.4000	215.7760	723.7455

SOIL Z	SOIL Q	SOIL T
-.05	.0785	38.71
-1.00	.0799	20.78

Chapter 4. Program Structure

The structure of OSU1DPBL is outlined in this chapter. In section 4.1 the COMMON blocks are listed and their elements are described. In section 4.2 the program SUBROUTINES and their arguments are listed and described, along with the COMMON block elements used, other subroutines called, and important data. Section 4.3 contains other subprograms (BLOCK DATA statements and FUNCTIONs). A complete listing of the OSU1DPBL FORTRAN source code is found in Appendix D.

4.1 Global PARAMETERS and COMMON Blocks

A number of constants and variables are carried as global PARAMETERs or in COMMON blocks. A description follows each element along with its units; if no units are listed that element is nondimensional. Note that the units the elements have in their COMMON block differ from those in the model output.

4.1.1 Global PARAMETERs

NLEVD Number of dimensioned output levels.
NLEVI Number of dimensioned input levels.
NSOLD Number of dimensioned soil layers.
ngrid Number of model output grids.

4.1.2 COMMON blocks

An astrisk (*) indicates that this parameter is initially specified in the control (input) file.

/FIELDS/ UN(NLEVD),UNM(NLEVI),VN(NLEVD),VNM(NLEVI),RN(NLEVD), RNM(NLEVI), QN(NLEVD),QNM(NLEVI),UG(NLEVD),VG(NLEVD)

UN(NLEVD) Updated u wind component (m s^{-1}).
UNM(NLEVI) Initial/previous u wind component (m s^{-1}).
VN(NLEVD) Updated v wind component (m s^{-1}).
VNM(NLEVI) Initial/previous v wind component (m s^{-1}).
RN(NLEVD) Updated temperature (K).
RNM(NLEVI) Initial/previous temperature (K).
QN(NLEVD) Updated mixing ratio (K).

QNM(NLEVI)	Initial/previous mixing ratio (kg kg^{-1}, nondimensional).
UG(NLEVD)	Zonal geostrophic wind component (m s^{-1}).
VG(NLEVD)	Meridional geostrophic wind component (m s^{-1}).

/GRID/ SS(NLEVD),SSK(NLEVD),MZ,MZM,NOOFGR

SS(NLEVD)	sigma height coordinate, $\sigma = p/p_s$.
SSK(NLEVD)	σ^κ ($\kappa \equiv R_d/C_p$).
MZ	Number of output levels.
MZM	MZ − 1.
NOOFGR	Grid identifier (default is 1 corresponding to a 20 meter resolution, 6 is A18 resolution comparable to AFGL GSM). See section 3.2.2.

/PBL/ DUDT(NLEVD),DVDT(NLEVD),DTDT(NLEVD),DWDT(NLEVD), VERT(NLEVD),ZZ(NLEVD),WINIT(NLEVD),HPBL,MZBL,DELT2,RICR, PINK,DTNW,KOOL,PBLK(NLEVD),CLOUDK(NLEVD),ZLCL,CLTOP,DCZ, IFCLD

DUDT(NLEVD)	u on input to PBL (m s^{-1}), $\partial u/\partial t$ on output (m s^{-2}).
DVDT(NLEVD)	v on input to PBL (m s^{-1}), $\partial v/\partial t$ on output (m s^{-2}).
DTDT(NLEVD)	θ on input to PBL (K), $\partial \theta/\partial t$ on output (K s^{-1}).
DWDT(NLEVD)	q on input to PBL, $\partial q/\partial t$ on output (s^{-1}).
VERT(NLEVD)	Input vertical motion field (m s^{-1}).
ZZ(NLEVD)	Grid levels (m).
WINIT(NLEVD)	Initial mixing ratio profile used for linear damping.
HPBL	Boundary layer height (m).
MZBL	Number of levels for calculations of boundary layer.

parameters, including then level equal to or just

above the HPBL (MZBL is the 1st level above HPBL).

DELT2	Time step (actual time step for each iteration, s).
RICR	Critical Richardson number (default = 0.5).
PINK	p power in K profile (default = 2).
DTNW	Time for Newtonian cooling (s).
KOOL	Newtonian cooling index (default = 0, off).
PBLK(NLEVD)	Diffusivity coefficients due to turbulence (m^2 s^{-1}).
CLOUDK(NLEVD)	Diffusivity coefficients due to clouds (m^2 s^{-1}).
ZLCL	Bottom of cloud layer (m).
CLTOP	Top of cloud layer (m).
DCZ	Thickness of the cloud layer (m).

IFCLD	Cloud diffusivity flag (not implemented in this version).

/SFCL/ TS,WS,CM,CH,U2,V2,T2,TH2,W2,ZZ2,Z0,Z0H,BETA,RIRAD,RIB,RIF TSNOW,Z01,CBAGK

TS	Surface temperature (K).
WS	Effective surface moisture (EVAP = -CH*(W2-WS); defines WS.
CM	Drag coefficient for momentum (m s^{-1}).
CH	Drag coefficient for heat and moisture (m s^{-1}).
U2	u wind component at 1st model level (m s^{-1}).
V2	v wind component at 1st model level (m s^{-1}).
T2	Temperature at 1st model level (K).
TH2	Potential temperature at 1st model level (K).
W2	Mixing ratio at first model level.
ZZ2	Height of 1st model layer (m).
Z0	Roughness length for momentum (m, 0 over the sea).
Z0H	Roughness length for heat (m).
BETA	E/E_p.
RIR	Radiation Richardson number.
RIB	Bulk Richardson number.
RIF	Flux Richardson number.
TSNOW	Snow temperature (K).
Z01	Actual roughness (m, calculated over the sea).
CBAGK	Background diffusivity coefficient (m^2 s^{-1}, 0 by default).

/AUXIL/ PSFC,HEAT,TAOX,TAOY,EVAP,XL,CG,THERM,DELTAT,FH,PRCP,DEW, ACCP,ACCD,UFLX(NLEVD),VFLX(NLEVD),TFLX(NLEVD)

PSFC	Surface pressure (Pa).
HEAT	Surface heat flux (K m s^{-1}).
TAOX	Surface stress (m^2 s^{-2}, zonal).
TAOY	Surface stress (m^2 s^{-2}, meridonal).
EVAP	Surface moisture flux (m s^{-1}).
XL	Monin-Obukhov length (m).
CG	Layered average temperature excess (K).
THERM	Scaled virtual temperature excess (K).
DELTAT	Input time step (s).
FH	Coriolis parameter (s^{-1}).
PRCP	Precipitation at current time step (m s^{-1}).
DEW	Dew at current time step (m s^{-1}).
ACCP	Accumulated precipitation (m).

ACCD	Accumulated dew (m).
UFLX(NLEVD)	Zonal momentum flux (kg m^2 s^{-1}).
VFLX(NLEVD)	Meridonal momentum flux (kg m^2 s^{-1}).
TFLX(NLEVD)	Temperature flux (K m s^{-1}).
QFLX(NLEVD)	Moisture (mixing ratio) flux (m s^{-1}).

/AUXI2/ EP,ETOT,PR

EP	Potential evapotranspiration (m s^{-1}).
ETOT	Accumulated evapotranspiration (m).
PR	Prandtl number (0.74 by default).

/RAD/ FDOWN,MO,DY,TSUN,CLC,TREF,SLO,SLA,ALBEDO,IFCRI,IFPR,SOLARN

FDOWN	Total downward radiative flux (W m^{-2}).
MO	Month.
DY	Elapsed days.
TSUN	Greenwich time (hr).
CLC	Fractional cloud cover.
TREF	Reference temperature for downward longwave radiation and snow (273.16 K by default).
SLO	Longitude.
SLA	Latitude.
ALBEDO	Albedo (fraction).
IFCRI	Flag for cloud-radiation interaction, 1 = cloud cover diagnosed, clouds affect radiation 0 = no clouds diagnosed -1 = clouds diagnosed, clouds do not affect radiation.
IFPR	Flag for parameterized downward longwave radiation, 0=specifed temperature, 1= method following Satterlund, and Paltridge and Platt (default).
SOLARN	Net downward solar radiation, (1-ALBEDO)*S (W m^{-2}).

/SOIL/ WSOIL(NSOLD),CMC,NSOIL,SSOIL,TSOIL(NSOLD),ESD

WSOIL(NSOLD)	Volumetric water content.
CMC	Canopy water content (m).
NSOIL	Number of soil layers.
SSOIL	Soil heat flux (positive upward, W m^{-2}).
TSOIL(NSOLD)	Soil temperature (K).
ESD	Equivalent snow depth (m).

/SOIL1/ IFTC,TSO0,SIGMAF,TSOSAT,TWILT,SCANOP,PC,RC,KWILT,CFACTR, TSOREF

IFTC	Flag = 0, transpiration and canopy package not activated. Any non-zero value activates the transpiration and canopy package.
TSO0	Air dry value.
SIGMAF	Plant shading factor for reduction of direct evaporation.
TSOSAT	Saturation volumetric water content used to determine runoff situations. Default uses the saturation value for soil type 'ISOIL'.
TWILT	Wilting point for plant transpiration. We have not implemented a check for wilting after THETA drops below TWILT. In order to do this, we have to store the logical variable KWILT for each grid point and switch KWILT to true once THETA at the root zone drops below TWILT.
SCANOP	Capacity of water storage by canopy. Default model value = 0.002 m.
PC	Plant coefficient. Fractional value for which a plant reduces transpiration.
RC	Canopy resistance (s m^{-1}), constant if specified in control file, calculated from PC if PC is specified. See description of PC, Record 11, section 3.2.2.
KWILT	"false": water at root zone not dropped below TWILT, "true": water at root zone dropped below TWILT.
CFACTR	Exponent factor of canopy/scanopy in reducing transpiration due to deficit of water (default = 0.5).
TSOREF	Reference value of THETA for transpiration reduction due to water deficit.

/SOIL2/ DSOIL(NSOLD),ISOIL,IFSOIL

DSOIL(NSOLD)	Vertical coordinate for soil moisture and temperature (m). Dimensioned 10. Default is two layer model with ZSOIL(1) = -0.05 m and ZSOIL(2) = -1.0 m.
ISOIL	Soil type, 1 to 11: 1. Sand, 2. Loamy sand, 3. Sandy loam, 4. Silt loam, 5. Loam, 6. Sandy clay loam, 7. Silty clay loam, 8. Clay loam, 9. Sandy clay, 10. Silty clay, 11. Clay.
IFSOIL	flag = 1 the coeffieients of diffusivity and

hydraulic conductivity are computed using the power law directly (default).flag = 2 linear interpolation is done using a pre-calculated table of coefficients. The disadvantage of this option is in a general circulation model when soil type is allowed to vary and the tables need to be re-initialized often.

/SOIL3/ B(11), SATPSI(11), SATKT(11), TSAT(11)

B(11) — Value used in the calculation of soil diffusivity and hydraulic conductivity; a function of the 11 USDA soil textural classes; see BLOCK DATA A2 in the model code (Appendix G.1) for the values of B, SATPSI, SATKT, and TSAT. The 11 USDA soil textural classes are described in this section under /SOIL2/, ISOIL.

SATPSI(11) — Saturation moisture potential.

SATKT(11) — Saturation hydraulic conductivity.

TSAT(11) — Saturation volumetric moisture content.

/SOIL4/ TBOT, ZBOT

TBOT — Soil temperature at bottom of the model layer (283.16 K by default). This is another boundary value for the prognostic equation.

ZBOT — Coordinate of the bottom model layer (3 m by default).

/HCALC/ MZH,TIMEIS

MZH — Grid level at/just above HPBL; tendencies are computed up to this level.

TIMEIS — Model time (hours).

/SNOW/ FLX1,FLX2,FLX3

FLX1 — Heat flux due to warming or cooling of rain ($W\ m^{-2}$).

FLX2 — Heat flux due to conversion of rain water to ice ($W\ m^{-2}$).

FLX3 — Heat flux due to melting snow ($W\ m^{-2}$).

/HYDRO/ ALFA(200),BETA(200)

ALFA(200) — Hydrostatic equation coefficients.

BETA(200) — Hydrostatic equation coefficients.

/ABCI/ AI(NSOLD),BI(NSOLD),CI(NSOLD)

AI(NSOLD)	Lower diagonal array for a tri-diagonal matrix (s^{-1}).
BI(NSOLD)	Diagonal array (s^{-1}).
CI(NSOLD)	Upper diagonal array (s^{-1}).

/LUN/ LUNC,LUNB,LUND

LUNC	Input control file.
LUNB	Binary output file.
LUND	File of dumped initial parameters.

/WFK74/ ALF(7,2)

ALF(7,2)	Table of coefficients for calculation of saturation vapor pressure.

Gravity wave drag calculation: Added common block and its variables

INPUT/OUTPUT:

/gwave/vartpo,hktpo,gwtim,dudtw,dvdtw,dupdt,tau,tauu,tauv

vartpo: an input constant; the variance of topography

hktpo: an input constant; the horizontal wavelength

gwtim: an input constant; equilibrium time scale of a gravity wave

dudtw: an output array; wave induced deceleration of u-wind

dvdtw: an output array; wave induced deceleration of v-wind

dupdt: an output array; parallel wind component

tau: an output array: wave momentum flux (total)

tauu: an output array: x-component wave momentum flux

tauv: an output array: y-component wave momentum flux

4.2 SUBROUTINEs and their Arguments

In this section the SUBROUTINEs used in OSU1DPBL are briefly described, their arguments are given and defined, COMMON blocks and the elements used are listed, and other SUBROUTINEs called are named. Also, some important DATA statements are defined and units are given; unless otherwise noted constants are nondimensional. More detailed information on the COMMON BLOCK elements can be found in section 4.1.2. Further information is available in comment statements throughout the model code found in Appendix D.1. After the program driver (PBLDRV) is described the remaining SUBROUTINEs are listed in alphabetic order.

PROGRAM PBLDRV

While PBLDRV is not a SUBROUTINE, it is the main program that drives OSU1DPBL and is included here for completeness.

COMMON BLOCKS/ELEMENTS USED:

INPUT OR INITIALIZED:

/FIELDS/	UG, VG
/GRID/	SS, SSK (CURRENT), NOOFGR, MZ, MZM
/SOIL/	WSOIL, CMC, NSOIL, TSOIL, ESD
/SOIL1/	IFTC, TSO0, SIGMAF, TSOSAT, TWILT, SCANOP, PC, TSOREF
/SOIL2/	DSOIL, ISOIL
/PBL/	ZZ (CURRENT), WINIT, RICR, PINK, DTNW, KOOL, IFCLD
/SFCL/	Z0, TSNOW
/AUXIL/	PSFC, PRCP, UFLX, VFLX, TFLX, QFLX
/RAD/	FDOWN, MO, DY, CLC, TREF, SLO, SLA, ALBEDO, IFCRI, IFPR
/AUX12/	ETOT
/XLUN/	LUNC
/HCALC/	TIMEIS (CURRENT)
/gware/	vartpo, hktpo, gwtim, dudtw(NLEVD), dvdtw(NLEVD), dupdt(NLEVD), tau(NLEVD), tauu(NLEVD), tauv(NLEVD)

OUTPUT OR MODIFIED:

/FIELDS/	UN, UNM, VN, VNM, RN, RNM, QN, QNM
/GRID/	SSK (UPDATED)
/SOIL/	SSOIL
/PBL/	DUDT, DVDT, DTDT, DWDT, ZZ (UPDATED), MZBL, DELT2
/SFCL/	TS, WS, U2, V2, T2, TH2, W2, ZZ2

/AUXIL/	DEW, ACCP, ACCD
/RAD/	TSUN
/XLUN/	LUNB, LUND
/HCALC/	TIMEIS (UPDATED)

SUBROUTINES CALLED: WINTB (FOR MACINTOSH), TIME and DATE (for VAX), ZTOSIG, HFAK, CHACHA, SIGTOZ, SUN, SFLX, PBLL, SVP, SSHEAT, ERR1, PRINT

DATA:

INIL	Number of levels in a particular grid.
IGRID	Grid level array for the 6 different grids.
ZUNIT	Unit used to multiply by IGRID to get actual height.
INIT	Flag for printout after first timestep.
MZ0	Used in vertical grid fit in SUBROUTINE CHACHA.
XSKIP	Used in vertical grid fit in SUBROUTINE CHACHA.
G	Gravitaitional constant (9.806 m s^{-2}).
RD	Gas constant for dry air (287.0 J kg^{-1} K^{-1}).
GRD	G/RD (0.0342 K m^{-1}).
MBTOKA	Constant used to convert from mb to Pa (100 Pa mb^{-1}).
CP	Specific heat of dry air (1004.5 J kg^{-1} K^{-1}).

SUBROUTINE CHACHA (XO,ZO,MO1,MO2,XI,ZI,I1,I2,XSKIP,Q)

Fits data to the specified vertical grid.

ARGUMENTS:

XO	Output function value on the new grid, dimensioned (1:MO2).
ZO	Grid coordinate on which the function is to be interpolated, dimensioned(1:MO2).
MO1	Starting point for output grid.
MO2	Ending point for output grid.
XI	Input function value, dimensioned (1:I2).
ZI	Input grid coordinate, dimensioned (1:I2).
I1	Starting point to interpolate.
I2	Ending point to interpolate.
XSKIP	Interpolation only occurs when XO(I)=XSKIP.
Q	Work array.

SUBROUTINE CLOUD (JPBL, CLC)

This routine calculates the fractional cloud cover as a function of the maximum relative humidity in the boundary layer and the relative humidity variance at the same level; the variance depends on both turbulent and mesoscale (subgrid) effects.

ARGUMENTS:

INPUT:

JBPL	First level above the boudary layer top.

OUTPUT:

CLC	Fractional cloud cover.

COMMON BLOCKS/ELEMENTS USED:

INPUT:

/SFCL/	TS, WS, TH2
/PBL/	RN(NLEVD), WN(NLEVD), ZZ(NLEVD), PBLK(NLEVD)
/AUXIL/	PSFC, HEAT, TAOX, TAOY, EVAP
/GRID/	SS(NLEVD), SSK(NLEVD)

SUBROUTINES CALLED: SVP.

SUBROUTINE DFKT (DF,KT,THETA)

Compute soil water diffusivity and hydraulic conductivity.

ARGUMENTS:

INPUT:

THETA	Volumetric water content.

OUTPUT:

DF	Soil water diffusivity (m^2 s^{-1}).
KT	Hydraulic conductivity (m s^{-1}).

COMMON BLOCKS/ELEMENTS USED:

INPUT:

/SOIL2/	ISOIL, IFSOIL
/SOIL3/	B, SATPSI, SATKT, TSAT

DATA:

KDFKT	flag, = 0 for initial calculation of DF and KT, = ISOIL after initialization.

SUBROUTINE ERR1 (IROW,ICOL)

This is an error-checking routine designed to inform the user if there is a problem in SUBROUTINE CHACHA.

ARGUMENTS:

INPUT:

IROW	Row index returned from call to subroutine CHACHA.
ICOL	Column returned from call to subroutine CHACHA.

SUBROUTINE HFAK (S,N)

Computes factors for use in the hydrostatic equation. Output through COMMON HYDRO.

ARGUMENTS:

INPUT:

S	Sigma vector.
N	Number of levels.

OUTPUT:

None.

COMMON BLOCKS/ELEMENTS USED:

OUTPUT:

/HYDRO/ ALFA, BETA

DATA:

CP	Specific heat of dry air (1004.5 J kg^{-1} K^{-1}).
G	Gravitational constant (9.806 m s^{-2}).
RGAS	Gas constant for dry air (287.0 J kg^{-1} K^{-1}).

SUBROUTINE HFLX (S,TS,TS1,T1,Z1)

Computes the soil heat flux at the surface.

ARGUMENTS:

INPUT:

TS	Surface temperature (K).
TS1	First layer soil temperature (K).
T1	First soil layer volumetric water content.
Z1	Coordinate of the first soil layer (m).

OUTPUT:

S	Soil heat flux (W m^{-2}).

SUBROUTINES CALLED: KTSOIL

SUBROUTINE HRT (RHSTS,TS,TSOIL,THETA,NSOIL,Z,YY,ZZ1)

Computes the tendency terms for the soil thermodynamic diffusion equation and the matrix elements for the implicit time-integration scheme.

ARGUMENTS:

INPUT:

RHSTS	Right hand side of the soil thermal diffusion equation.

OUTPUT:

TS	Surface temperature (K).
TSOIL	Soil temperature (K), dimensioned NSOIL.
THETA	Soil volumetric water content, dimensioned NSOIL.
NSOIL	Number of soil layers.
Z	Soil layer coordinates, dimensioned NSOIL.
YY, ZZ1	Factors to use the sfc energy balance as boundary condition.

COMMON BLOCKS/ELEMENTS USED:

INPUT:

/SOIL2/	ISOIL
/SOIL3/	TSAT
/SOIL4/	TBOT, ZBOT

OUTPUT:

/ABCI/	AI, BI, CI

SUBROUTINES CALLED: KTSOIL

DATA:

CSOIL	Volumetric heat capacity, soil (1.25×10^6 J m^{-3} K^{-1}).
CH2O	Volumetric heat capacity, water (4.2×10^6 J m^{-3} K^{-1}).
CAIR	Volumetric heat capacity, air (1280.7 J m^{-3} K^{-1}).

SUBROUTINE HSTEP (TSOIL,RHSTS,DELTAT,NSOIL)

Updates the soil temperature field.

ARGUMENTS:

INPUT:

TSOIL	Soil temperature array (K).
RHSTS	Right hand side of the soil thermal diffusion equation.
DELTAT	Time step (s).
NSOIL	Number of soil layers.

OUTPUT:

TSOIL	Updated soil temperature array (K).
RHSTS	Updated right hand side of the soil thermal diffusion equation (K s^{-1}).

COMMON BLOCKS/ELEMENTS USED:

INPUT:

/ABCI/	AI, BI, CI

OUTPUT:

/ABCI/	AI (Updated), BI (Updated), CI (Updated)

SUBROUTINES CALLED: ROSR12

SUBROUTINE KTSOIL (DF,THETA)

Computes soil thermal conductivity.

ARGUMENTS:

INPUT:

THETA	Volumetric water content of the soil layer.

OUTPUT:

DF	Thermal diffusivity of the soil layer.

COMMON BLOCKS/ELEMENTS USED:

INPUT:

/SOIL2/	ISOIL
/SOIL3/	SATPSI, TSAT

DATA:

KDFKT	flag, = 0 for initial calculation of DF and KT, = ISOIL after initialization.

SUBROUTINE LCL (T,P,Q,PLCL,TLCL)

Finds lifting condensation level data.

ARGUMENTS:

INPUT:

T	Temperature (K)
P	Pressure (Pa)
Q	Specific humidity (kg kg^{-1})

OUTPUT:

PLCL	Lifting condensation level pressure (Pa)
TLCL	Saturation point temperature (K)

COMMON BLOCKS/ELEMENTS USED:

INPUT:

/WFK74/ ALF(7,2)

SUBROUTINES CALLED: TDEW

DATA:

EPS	Ratio molecular weight water vapor/dry air (0.622).
TO	Triple point of water (273.16 K).
CP	Specific heat of dry air (1004.5 J kg^{-1} K^{-1}).
RGAS	Gas constant for dry air (287.0 J kg^{-1} K^{-1}).

SUBROUTINE PBLL (IFREE,ENVK,IFKPBL,RKFAC,RB2)

This subroutine contains the code necessary to compute the tendencies due to boundary layer mixing. Arguments passed as input are used as the controlling parameters for the free atmospheric diffusion and local generation in the stable boundary layer. Arguments passed as output aare used only for print out.

ARGUMENTS: Most, input/output through COMMON blocks.

INPUT:

IFREE	a flag for free atmospheric diffusion calculation (1 for true)
IFKPBL	a flag for local generation of turbulence in the stable boundary layer
RKFAC	a real factor to enhance/reduce $l_{0,h}$ in the free atmosphere

OUTPUT:

ENVK	an array containing K_m (only for print)
RB2	the bulk richardson number computed for the lowest level (only for print)

COMMON BLOCKS/ELEMENTS USED:

INPUT:

/PBL/	ZZ, WINIT, MZBL, DTBL, RICR, PINK, DTNW, KOOL, IFCLD
/SFCL/	TS, WS, CM, CH, U2, V2, T2, TH2, W2, ZZ2, CBAGK
/AUXIL/	PSFC
/RAD/	CLC
/GRID/	SS, SSK
/AUX12/	PR

OUTPUT:

/PBL/	UN, VN, RN, WN, HPBL, PBLK, CLOUDK, ZLCL, CLTOP, DCZ
/SFCL/	RIF
/AUXIL/	HEAT, TAOX, TAOY, EVAP, XL, CGH, THERM, UFLX, VFLX, TFLX, WFLX
/HCALC/	MZH

SUBROUTINES CALLED: STBCLC, UNSCLC

DATA:

VK	Von Kármán constant (0.40).

G	Gravitational acceleration (9.806 m s^{-2}).
FAK	Coefficient in countergradient term (8.5).
BETAM	Nondimensional profile function for shear, unstable case (15.0).
BETAH	Nondimensional profile function for heat, unstable case (15.0).
SFFRAC	Surface layer fraction of boundary layer depth (0.1).
FBC	Factor used in determining atmospheric diffusion (0.5).
ONET	Coefficient in profile function for momentum (0.333).
CCCRT	Critical RH value used in unstable-case fractional cloud cover calculation (40.0%).
C4,C5,C6	More critical RH values used in unstable-case fractional cloud cover calculation (123.6,34.0, C6=(CCCRT-C5)/(100.0-C5)/CCCRT.
BGK	Used with CBAGK (see COMMON BLOCK /SFCL/).
CCON	FAK x SFFRAC x VK.
BINM, BINH	BETAM x SFFRAC, BETAH x SFFRAC.

SUBROUTINE PRINT

All binary output is written from this routine.

ARGUMENTS: None, input/output through COMMON BLOCKs.

COMMON BLOCKS/ELEMENTS USED:

INPUT:

/FIELDS/	UN, VN, RN, QN, UG, VG
/GRID/	SS, SSK, MZ, MZM, NOOFGR
/SOIL/	WSOIL, CMC, NSOIL, SSOIL, TSOIL, ESD
/SOIL2/	DSOIL, ISOIL
/PBL/	ZZ, HPBL, MZBL, PBLK, CLOUDK, ZLCL
/SFCL/	CM, CH, TS, T2, TH2, W2, ZZ2, Z0, RIR, RIB, RIF
/AUXIL/	PSFC, HEAT, TAOS, TAOY, EVAP, XL, CG, THERM, FH, PRCP, DEW, ACCP, ACCD, FUL, FVL, FHL, FWL
/RAD/	FDOWN, MO, DY, CLC
/AUX12/	EP, ETOT, PR
/SNOW/	FLX1, FLX2, FLX3
/XLUN/	LUNB
/HCALC/	JPBL, HO

SUBROUTINES CALLED: LCL, SVP, TDEW, SP, TOPQ

SUBROUTINE ROSR12 (PP,AA,BB,CC,DD,DELT,M)

Inverts a tri-diagonal matrix.

ARGUMENTS:

INPUT:

AA	Lower diagonal elements.
BB	diagonal elements.
CC	Upper diagonal elements.
DD	Forcing of the tri-diagonal matrix equation, [ ]p = D.
M	Dimension of all arrays.

OUTPUT:

P	Solution of the tri-diagonal matrix equation, [ ]p = D.
DELT	Working array.

SUBROUTINE SEC (EC,EPOTNL,CANOPY)

Computes canopy evaporation.

ARGUMENTS:

INPUT:

EPOTNL	Potential evaporation (m s^{-1}).
CANOPY	The canopy water content (m).

OUTPUT:

EC	Canopy evaporation (m s^{-1}).

COMMON BLOCKS/ELEMENTS USED:

INPUT:

/SOIL1/	SIGMAF, SCANOP, CFACTR

SUBROUTINE SEDIR (EDIR,EPOTNL,THETA1,Z1)

Compute direct evaporation from bare soil.

ARGUMENTS:

INPUT:

EPOTNL	Potential evaporation (m s^{-1}).
THETA1	First soil layer volumetric water content.
Z1	Depth of the first soil layer (m).

OUTPUT:

EDIR	Direct evaporation (m s^{-1}).

COMMON BLOCKS/ELEMENTS USED:

INPUT:

/SOIL1/	IFTC, TSO0, SIGMAF

SUBROUTINES CALLED: DFKT

DATA:

DF0	Flag (=0) when determining soil moisture diffusivity and hydraulic conductivity for air dry value, TSO0.

SUBROUTINE SET (ET,NSOIL,EPOTNL,THETA,CANOPY,Z)

Computes transpiration due to plants.

ARGUMENTS:

INPUT:

NSOIL	Number of soil layers.
EPOTNL	Potential evaporation (m s^{-1}).
THETA	Volumetric water content.
CANOPY	The canopy water content (m).
Z	Coordinate of the soil layer (m).

OUTPUT:

ET	Transpiration rate (m s^{-1}).

COMMON BLOCKS/ELEMENTS USED:

INPUT:

/SOIL1/	SIGMAF, TWILT, SCANOP, PC, KWILT, CFACTR, TSOREF

SUBROUTINE SFLX (F,S,PSFC,PRCP,DEW,DT,IFHF,IFSNO)

This subroutine is responsible for calculating surface exchange coefficients, estimating potential evapotranspiration from the modified-Penman surface energy balance method, and iterating the soil model.

ARGUMENTS:

INPUT:

F	Net downward radiation = solar + downward atmospheric (positive downward, W m^{-2}).
PSFC	Surface pressure (Pa).
PRCP	Precipitation rate (m s^{-1}).
DT	Time step (s).
IFHF	Flag for soil heat flux (1 = yes, 0 = no).
IFSNO	Flag for snow (1 = yes, 0 = no).

OUTPUT:

S	Soil heat flux (positive downward, W m^{-2}).
DEW	Dew fall rate (m s^{-1}).

COMMON BLOCKS/ELEMENTS USED:

INPUT:

/SFCL/	T1 (PRESENT), U2, V2, T2, TH2, Q2, Z, ZO, TO
/SOIL/	SMC, CMC, NSOIL, SSOIL, STC
/SOIL2/	ZSOIL, ISOIL
/AUX12/	PR

OUTPUT:

/SFCL/	T1 (UPDATED), Q1, CM, CH, BETA, RIR, RIB, ZO1
/SOIL/	ESD
/AUX12/	EP, ETOT
/SNOW/	FLX1, FLX2, FLX3

SUBROUTINES CALLED: HFLX, SVP, SMFLX, KTSOIL, SHFLX, TDEW

DATA:

ELV	Latent heat of condensation (2.5 x 10^6 J kg^{-1}).
SIGMA	Stephan-Boltzmann constant (5.67 x 10^{-8} W m^{-2} K^{-4}).
CP	Specific heat of dry air (1004.5 J kg^{-1} K^{-1}).
RGAS	Gas constant for dry air (287.0 J kg^{-1} K^{-1}).
EXMCH	Used in calculating surface exchange coefficients under stable conditions (-1.0).
B1	Used in calculating surface exchange coefficients

	under unstable conditions (9.4).
CUS	Used in calculating surface exchange coefficient for momentum (7.4).
RCUCT	Used in relating momentum and heat exchange coefficients (0.716).
VK	Von Kármán constant (0.40).
G	Gravitational acceleration (9.806 m s^{-2}).
SFAK	(4 x SIGMA x RGAS)/CP (6.48 x 10^{-8} W m^{-2} K^{-4}).
ELCP	ELV/CP (2.4888 x 10^{3} K).
CPICE	Specific heat capacity for ice (2.106 x 10^{3} J kg^{-1} K^{-1}).
ELI	Latent heat of fusion (3.335 x 10^{5} J kg^{-1}).
DFS	HAS TO DO WITH SNOW HEAT FLUX? (0.13).
CPH2O	Specific heat for water (4.218 x 10^{3} J kg^{-1} K^{-1}).

SUBROUTINE SHFLX (S,TSOIL,THETA,NSOIL,TS,DELTAT,YY,ZZ1)

Computes the *soil* heat flux.

ARGUMENTS:

INPUT:

S	Soil heat flux defined as positive downward (W m^{-2}).
TSOIL	Layer averaged soil temperature (K) dimensioned NSOIL. The internal default number of layer is 2 with top layer 5 cm thick and layer 95 cm thick. TSOIL is a prognostic variable, on input the value for the current time step is given.
THETA	Layer averaged volumetric water content for the soil dimensioned NSOIL. This variable should be updated by the routine SMFLX before this routine is called.
NSOIL	Number of soil layers to be used. If the number is not 2, the internal parameter Z (in labeled COMMON SOIL2) needs to be re-initialized.
TS	Surface temperature (K). This serves as a boundary value for the prognostic equation.
DELTAT	Time step for updating TSOIL (s). A practical limit is 2 hours. For thin layers, a smaller time step would be needed.
YY,ZZ1	Factors to calculate TS implicitly together with TSOIL.

OUTPUT:

S	Updated soil heat flux (W m^{-2}).
TSOIL	Layer averaged soil temperature (K) dimensioned NSOIL. TSOIL is a prognostic variable, on output the updated value for the next time step is returned.
TS	Updated surface temperature (K). This serves as a boundary value for the prognostic equation.

COMMON BLOCKS/ELEMENTS USED:

INPUT:

/SOIL2/ Z, ISOIL

/SOIL4/ TBOT, ZBOT

OUTPUT:

/XLUN/ LUNB, LUNC

SUBROUTINES CALLED: HRT, HSTEP, HFLX

SUBROUTINE SIGTOZ (Z,T,Q,N)

Computes heights at each of the σ levels.

ARGUMENTS:

INPUT:

T	Temperature (K).
Q	Mixing ratio (kg kg^{-1}).
N	Number of levels.

OUTPUT:

Z	Height (m).

COMMON BLOCKS/ELEMENTS USED:

INPUT:

/HYDRO/ ALFA, BETA

SUBROUTINE SMFLX (EVAP,RUNOFF,THETA,NSOIL,CANOPY,EPOTNL, DELTAT,PRECIP)

Computes soil moisture flux. The soil moisture content (per unit volume) THEAT is a dependent variable that is updated, as well as the canopy water content (CANOPY), through prognostic equations.

ARGUMENTS:

INPUT:

EVAP	Actual evaporation (m s^{-1}).
RUNOFF	Any precipitation that cannot flow through the top layer within a given time step is considered runoff (m s^{-1}).
THETA	Layer averaged volumetric water content for the soil dimensioned NSOIL. The internal default number of layers is 2 with top layer 5 cm thick and bottom 95 cm thick. THETA is a prognostic variable, on input the value for current time is given.
NSOIL	Number of soil layer to be used. If the number is not 2, the internal parameter Z (in labeled COMMON SOIL2) needs to be re-initialized.
CANOPY	Canopy water content (m) If the internal parameter IFTC (in COMMON SOIL1) is given a non-zero value. Update to next time step is done. When IFTC is zero, CANOPY is not included.
EPOTNL	Potential evaporation (m s^{-1}) from modified Penman.
DELTAT	Time step for updating THETA and CANOPY (s). A practical limit is 2 hours. For thin layers, a smaller time step would be needed.
PRECIP	Precipitation rate (m s^{-1}).

OUTPUT:

EVAP	Updated actual evaporation (m s^{-1}).
THETA	Updated layer averaged volumetric water content for the next time step for the soil dimensioned NSOIL.
CANOPY	Updated canopy water content (m).

COMMON BLOCKS/ELEMENTS USED:

INPUT:

/SOIL1/	IFTC, SIGMAF, TSAT, SCANOP
/SOIL2/	Z, ISOIL, IFSOIL

SUBROUTINES CALLED: THSAT, SEDIR, SET, SEC, SRC, SRT, SSTEP

DATA:

KDFKT	flag, = 0 for initial calculation of DF and KT, = ISOIL after initialization.

SUBROUTINE SP (SS,PSFC,PLCL,ZZ,J,MZ,ZSP,NLEVD)

Computes geopotential height of the LCL.

ARGUMENTS:

INPUT:

SS	Sigma value.
PSFC	Surface pressure (Pa).
ZZ	Coordinate of the boundary layer (m).
J	Index for which the SP point is sought.
MZ	Number of atmospheric layers.
NLEVD	Number of dimensioned output levels.

OUTPUT:

PLCL	Lifting condensation level pressure (Pa).
ZSP	Saturation point height (m), if none found, ZSP = -1.

DATA:

CP	Specific heat of air (1004.5 J kg^{-1} K^{-1}).
LV	Latent heat (2.5E+6 J kg^{-1}).

SUBROUTINE SRC (RHSCT,EC,PRECIP)

Computes the time tendency for canopy water.

ARGUMENTS:

INPUT:

EC	Canopy evaporation (m s^{-1}).
PRECIP	Precipitation rate (m s^{-1}).

OUTPUT:

RHSCT	Right hand side of the soil hydrological diffusion equation (s^{-1}).

COMMON BLOCKS/ELEMENTS USED:

INPUT:

/SOIL1/ SIGMAF

SUBROUTINE SRT (RHSTT,RUNOFF,EDIR,ET,THETA,NSOIL,PRECIP,Z

Computes the tendency of the soil hydrology diffusion equation and matrix coefficients for the implicit time integration.

ARGUMENTS:

INPUT:

EDIR	Direct evaporation (m s^{-1}).
ET	Transpiration rate (m s^{-1}).
THETA	Volumetric water content.
NSOIL	Number of soil layers.
PRECIP	Precipitation rate (m s^{-1}).
Z	Coordinate of the soil layers (m).

OUTPUT:

RHSTT	Right hand side of soil hydrology diffusion equation (s^{-1}).
RUNOFF	Excess precipitation that becomes runoff (m s^{-1}).

COMMON BLOCKS/ELEMENTS USED:

INPUT:

/SOIL1/ TSAT

OUTPUT:

/ABCI/ AI, BI, CI

SUBROUTINES CALLED: DFKT

DATA:

DSAT	Initial value of soil moisture diffusivity (0.0 m^2 s^{-1}).

SUBROUTINE SSHEAT (Q,T,P)

Computes super-saturation adjustment if the mixing ratio exceeds its saturation value.

ARGUMENTS:

INPUT:

Q	Supersaturation mixing ratio, Q greater than QSAT(T) (kg kg^{-1}).

T	Temperature (K).
P	Pressure (Pa).

OUTPUT:

Q	Adjusted saturation mixing ratio (kg kg^{-1}).
T	Adjusted temperature (K).

DATA:

CP	Specific heat of air (1004.5 J kg^{-1} K^{-1}).
LV	Latent heat (2.5 x 10^6 J kg^{-1}).

SUBROUTINE SSTEP (THETA,CANOPY,RHSTT,RHSCT,DELTAT,NSOIL, RUNOFF)

Updates both soil and canopy water content.

ARGUMENTS:

INPUT:

THETA	Volumetric water content.
CANOPY	Canopy water content (m).
RHSTT	Right hand side of the soil hydrological diffusion equation (s^{-1}).
RHSCT	Right hand side of the canopy prediction equation (m s^{-1}).
DELTAT	Time step (s).
NSOIL	Number of soil layers.

OUTPUT:

THETA	Updated volumetric water content.
CANOPY	Updated canopy water content (m).
RUNOFF	Any precipitation that cannot flow through the top layer within a given time step is considered runoff (m s^{-1}).

COMMON BLOCKS/ELEMENTS USED:

INPUT:

/SOIL1/	IFTC, SCANOP
/ABCI/	AI, BI, CI

SUBROUTINES CALLED: ROSR12

SUBROUTINE SUN

All radiation information is calculated in this subroutine (solar, terrestrial, atmospheric); output through COMMON RAD.

ARGUMENTS: None, input/output through COMMON block RAD.

COMMON BLOCKS/ELEMENTS USED:

INPUT:

/FIELDS/ RNM, QNM
/PRL/ ZZ
/GRID/ SS, MZ, NOOFGR
/RAD/ MO, DY, HO, CLC, SLO, SLA, ALBEDO, IFCRI, IFPR
/AUXIL/ PSFC

OUTPUT:

/RAD/ FDOWN, TREF, SOLARN

DATA:

PI	π used in solar elevation calculations (3.14159).
DNF	Constant multiplied by day of year to convert to angle in full circle (0.986).
HNF	Used in conversion from hour of day to hour angle of sun (15.0 degrees/hour).
XA1	Solar constant used with SFI to determine incoming solar radiation under clear sky conditions (990.0 W m^{-2}).
XA2	Empirical reduction factor used with SFI to determine incoming solar radiation under clear sky conditions (-30.0 W m^{-2}).
C1	Stephan-Boltzmann constant (5.67 x 10^{-8} W m^{-2} K^{-4}).
C2	Constant used in calculating downward longwave radiation from clouds (60.0 W m^{-2}).

SUBROUTINE SVP (QS,ES,P,TA)

Calculates saturation vapor pressure.

ARGUMENTS:

INPUT:

P	Pressure (Pa).
TA	Temperature (K).

OUTPUT:

QS	Saturation mixing ratio (kg kg^{-1}).

ES Saturation vapor pressure (Pa).

COMMON BLOCKS/ELEMENTS USED:

INPUT:

/WFK74/ ALF(7,2)

DATA:

EPS	Ratio molecular weight water vapor/dry air (0.622).
T0	Triple point of water (273.16 K).

SUBROUTINE TDEW (Q,P,TA,TD)

Calculate the dew-point temperature by isobaric-adiabatic cooling.

ARGUMENTS:

INPUT:

Q	Mixing ratio (kg kg^{-1}).
P	Pressure (Pa).
TA	Temperature (K).

OUTPUT:

TD	Dew point temperature (K).

COMMON BLOCKS/ELEMENTS USED:

INPUT:

/WFK74/ ALF(7,2).

DATA:

EPS	Ratio molecular weight water vapor/dry air (0.622).
T0	Triple point of water (273.16 K).

SUBROUTINE THSAT (THETA)

Finds volumetric water content.

ARGUMENTS:

INPUT:

None.

OUTPUT:

THETA	Volumetric water content

COMMON BLOCKS/ELEMENTS USED:

INPUT:

/SOIL2/	ISOIL
/SOIL3/	TSAT

SUBROUTINE TOPQ (Q2,T2,P2,Q1,T1,P1)

Provides temperature and saturation mixing ratio at level 2 given equivalent potential temperature at level 1 (the surface).

ARGUMENTS:

INPUT:

Q1	Saturation mixing ratio (kg kg^{-1}).
T1	Temperature (K).
P1	Pressure (Pa).
P2	Pressure (Pa).

OUTPUT:

Q2	Saturation mixing ratio (kg kg^{-1}).
T2	Temperature (K).

SUBROUTINES CALLED: SVP

DATA:

CP	Specific heat of dry air (1004.5 J kg^{-1} K^{-1}).
DTDP	Change in temperature with pressure (4.5×10^{-4} K Pa^{-1})
G	Gravitational constant (9.806 m s^{-2}).
LV	Latent heat of condensation (2.5×10^{6} J kg^{-1}).
RGAS	Gas constant for dry air (287.0 J kg^{-1} K^{-1}).

SUBROUTINE ZTOSIG (S,T,Q,Z,N)

Computes σ as a function of Z.

ARGUMENTS:

INPUT:

T	Temperature (K).
Q	Mixing ratio (kg kg^{-1}).
Z	Height (m).
N	Number of levels.

OUTPUT:

S	Sigma vector = P(I)/PSFC.

DATA:

CP	Specific heat of dry air (1004.5 J kg^{-1} K^{-1}).
G	Gravitational constant (9.806 m s^{-2}).
RGAS	Gas constant for dry air (287.0 J kg^{-1} K^{-1}).

SUBROUTINE SFCXCH (T1,T2,TH2,Q1,Q2,Z,Z0,Z0H,Z01,S2,SPD,RIB, CM,CH)

Finds the bulk Richardson number and surface exchange coefficients for momentum and heat.

ARGUMENTS:

INPUT:

T1	Surface temperature from surface energy balance (K).
T2	Air temperature from first model level (K).
TH2	Potential temperature from first model level (K).
Q1	Surface specific humidity from surface energy balance.
Q2	Specific humidity from the first model leve.
Z	Height of first model level (m).
Z0	Roughness length for momentum (m, 0 over the sea).
Z0H	Roughness length for heat (m).
Z01	Actual roughness length for hmomentum (m, calculated over the sea).
S2	Square of wind speed at the first model level (m^2 s^{-2}).
SPD	Wind speed at the first model level (m s^{-1}).

OUTPUT:

RIB	Bulk Richardson number.
CM	Surface exchange coefficient for momentum (m s^{-1}).
CH	Surface exchange coefficient for heat (m s^{-1}).

COMMON BLOCKS/ELEMENTS USED:

INPUT:

/SOIL2/	ISOIL
/SOIL3/	TSAT

Description of variables

subroutine gwls(psfc)

This subroutine calculates the acceleration of u and v wind components due to wave stress divergence. The gravity wave stress is computed for linear, monochromatic, and sinusoidal gravity waves with a zero-order lower boundary condition and the wave stress saturation condition with respect to convective instability (Kim and Mahrt, 1991).

ARGUMENTS:

INPUT:

psfc: surface pressure

COMMON BLOCKS USED/ADDED

INPUT: see main subroutine for description

/fields/

/grid/

/pbl/

/sfcl/

INPUT/OUTPUT:

/gwave/vartpo,hktpo,gwtim,dudtw,dvdtw,dupdt,tau,tauu,tauv

LOCAL VARIABLES

theta, upl, taucnv; potential temperature, parallel wind, and wave stress divergence at full level

tht, uht, vht, bf, vwl, tausat: θ, u, v, N, vertical wave number, and saturated wave stress at half level

tmpht, ssht,rho: temperature, σ value, and density at half level

dz, gam, gamp: layer thickness, γ, $gamma'$ at half level (see Kim and Mahrt, 1991)

CONSTANTS

cp, rd: specific heat and gas constant of dry air

rkapa, rkpinv, gcp: $\kappa = R_d/C_p$, $1/\kappa = C_p/R_d$, g/C_p

hleng: horizontal wavelength of the topography

utop, vtop, ttop, sstop: u, v, θ, and σ at the mountain-top level (do loop 10)

bftop, uvtop, ptop, rhotop: N, $|V|$, pressure, and density at the mountain top level

hsmax, taus: maximum value of topographic variance and surface stress (see Kim and Mahrt, 1991)

cnst0, cnst1: $\rho N|V|$ and $N/(\rho|V|^3$ at the mountain top level to be used to compute γ and γ'

ufac: magnitude of x component of unit vector parallel to the surface wind vfac*: magnitude of the y component of unit vector parallel to the surface wind

__subroutine gws__(psfc)

This subroutine calculates the acceleration of u and v wind components due to wave stress divergence. The gravity wave stress is computed for linear, monochromatic, and sinusoidal gravity waves with a first-order lower boundary condition and the wave stress saturation condition with respect to convective instability (Kim and Mahrt, 1991).

common blocks, local variables and constants are the same as the subroutine gwls except for the additional variable **phi**

phi: vertical wave phase at half level

__subroutine gwlss__(psfc)

This subroutine calculates the acceleration of u and v wind components due to wave stress divergence. The gravity wave stress is computed for linear, monochromatic, and sinusoidal gravity waves with a zero-order lower boundary condition and the wave stress supersaturation condition with respect to convective instability (Kim and Mahrt, 1991).

common blocks, local variables and constants are the same as the subroutine gwls except for the additional variable sps

ADDITIONAL VARIABLES TO subroutine gwls

sps: degree of supersaturation at half level

__subroutine gwss__(psfc)

This subroutine calculates the acceleration of u and v wind components due to wave stress divergence. The gravity wave stress is computed for linear, monochromatic, and sinusoidal gravity waves with a first-order lower boundary condition and the wave stress supersaturation condition with respect to convective instability (Kim and Mahrt, 1991 or user's guide).

common blocks, local variables and constants are the same as the subroutine gwls except for the additional variable **phi** and sps

ADDITIONAL VARIABLES TO subroutine gwls

phi: vertical wave phase at half level

sps: degree of supersaturation at half level

---

* **ufac** and **vfac** are multiplied by an equilibrium time scale and used to convert the deceleration of the parallel wind to the deceleration of the x and y wind components

4.3 Other Subprograms

OSU1DPBL contains other subprograms which are described in the following sections.

4.3.1 BLOCK DATA

In the four BLOCK DATA all common block elements are initialized (a Machintoch FORTRAN compiler requirement), some with real data, other with dummy values (zeros). The table below lists the BLOCK DATA subprograms, the common blocks they contain, and the elements that are initialized with real data.

BLOCK DATA	Variable Category	COMMON blocks	Elements Initialized
A1	Radiation	/AUX12/	PR, ETOT
		/SNOW/	FLX1, FLX2, FLX3
		/RAD/	TREF, IFPR
		/SFCL/	TSNOW, CBAGK
A2	Soil Model	/SOIL/	NSOIL
		/SOIL1/	SATT, KWILT, CFACTR
		/SOIL2/	Z(11), IFSOIL
		/SOIL3/	B(11), SATPSI(11), SATKT(11), TSAT(11)
		/SOIL4/	TBOT, ZBOT
A3	"α" tables	/WFK74/	ALF(7,2)
A4	Logical units & misc.	/PBL/	RICR,PINK, KOOL, PBLK(100)
		/GRID/	NOOFGR
		/XLUN/	LUNC, LUNB, LUND

4.3.2 FUNCTIONs

Four FUNCTION subprograms are included in OSU1DPBL.

FUNCTION DQSDT (TA,P)

Calculates change of saturation mixing ratio with temperature.

ARGUMENTS:

INPUT:

TA	Temperature in °C.
P	Pressure in Pa.

OUTPUT:

DSQDT	As noted above.

COMMON BLOCKS/ELEMENTS USED:

INPUT:

/WFK74/ ALF(7,2)

DATA:

EPS	Ratio molecular weight water vapor to dry air (0.622).
T0	Reference temperature (273.16 K).

FUNCTION T2M (PZ, PT2, PHABS, PTST, PUST, PVIRFX)

Calculates the potential temperature at 2 meters, following Holtslag (1987).

ARGUMENTS:

INPUT:

PZ	Height of first model layer (m).
PT2	Potential temperature at first model layer (°K).
PHABS	Absolute temperature for Obukhov length (°K).
PTST	θ_* (°K).
PUST	u_* (m s^{-1}).
PVIRFX	Virtual heat flux (W m^{-2}).

OUTPUT:

T2M	As noted above.

FUNCTION FPSIM (ETA)

Calculates the stability correction function in the surface layer wind profile.

ARGUMENTS:

INPUT:

ETA z/L (z/Obukhov length).

OUTPUT:

FPSIM As noted above.

FUNCTION FPSIH (ETA)

Calculates the stability correction function in the surface layer temperature profile.

ARGUMENTS:

INPUT:

ETA z/L (z/Obukhov length)

OUTPUT:

FPSIH As noted above.

APPENDIXES

A. OSU1DPBL Users

B. Model Changes for version 1.0.4
   - From version 1.0.3
   - From version 1.0.2
   - From version 1.0.1
   - Future proposed additions and changes
   - Current model limitations
   - Gravity wave model

C. Model references

D. Source Codes
   - OSU1DPBL.for
   - PRINT1DPBL.for

Appendix A OSU1DPBL Model Users

User	Comments/Uses
Sam Chang, Douglas Hahn Phillips Laboratory Atmospheric Sciences Division Atmospheric Prediction Branch Hanscom AFB, MA 01731-5000 USA	entire model coupled with global model (sent code)
A. A. M. Holtslag Royal Netherlands Meteorological Institute (KNMI) P. O. Box 201 3730 AE de Bilt THE NETHERLANDS	PBL model Operational forecasting/ boundary layer studies (sent code)
Tom Lyons Huang Xinmei Environmental Science Murdoch University Murdoch, Western Australia, 6150 AUSTRALIA	Entire model (sent code)
Tom Lyons Dick Smirk Alcoa of Australia Limited PO Box 252 Applecross, Western Australia 6153 AUSTRALIA	Evaporation from industrial wastes (sent code)
Alistair Culf Institute of Hydrology Wallingford Oxfordshirt OX10 8BB UNITED KINGDOM	Entire model/energy balance for vegetation (sent code)
Paul Ruscher Department of Meteorology Florida State University Tallahassee, FL 32302 USA	Entire model/ local weather forecasting (sent code)

Richard Cuenca Water Resources Engineering Team Bioresource Engineering Gilmore Hall, Oregon State University Corvallis, OR 97331-3906 USA	Entire model/emphasis on plant/soil studies (using our code)
John Eise National Weather Service RR3 Box 578 Amarillo, TX 79107 USA	Entire model/local weather forecasting (sent code)
H. A. R. de Bruin and colleagues Department of Meteorology Wageningen Agricultural University Duivendaal 2 6701 AP Wageningen THE NETHERLANDS	Soil/plant studies (sent code)
Trevor Scholtz Atmospheric Environmental Service (AES) CANADA	Entire model/ atmospheric chemistry/ soil chemistry (sentcode)
Dr. Mike McCorcle Department of Agronomy Iowa State University Ames, Iowa 50011 USA	Soil/plant (wrote own code)
Professor Jan Paegel Department of Meteorology University of Utah Salt Lake City, Utah 84112 USA	Soil/plant studies (McCorkle code)
Prof. Moid Ahmad Department of Geophysical Sciences Ohio University 316 Clippinger Lab Athens, OH 45701 USA	Evapotranspiration/ climate modification (sent code)
James Cramer HQ AF Global Weather Central/SDDC Offutt AFB Omaha, NE 68113-5000 USA	Entire model/clouds, low-level winds, moisture and temperature (sent code)

Peter Rice Global Weather Central GWC/SDDC Offutt AFB Omaha, NE 68113-5000 USA	Evaporation (Phillips Lab. code)
David Zehr USAF/ETAC DNO Scott AFB, IL 62225 USA	Low-level winds (sent code)
Hua-Lu Pan and Ken Mitchell Development Division, National Meteorological Center National Weather Service/NOAA W/NMC22 WWB, Room 204 Washington, D. C. 20233 USA	Evaporation (wrote own code)
Stefan Gollvik Swedish Meteorological and Hydrological Institute (SMHI) S-60176 Norrköping SWEDEN	PBL model/regional weather forecasting (KNMI code)
National Center for Atmospheric Research (NCAR) MMM Divsion PO Box 3000 Boulder, CO 80307-3000 USA	PBL model in NCAR Community Climate Model (KNMI code)

Appendix B. Model Changes

The OSU1DPBL model continues to undergo change. The sections in this appendix address the many changes made to the model since version 1.0.1.

B.1 Changes from version 1.0.3 to version 1.0.4

Jinwon Kim's Ph.D. thesis work involved adding free atmospheric diffusion and local generation of turbulence in the stable boundary layer, and gravity wave drag to the model.

Michael Ek and Larry Mahrt's cloud package captures the most important interaction between boundary-layer clouds and boundary layer-development, namely the reduction of incoming solar radiation and its impact on the surface energy balance. The new formulation of boundary-layer cloud cover includes the influence of turbulent and meso-scale subgrid variability on the averaged boundary-layer cover.

Other changes are noted in the comments at the beginning of and throughout the model code, such as a critical Richardson number of unity (RICR = 1).

B.2 Changes from version 1.0.2 to version 1.0.3

Significant changes were made to subroutines PBLL and SFLX following suggestions by A. A. M. Holtslag who spent the summer of 1989 at Oregon State University. These changes are outline in detail in the extensive comment section at the beginning of the model code, and include changes to surface exchange coefficients, two-meter temperature and wind calculations, the critical richardson number, minimum boundary layer depth, similarity profile functions, and the soil moisture excess; and additions of separate heat and momentum roughness lengths, displacement height, and canopy resistance.

Cloud cover is now calculated following a modified form of Chu (1986) and Slingo (1980); this is discussed in the model physics chapter. The boundary layer cloud package is used only for determining fractional cloud cover which modifies the boundary layer by reducing incoming solar radiation and changing downward atmospheric radiation. This cloud cover calculation and cloud-radiation interaction is now controlled by a three-way flag. For IFCRI = 1 cloud cover is calculated using the new cloud package and there is radiation reduction due to fractional cloud cover; for IFCRI = -1 cloud cover is calculated but there is no cloud-radiation feedback; for IFCRI = 0 there is no cloud cover calculation.

The parameterized downward atmospheric radiation method has been tested and appears adequate for non-cloudy cases. So the flag for parameterized radiation has been removed from control file and is hardwired at IFPR=1.

B.3 Changes from version 1.0.1 to version 1.0.2

A grid with a 20 meter resolution was introduced (grid #1 in the model); the previous model had a grid with a resolution of 50 meters (grid #6).

A cap (maximum value) was put on the countergradient term for heat (CGH), based on Deardorff (1966). The countergradient term for moisture was removed (CGW = 0) due to the breakdown of the similarity formulation of that term for near-neutral conditions. There will be no future references to the countergradient term for moisture in the user's guide or model code.

The critical Richardson number (RICR) has been changed from 1.0 to 0.5.

Vertical advection of momentum is now included in OSU1DPBL.

Clouds in SUBROUTINE SUN are turned off by means of a new flag for cloud-radiation interaction (IFCRI) until a more viable cloud scheme is developed. (See Future changes in the next section). IFCRI is set to zero in COMMON block RAD which is described in section 4.1.2.

The soil heat capacity code in SUBROUTINE HRT was changed to include the contribution by the air in the soil. Although this was only a minor change, it was simple and made for completeness.

Many COMMON block elements have been changed so that they are "common" throughout OSU1DPBL. This is described further in the next section.

Many of the hard-wired values for albedo, soil type, etc, are no longer hard-wired. This allows more freedom to make changes in OSU1DPBL through the control file input data. These parameters listed below must now be initialized in the control file. (See section 4.1.2 on COMMON blocks for more detailed descriptions.)

parameter	description	original default value
ALBEDO	albedo	0.23
ISOIL	soil type	6 (sandy clay loam)
TWILT	plant wilting pt	0.12
PC	plant coefficient	0.6
SIGMAF	shading factor	0.7
TSO0	air dry value	0.25
TSOREF	reference value	0.25
CLC	cloud cover	0.0
CMC	canopy water content	0.0
SCANOP	canopy saturation	0.002 meters (2 mm)
IFCLD	cloud diffusivity flag	0
IFTC	plant transpiration flag	1

B.4 Future Changes

We feel that our formulation, as well as all existing formulations, for turbulent transport by boundary-layer clouds are inadequate. The interplay between boundary-layer clouds and turbulence varies dramatically between different boundary-layer situations. The failure to understand the basic physics of these situations limits our ability to construct useful parameterizations. As a result we must start with existing and new analyses of observations for relatively simple situations. These are best found over the oceans.

In addition, a radiation package would eliminate one of the most serious shortcomings of the model when it is operated in a stand-alone mode. In keeping with the philosophy of the model, a requirement of this radiation package is that it be simple and not computationally expensive Several possibilities exist.

Formulations for the surface exchange coefficients and profile functions following Holtslag and Beljaars (1989) tested in the model during the summer of 1989. The formulations have potential problems under stable conditions, so the present stable formulation following Mahrt (1987) is being retained, although future study is planned.

There is some potential confusion with different COMMON block elements with identical names, or the same COMMON block elements with different names in different subroutines in OSU1DPBL. The COMMON block elements have been or are being changed so that they are "common" throughout OSU1DPBL. The following list is what remains to be changed.

COMMON Block	Element	Also called... / in...
PBL	DUDT	UN / SUBROUTINE PBLL
	DVDT	VN / SUBROUTINE PBLL
	DTDT	RN / SUBROUTINE PBLL
	DWDT	WN / SUBROUTINE PBLL
	DELT2	DTBL / SUBROUTINE PBLL
SFCL	TS	T1 / SUBROUTINE SFLX
	WS	Q1 / SUBROUTINE SFLX
	W2	Q2 / SUBROUTINE SFLX
	ZZ2	Z / SUBROUTINE SFLX
AUXIL	CG	CGH / SUBROUTINE PBLL
RAD	TSUN	HO / BLOCK DATA A1
	TSUN	HO / SUBROUTINE SUN
HCALC	MZH	JPBL / SUBROUTINE PRINT
	TIMEIS	HO / SUBROUTINE PRINT
SOIL	WSOIL	SMC / SUBROUTINE SFLX
	TSOIL	STC / SUBROUTINE SFLX
SOIL2	ZSOIL	DSOIL / PROGRAM PBLDVR
	ZSOIL	Z / BLOCK DATA A2
	ZSOIL	DSOIL / SUBROUTINE PRINT
	ZSOIL	Z / SUBROUTINE SHFLX
	ZSOIL	XZ / SUBROUTINE HRT
	ZSOIL	Z / SUBROUTINE KTSOIL
	ZSOIL	Z / SUBROUTINE DFKT
	ZSOIL	Z / SUBROUTINE THSAT

There are still several statements in the OSU1DPBL code that have been "commented-out" as a part of model development in converting between the different compilers used to run the model.

Running the model on the Macintosh II was suspended due to FORTRAN compiler problems, so the more user friendly Hypercard application that was under development is on hold until a more suitable compiler for the Macintosh is found.

As before, we continue to make the model documentation more complete within OSU1DPBL and in the user's guide by making comments complete and uniform and trying to define most everything, listing alogrithm sources, and using similar style FORTRAN. A computer version of the user's guide is currently available for the Macintosh, while we are considering a user's guide for the model in a UNIX format ("man" pages).

B.5 Some model limitations

The present model resolution does not allow for clear air radiative cooling, although this is an important process in the energy balance, especially in very stable cases, e.g. nighttime.

The original air-dry (TSOO) default value of 0.25 was much higher than actual values in order to compensate for the underestimation of the vertical gradients of soil moisture near the soil surface because of a lack of model resolution at the surface.

Forested or natural grass regions lead to organic debris at the surface (dead grass, leaves, etc.) which have very low hydraulic and thermoconductivity when dry. This can be included in the present model only by adjusting the property values of the upper soil layer.

The soil neglects upward diffusion of water through the bottom of the soil layer which could cause significant errors during long drying periods.

The model does not allow for poor drainage conditions at the bottom of the soil layer where the effective hydraulic conductivity, $K(\Theta)$ is small.

No special consideration is made for the soil-ice phase.

B.6 Application of the gravity wave model: Problems and suggestions

For the application of the gravity wave drag model to large scale models, several problems need to be considered. The problems include the determination of the wave amplitude at the ground surface (same as the effective mountain height), definition of the *surface* flow which is directly related to the generation of gravity waves, the influence of the boundary layer turbulence on the generation of gravity waves, and the influence of the residual layer on the propagation of gravity waves.

1. *Surface* wind and stratification

In the current model, the surface wind is defined as the mean wind in a layer containing the top of the mountain (or the variance of topographic height). The surface stratification is calculated for the same layer as the mean wind (Fig. 1). If the stratification determined in this way is neutral or unstable at the mountain top level due to a deep boundary layer, wave stress at the surface becomes zero (no gravity waves) and wave drag is not computed.

2. Effective mountain height

The effective mountain height is determined by (5) where the wave amplitude at the surface is assumed to be equal to the effective mountain height. The effective height must be estimated for each individual grid box. The mountain height η_0 in (5) for a model grid box is usually assigned by the root-mean-square value of high resolution topographic data (Palmer *et al.*, 1986; MacFarlane, 1987; Stern and Pierrehumbert, 1988).

The influence of the boundary layer turbulence on the generation of gravity waves is not clearly known. It has been assumed that when the mixed layer develops during the day, the resulting turbulence would rapidly dissipate coherent wave motions so that topographic gravity waves are nonexistent during daytime (Palmer *et al.*, 1986). However, case studies for 6 and 25 March ALPEX suggest that the effective mountain height can be well approximated by (5) even though the observations are taken during the daytime. This may suggest that even in the presence of a mixed layer, gravity waves can still be induced and can propagate above if the dissipation time scale of turbulence is longer than the time scale for the vertical propagation of wave energy. In any case, the net influence of the boundary layer is expected to reduce the influence of topographic variations. During the night where the boundary layer is usually shallow and stably stratified, influence of the boundary layer would be small, if not negligible.

For model applications, several different approaches can be tested for daytime simulations:

(1) Like other modelling studies, gravity wave drag is neglected whenever the mixed layer is developed during the daytime.

(2) Even though turbulence can eliminate gravity waves entirely in the boundary layer, gravity waves still can be generated if the boundary layer has below the mountain top. An alternative to the approach (1) is to replace η_0 with $\eta_0 - H_{pbl}$ in (5), where H_{pbl} is the depth of the boundary layer.

(3) If the boundary layer is stably-stratified, as is sometimes observed in the upper part of the mixed layer, that stable boundary layer would be able to maintain gravity waves. With this assumption, η_0 is replaced with $\eta_0 - D_{pbl}$ where D_{pbl} is the depth of the unstable portion of the mixed layer.

For the approaches (2) and (3), topographically-generated gravity waves will be nonexistent for a deep mixed layer. Variation of the surface topography can cause the variation of the inversion height at the top of the mixed layer which can be another source of gravity waves near the surface. This case must be considered further and requires knowledge of the variation of the boundary layer depth over uneven topography.

3. Vertical propagation of gravity waves: nighttime

The current formulation of gravity wave drag assumes that whenever gravity waves encounter neutral or unstable layers during vertical propagation, gravity waves are totally dissipated in the layer. In the real atmosphere, neutral or unstable mean flow will not be frequent in the free atmosphere. However, such layers can temporarily appear in numerical models.

In column model simulations, neutral or unstable layers in the free atmosphere are most frequently and systematically appear in the residual layer, especially when the mixed layer collapses in the early evening. The lack of stratification in the modelled residual layer is a consequence of the lack of radiative heat transfer, large-scale advection, or insufficient turbulent mixing. At any case, if the daytime mixed layer grows to a level much higher than the top of the mountain and significant stratification fails to be developed in the residual layer during the night, the current model will predict unrealistically small gravity wave drag. Such problems are expected to be less severe for two- or three-dimensional models. One way of avoiding such problems is to start the wave drag computation from a level higher than the top of the daytime mixed layer (some previous modelling studies start the wave drag calculation from the 850 mb level).

Appendix C
References

Al Nakshabandi, G. and H. Kohnke, 1965: Thermal conductivity and diffusivity of soils as related to moisture tension and other physical properties, *Argic. Meteorol.*, **2**, 271-279.

Alhberg, H. J., E. N. Nilson and J. L. Walsh, 1967: *The Theory of Splines and their Applications*, Academic Press, 284 pp.

Baer, F. and T. J. Simons, 1970: Computational stability and time truncation of coupled nonlinear equations with exact solutions. *Mon. Wea. Rev.*, **98**, 665-679.

Brenner, S., C.-H. Yang and K. Mitchell, 1984: *The AFGL Global Spectral Model: Expanded Resolution Baseline Version*. Rept. No. AFGL-TR-84-0308, Air Force Geophysics Laboratory, Hanscom AFB, 72 pp. [ADA160370]

Businger, J. A., J. C. Wyngaard, Y. Izumi and E. F. Bradley, 1971: Flux-profile relationships in the atmospheric surface layer. *J. Atmos. Sci.*, **28**, 181-189.

Charnock, H., 1955: Wind stress on a water surface. *Quart. J. Roy. Meteor. Soc.*, 81, 639-640.

Chu, C.-T., 1986: Parameterization of shallow convection in the boundary layer. M. S. thesis, Department of Atmospheric Sciences, Oregon State University, Corvallis, 83 pp.

Clapp, R. B. and G. M. Hornberger, 1978: Empirical equations for some soil hydraulic properties. *J. Water Resources Res.*, **14**, 601-604.

* Collier and Lockwood, 1974. See p. 118 of this manual.

Dalrymple, P. C., 1966: A physical climatology of the Antarctic plateau. *Studies in Antarctic Meteorology* (M. J. Rubin, ed.). Vol. 9 of the Antarctic Research Series, American Geophysical Union, Washington, 195-231.

Deardorff, J. W., 1966: The countergradient heat flux in the lower atmosphere and in the laboratory. *J. Atmos. Sci.*, **23**, 503-506.

Ek, M. and L. Mahrt, 1991: A formulation for boundary-layer cloud cover (~~submitted to~~ ~~to appear~~ *Ann. Geophys.* ~~ser. B~~). 9, 716-724.

Fairall, C. W., J. E. Hare and J. B. Snider, 1990: An eight-month climatology of marine stratocumulus cloud fraction, albedo, and integrated liquid water. *J. Climate*, **3**, 847-864.

Gray, D. M. and D. H. Male, 1981: *Handbook of Snow*. Pergamon Press, Toronto, 776 pp.

Holtslag, A. A. M., 1987: Surface fluxes and boundary-layer scaling; models and applications. KNMI Sci. Rep. 87-02.

Holtslag, A. A. M. and F. T. M. Nieuwstadt, 1986: Scaling the atmospheric boundary layer. *Bound.-Layer Meteorol.*, **36**, 201-209.

Holtslag, A. A. M. and H. A. R. de Bruin, 1988: Applied modeling of the nighttime surface energy balance over land. *J. Appl. Meteorol.*, **27**, 689-704.

Holtslag, A. A. M. and A. C. M. Beljaars, 1989: Surface flux parameterization schemes; developments and experiences at KNMI. ECMWF Workshop on Parameterization of Fluxes and Land Surfaces, 24-26 Oct., 1988, pp. 121-147, Reading, England. (Also as KNMI Sci. Rep. 88-06, 1988.)

Holtslag, A. A. M., E. I. F. de Bruijn and H.-L. Pan, 1990: A high-resolution air mass transformation model for short-range weather forecasting. *Mon. Wea. Rev.*, **118**, 1561-1575.

Holtslag, A. A. M. and M. Ek, 1990: Simulation of surface fluxes and skin temperature: Preliminary results for the pine forest in HAPEX-MOBILHY. Preprint Ninth Symposium on Turbulence and Diffusion, Am. Met. Soc., Roskilde, Denmark, 30 Apr - 3 May, pp 188-191. To be submitted to *Bound.-Layer Meteor.*

Kasten, F. and G. Czeplak, 1980: Solar and terrestrial radiation dependent on the amount and type of cloud. *Solar Energy*, **24**, 177-189.

Kim, J. and L. Mahrt, 1991a: Turbulent transport in the free atmosphere. To be submitted to *Bound.-Layer Meteor.*

Kim, J. and L. Mahrt, 1991b: Momentum transport by gravity waves. To be submitted to *J. Atmos. Sci.*

Kondo, J. O., O. Kanechika and N. Yasuda, 1978: Heat and momentum transfers under strong stability in the atmospheric surface layer. *J. Atmos. Sci.*, **35**, 1012-1021.

Liou, K.-N., 1976: On the absorption, reflection and transmission of solar radiation in cloudy atmospheres. *J. Atmos. Sci.*, **33**, 798-805.

Louis, J.-F., 1979: A parametric model of vertical eddy fluxes in the atmosphere. *Bound.-Layer Meteorol.*, **17**, 187-202.

Louis, J.-F., M. Tiedtke and J. F. Geleyn, 1982: A short history of the operational PBL-Parameterization of ECMWF. Workshop on planetary boundary-layer parameterization, European Centre for Medium Range Weather Forecasts, Shinfield Park, Reading, Berks, U. K.

Lowe, P. R. and J. M. Ficke, 1974: Computation of saturation vapor pressure. *United States Environmental Prediction Research Facility, Naval Postgraduate School, Monterey, CA., ENVPREDRSCHFAC Technical Paper No. 4-74*, March, 27 pp.

Mahrt, L., 1987: Grid-averaged surface fluxes. *Mon. Wea. Rev.*, **115**, 1550-1560.

Mahrt, L. and M. Ek, 1984: The influence of atmospheric stability on potential evaporation. *J. Clim. Appl. Meteorol.*, **23**, 222-234.

Mahrt, L. and H.-L. Pan, 1984: A two-layer model of soil hydrology. *Bound.-Layer Meteorol.*, **29**, 1-20.

Mahrt, L., M. Ek, J. Kim and A. A. M. Holtslag, 1991: *Boundary-layer parameterization for a global spectral model*. Final contract report (PL-TR-91-2031) to Atmospheric Prediction

Branch, Phillips Laboratory, Hanscom AFB, MA, 210 pp. Oregon State University, Corvallis.

Mahrt, L., H.-L. Pan, P. Ruscher and C.-T. Chu, 1987: *Boundary-layer parameterization for a global spectral model.* Final contract report (AFGL-TR-87-0246) to Atmospheric Prediction Branch, Air Force Geophysics Laboratory, Hanscom AFB, MA, 182 pp. Oregon State University, Corvallis.

Mahrt, L., J. O. Paumier, H.-L. Pan and I. Troen, 1984: *A boundary-layer parameterization for a general circulation model.* Final contract report (AFGL-TR-84-0063) to Atmospheric Prediction Branch, Air Force Geophysics Laboratory, Hanscom AFB, MA, 179 pp. Oregon State University, Corvallis.

Marchuk, G. I., 1974: *Numerical Methods in Weather Prediction*, Academic Press, 277 pp.

Monteith, J. L., 1965: Evaporation and environment. *Symp. Soc. Exp. Biol.*, **19**, 205-234.

Monteith, J. L., 1981: Evaporation and surface temperature. *Quart. J. Roy. Meteor. Soc.*, **107**, 1-27.

Oke, T.R., 1978: *Boundary-layer Climates*. Methuen, London, 372 pp.

Paltridge, G. W. and C. M. R. Platt, 1976: Radiative processes in meteorology and climatology in *Developments in Atmospheric Science, 5.* Elsevier Scientific Publ. Co., Amsterdam, 318 pp.

Pan, H.-L. and L. Mahrt, 1987: Interaction between soil hydrology and boundary-layer development. *Bound.-Layer Meteorol.*, **38**, 185-202.

Ruscher, P. H., 1987: An examination of structure and parameterization of turbulence in the stably-stratified atmospheric boundary layer. Ph. D. thesis, Department of Atmospheric Sciences, Oregon State University, Corvallis, 170 pp.

Ruscher, P. H., 1991: A formulation of the very stable boundary layer in a simple atmospheric model. To be submitted to *Mon. Wea. Rev.*

Satterlund, D. R., 1979: Improved equation for estimating long wave radiation from the atmosphere. *J. Water Resources Res.*, **15**, 1649-1650.

Troen, I. and L. Mahrt, 1986: A simple model of the atmospheric boundary layer: Sensitivity to surface evaporation. *Bound.-Layer Meteorol.*, **37**, 129-148.

Tuccillo, J. J., 1987: Impact of snow cover on NGM forecast temperature. *NWS West. Region Tech. Attach.*, **87**, No. 2, 7 pp.

* Collier, L. R. and J. G. Lockwood, 1974: The estimation of solar radiation under cloudless skies with atmospheric dust. Quart. J. Roy. Meteorol. Soc., 100, 678-681.